UC Merced
UC Merced Electronic Theses and Dissertations

Title
Controls on marine community respiration

Permalink
https://escholarship.org/uc/item/8np8p4pm

Author
Wilson, Jesse Mac

Publication Date
2017

Peer reviewed|Thesis/dissertation

eScholarship.org Powered by the California Digital Library
University of California

UNIVERSITY OF CALIFORNIA MERCED

CONTROLS ON MARINE COMMUNITY RESPIRATION

A dissertation submitted in partial satisfaction of the requirements for the degree
Doctor of Philosophy

In

Environmental Systems
(Microbial Oceanography)

by

Jesse Mac Wilson

Committee in charge:

J. Michael Beman
Michael N. Dawson (Chair)
Emily Jane McTavish
Justin Yeakel

©

Jesse Mac Wilson, 2017

All rights reserved

The dissertation of Jesse Mac Wilson is approved, and is acceptable in quality and form for publication on microfilm and electronically:

_____

J. Michael Beman, Graduate Advisor

_____

Michael N. Dawson, Chair

_____

Emily Jane McTavish

_____

Justin Yeakel

University of California, Merced
2017

Table of Contents

List of Tables ..... **vi**

List of Figures ..... **vii**

Acknowledgements ..... **viii**

Curriculum Vitae ..... **x**

Abstract of Dissertation ..... **xiv**

1 Introduction **1**
- **1.1 Background** **1**
- **1.2 Scope of Dissertation** **3**
- **1.3 Organization of Dissertation** **3**
- **1.4 References** **4**

2 Ocean-scale patterns in community respiration rates along continuous transects across the Pacific Ocean **7**
- **2.1 Abstract** **7**
- **2.2 Introduction** **7**
- **2.3 Methods** **9**
  - 2.3.1 Autonomous sampling and data 9
  - 2.3.2 Respiration rate calculations 9
  - 2.3.3 Data analysis 12
- **2.4 Results** **12**
  - 2.4.1 Pacific-scale patterns in CR 12
  - 2.4.2 Relationships to environmental data 14
- **2.5 Discussion** **15**
- **2.6 References** **19**
- **2.7 Tables** **24**
- **2.8 Figures** **25**

3 Microbial community networks associated with variations in community respiration rates during upwelling in nearshore upwelling in nearshore Monterey Bay, California **31**
- **3.1 Abstract** **31**
- **3.2 Introduction** **31**
- **3.3 Methods** **32**
  - 3.3.1 Sample collection 32
  - 3.3.2 CR rate measurements 33
  - 3.3.3 Size fractionation 33
  - 3.3.4 Environmental data 34
  - 3.3.5 Microbial community assessment 34
  - 3.3.6 Statistical analyses 36
- **3.4 Results** **37**
  - 3.4.1 Temperature, oxygen, and upwelling 37
  - 3.4.2 Community respiration 37
  - 3.4.3 Microbial community dynamics 38

3.5 Discussion **40**
3.5.1 Spatial and temporal variation 40
3.5.2 Microbial community dynamics and CR 42
3.6 References **44**
3.7 Tables **52**
3.8 Figures **55**

4 Primary production, community respiration, and net community production along oxygen and nutrient gradients: environmental controls and biogeochemical feedbacks within and across 'marine lakes' **63**
4.1 Abstract **63**
4.2 Introduction **63**
4.3 Methods **65**
4.3.1 Study sites 65
4.3.2 Temperature, oxygen, and nutrient profiles 66
4.3.3 Production and respiration rate measurements and experiments 67
4.3.4 Statistical analyses 68
4.4 Results **68**
4.4.1 Oxygen, temperature, nutrient, and N* profiles 68
4.4.2 *In situ* rates in GPP, CR, and NCP 69
4.4.3 N and C additions 70
4.4.4 Rate measurements 71
4.5 Discussion **72**
4.5.1 Patterns in GPP, CR, and NCP within and across marine lakes 72
4.5.2 Effects of N and C on GPP, CR, and NCP in experimental additions 73
4.5.3 Effects of light, temperature, and oxygen on GPP, CR, and NCP 75
4.5.4 Implication for oxygen, carbon, and nutrient cycling 76
4.6 References **77**
4.7 Tables **83**
4.8 Figures **85**

5 Conclusion **93**

List of Tables

TABLE 2-1 r VALUES FOR RELATIONSHIPS AMONG ENVIRONMENTAL DATASETS IN DIFFERENT REGIONS OF THE PACIFIC.....24
TABLE 2-2 r^2 VALUES FOR COMPARISONS AMONG DIFFERENT AOU APPROACHES USED TO CALCULATE CR.....24
TABLE 2-3 r^2 VALUES FOR COMPARISONS AMONG DIFFERENT BDO APPROACHES USED TO CALCULATE CR.....24
TABLE 3-1 WEIGHTED GENE CORRELATION NETWORK ANALYSIS MODULES.....52
TABLE 3-2 LINEAR REGRESSION RESULTS RELATING THE SUM OF THE HELLINGER TRANSFORMED OTU ABUNDANCES FOR THE TWO MODULES THAT SIGNIFICANTLY CORRELATED WITH CR TO EACH ENVIRONMENTAL VARIABLE.....53
TABLE 3-3 TAXA IDENTIFICATION FOR TOP 7 OTUS IN MODULE 2 AND TOP 12 OTUS IN MODULE 6, AS IDENTIFIED BY WGCNA.....54
TABLE 4-1 LAKE AND EXPERIMENT INFORMATION.....83
TABLE 4-2 AVERAGE NUTRIENT CONCENTRATIONS.....84

List of Figures

FIGURE 2-1 MAP OF THE TRANSPACIFIC PATHS OF THE CALIFORNIA TO AUSTRALIA AND THE CALIFORNIA TO JAPAN GLIDERS AND SEA SURFACE TEMPERATURE....25
FIGURE 2-2 ENVIRONMENTAL DATA COLLECTED BY THE GLIDERS ALONG THE TWO TRANSECTS....26
FIGURE 2-3 BDO COMPUTED COMMUNITY RESPIRATION RATES ALONG THE TWO TRANSECTS....27
FIGURE 2-4 COMPUTED COMMUNITY RESPIRATION RATES ALONG THE TWO TRANSECTS....28
FIGURE 2-5 COMPUTED COMMUNITY RESPIRATION RATES ALONG THE TWO TRANSECTS....29
FIGURE 2-6 REGRESSION STATISTICS FOR BEST AIC DERIVED RELATIONSHIPS BETWEEN AOU-SLOPE-BASED CR2 DATA AND ENVIRONMENTAL DATA....30
FIGURE 3-1 STATION LOCATIONS IN MONTEREY BAY, CALIFORNIA....55
FIGURE 3-2 TEMPERATURE PROFILES FOR A) STATION K AND B) STATION O. OXYGEN PROFILES FOR C) STATION K AND D) STATION O....56
FIGURE 3-3 UPWELLING INDEXES....57
FIGURE 3-4 COMMUNITY RESPIRATION (CR) FOR A) STATION K AND B) STATION O ACCORDING TO DATE (COLOR)....58
FIGURE 3-5 REDUNDANCY ANALYSIS OF HELLINGER TRANSFORMED OTU ABUNDANCE MATRIX FOR THE SUBSAMPLED MICROBIAL COMMUNITY....59
FIGURE 3-6 ESOM FIGURES....60
FIGURE 3-7 THE SUM OF THE HELLINGER TRANSFORMED ABUNDANCES PLOTED AGAINST ENVIRONMENTAL CHARACTERISTICS OF INTEREST....62
FIGURE 4-1 LANDSAT IMAGE OF PALAU SHOWING THE LOCATION OF SAMPLING SITES....85
FIGURE 4-2 DEPTH PROFILES OF (A) DISSOLVED OXYGEN AND (B) TEMPERATURE FOR EACH LAKE IN WHICH RATES WERE MEASURED....86
FIGURE 4-3 DEPTH PROFILES OF (A) PO_3^{-4}, (B) NH_4^+, (C) $NO_3^- + NO_2^-$, AND (D) *N** IN HOLOMICTIC AND MEROMICTIC LAKES....87
FIGURE 4-4 DEPTH PROFILES OF (A) GPP, (B) CR, AND (C) NCP COLLECTED IN FIVE LAKES....88
FIGURE 4-5 RELATIONSHIPS BETWEEN OXYGEN CONCENTRATION AGAINST (A) GPP AND (B) CR....89
FIGURE 4-6 EFFECTS OF EXPERIMENTAL ADDITIONS OF NITROGEN, CARBON, AND NITROGEN + CARBON ON (A) GPP, (B) CR, AND (C) NCP....90
FIGURE 4-7 EFFECT SIZES (COHEN'S *D*) FOR EXPERIMENTAL ADDITIONS. EFFECT SIZES ARE SHOWN FOR ADDITIONS OF NITROGEN, CARBON, AND NITROGEN + CARBON ON (A) GPP, (B) CR, AND (C) NCP....91
FIGURE 4-8 EFFECT OF DEPTH TRANSPLANTS ON (A) GPP, (B) CR, AND (C) NCP....92

Acknowledgements

This dissertation was made possible by the generous support and guidance of many people over the course of my lifetime. I have been very lucky to have incredible mentors at every stage of my education and I will attempt to thank some of the many people who have helped me get to this point.

First and foremost, I would like to thank my graduate advisor, Dr. J. Michael Beman. He has enabled me to pursue my scientific interests by mentoring me throughout my graduate education. I learned many of the techniques that I used in this dissertation from him, he set up study sites and connections, read countless drafts, discussed thousands of ideas with me, and helped to prepare me for life after grad school. He did all of this while allowing me to find my own way and develop my own research ideas. I feel very fortunate to have had Mike as a role model in my life and I hope that I can achieve similar things with students one day.

My committee members, Mike Dawson, Mike Rappé, Jessica Blois, Justin Yeakel, and Emily Jane McTavish, have also been a huge help throughout this process and I would like to take the time to thank them for their assistance over the years. Mike Dawson has helped tremendously throughout the years with all things Palau and has been a wealth of information and discussions. He allowed me to audit classes that he taught and took the time to read and discuss several microbial ecology papers in preparation for my qualifying exam. Mike Rappé co-taught a summer course that helped me grow as both a graduate student and marine scientist. He took me on my first ocean research cruise, taught me molecular methods that I have used in this dissertation and will have in my tool belt from now on, and spent hours fishing for Mahi Mahi with me and the other graduate students on board the Kilo Moana. Jessica Blois has always been there to discuss ideas, to offer advice, and has always been warm and supportive. Justin Yeakel and Emily Jane McTavish each joined my committee and did me a huge service when they agreed to fill in during a busy research-filled summer. Both took the time to meet with me and discuss various chapters and provide advice. All of my committee members have made this dissertation possible and I owe them a huge debt of gratitude.

There have been many people throughout my education that influenced me going to graduate school by teaching me valuable information, techniques, and life lessons. My father has also been one of my greatest teachers throughout my life in all subjects. He fostered my love learning and taught me to approach everything with a scientific mindset. Dr. Steven Norris taught many of the classes that introduced me to field work and all things marine, Drs. Sally MacIntyre and Craig Carlson got me interested in microbial oceanography, Dr. Steve Sadro taught me several of the methods that I used in this dissertation (during which time I also received an amazing crash course in scientific writing and analysis), Dr. Michael Colvin taught me how to deal with large datasets and the code that I used for multiple chapters, and, finally, Dr. Donald Rodriguez mentored me at many stages throughout my higher education and easily had the largest influence on me becoming a scientist and teacher. I hope that I will be able to make the kind of difference that each of them has had in so many young people's lives. For these things and more I will always be eternally grateful.

This work was made possible by the generosity of the people at two field stations where I was fortunate to conduct the bulk of this dissertation's research and by Liquid Robots who built and deployed the wave gliders whose data was used. Coral Reef Research Foundation was an integral part of all the work that took place in Palau. Pat and Lori Colin have created an amazing lab and I was extremely lucky to work there. They have years of experience, are always interested in furthering scientific discovery, and work tirelessly to assist any researcher there. Their amazing employees have also made this dissertation possible. Gerda and Sharon are the marine lake experts and helped with a lot of the field work, Gerda maintained and collected data from oxygen sensors that were left in a lake throughout the 2016 El Nino that I will be analyzing in the near future, Emilo kept us safe while hiking through the jungle and paddling around the lakes, and Matt always safely got us where we needed to go. I was also extremely fortunate to work with Drs. Steve Litvin, Kerry Nickols, and Paul Leary at Hopkins Marine Station for the work conducted in Monterey Bay. Hopkins Marine Station and all of its researchers opened up their arms to us, giving us lab space, allowing us to use their boats and putting us up for the night during the many CR incubations that took place over that summer. Steve, Kerry, and Paul took us out on the water and made sure that we always had what we needed to complete our work. Steve was also the point of contact, coordinating our stays and research activities, and was an essential contributor to the paper that was developed from that work, reading and commenting on drafts and helping to acquire some of the data that we used in the models that we ran.

I would also like to acknowledge all the people who have helped me to complete this research over the years from the Beman Lab. I thank Matthew Meyerhof for starting the Palau work and for mentoring me in the lab; Curtis Hayden and Dr. Kelly Henry for carrying on the Palau work during the year that I had mono; and Elisabet Perez Coronel for helping me in Monterey Bay and for doing lab and field work with me over the years. I have also benefitted from many capable and intelligent undergraduates over the years including, Rodney Severson, Adrian Harris, Daniela Alonso, Angela Yu, Coral Quirino, and Mark Reynolds. They were each intelligent, eager, and helpful and I was very lucky to have their assistance throughout this project.

I was also extremely fortunate to have my girlfriend, Sarah Abboud, throughout most of my graduate education. She assisted me during my longest Palau field season where she carried buoys and equipment through the jungle, problem solved with me when things broke or were lost, and scienced the hell out of those marine lakes. She is a well-deserved coauthor on a paper that was published from that work, but she has helped me with tons of work throughout the years. Sarah has stayed up late discussing methods, troubleshooting stats, reading and rereading drafts, and just providing advice. Both Sarah and our dog, Mokey, have also been there emotionally for me, keeping me sane as I have stared at numbers, code, and words for countless hours.

Last, but not least, I would like to acknowledge the funding sources that went into this work, including the Eugene Cota Robles Fellowship, the Graduate Student Research Fellowship, and the Environmental Systems Summer Fellowship, all from UC Merced. Portions of this work were also funded by an NSF Dimensions of Biodiversity Award, which was awarded to Drs. J. Michael Beman, Jessica Blois, and Michael Dawson.

Curriculum Vitae

EDUCATION

Doctor of Philosophy in Environmental Systems — 2010-2017
University of California, Merced
Merced, California

Extension Courses in Marine Science — 2009-2010
University of California, Santa Barbara
Santa Barbara, California

Bachelor of Science in Environmental Science and Resource Management — 2004-2007
California State University, Channel Islands
Camarillo, California

Associate of Arts in Liberal Arts — 2001-2004
Santa Barbara City College
Santa Barbara, California

RESEARCH EXPERIENCE

Environmental Microbiology Graduate Researcher in the Beman Lab — 2010-2017
University of California, Merced
Merced, California

Center for Microbial Oceanography - Research and Education Summer Course — 2011
University of Hawaii at Manoa
Honolulu, Hawaii

Fisheries Intern for Cook Inlet Aquaculture Association — 2009
Kenai, Alaska

Wildlife Management Intern for the U.S. Army Corps of Engineers — 2008
Perkinsville, Vermont

TEACHING EXPERIENCE

Teaching Assistant — 2013-2016
University of California, Merced
Merced, California

Earth System Science Class and Lab Content Developer — 2015
University of California, Merced
Merced, California

Assessment as Pedagogy and Planning Project 2016
University of California, Merced
Merced, California

Center for Engaged Teaching and Learning 2014-2015
University of California, Merced
Merced, California

Geology Lab Technician 2006-2007
California State University, Channel Islands
Camarillo, California

OCEAN RESEARCH CRUISES

R/V Oceanus to Eastern Tropical North Pacific (Co-chief scientist) 2017 (28 days)
R/V Mussel Point to area off continental shelf of Northern California 2013 (1 day)
R/V Kilo Moana to Station ALOHA 2011 (10 days)

PUBLICATIONS

Wilson, J.M., S.S. Abboud, and J.M. Beman. (2017) "Primary production, community respiration, and net community production along oxygen and nutrient gradients: environmental controls and biogeochemical feedbacks within and across 'marine lakes'." *Frontiers of Marine Science*. doi.org/10.3389/fmars.2017.00012.

Meyerhof, M.S., J.M. Wilson, M.N. Dawson, and J.M. Beman. (2016) "Microbial community diversity, structure and assembly across oxygen gradients in meromictic marine lakes, Palau." *Environmental Microbiology* DOI: 10.1111/1462-2920.13416.

Wilson, J.M., R. Severson, and J.M. Beman. (2014) "Ocean-scale patterns in community respiration rates along continuous transects across the Pacific Ocean." *PLOS ONE* 9 (7): e99821.

Durham B. et al. (2014) "Draft genome sequence of marine alphaproteobacterial strain HIMB11, the first cultivated representative of a unique lineage within the Roseobacter clade possessing an unusually small genome." *Standards in Genomic Sciences* 9 (3).

Beman, J.M., V.J. Bertics, T. Braunschweiler, and J.M. Wilson. (2012) "Quantification of ammonia oxidation rates and the distribution of ammonia-oxidizing Archaea and Bacteria in marine sediment depth profiles from Catalina Island, California." *Frontiers in Microbiology* 3: 263.

Beman, J.M., and J.M. Wilson. "Aquatic Biomes." *The Nature Education: Knowledge Project*. www.nature.com/scitable/knowledge. Accepted.

Wilson, J.M., S.Y. Litvin, and J.M. Beman. "Microbial community networks associated with variations in community respiration rates during upwelling in nearshore Monterey Bay, California." In Prep.

Wilson, J.M, G. Ucharm, and J.M. Beman. "Ecosystem metabolism throughout the 2016 El Nino Southern Oscillation in a tropical marine lake." In Prep.

Wilson, J.M. and J.M. Beman. "Microbial community diversity and oxygen cycling in the marine lakes of Palau." In Prep.

PRESENTATIONS

Enviro-lunch Series 2011, 2012, 2013, 2016
Various topics (talks)
Merced, California

University of California Carbon Slam 2016
The dark side of the carbon cycle: simulating changing environmental conditions using natural gradients and mesocosms to study their effects on marine respiration (poster)
Palo Alto, California

Ocean Sciences Meeting 2016
Microbial community dynamics, community respiration, and net community production in Monterey Bay, a nearshore upwelling kelp forest environment (talk)
New Orleans, Louisiana

Ocean Sciences Meeting 2014
Marine Lakes as Model Systems for Understanding Interactions Between Marine Microbial Community Composition and Function (poster)
Honolulu, Hawaii

Ocean Sciences Meeting 2012
2011 C-MORE Summer Course Cruise Collective: Scales of Variability at Station ALOHA (poster)
Salt Lake City, Utah

Southern California Conference on Undergraduate Research 2007
Quantitative Method for Selecting the Best Subspecies of Channel Island Fox for a Mainland Breeding Program (poster)
Los Angeles, California

AWARDS

UC Merced Environmental Systems Summer Fellowship 2014, 2015, 2017
UC Merced, School of Engineering Outstanding Teaching Award 2016
UC Merced Graduate Division Summer Fellowship 2011, 2012
Eugene Cota-Robles Fellowship 2010-2012
Graduated Summa Cum Laude from CSU Channel Islands 2007
Environmental Science Program Honors at CSU Channel Islands 2007
Presenter at Southern California Conference on Undergraduate Research 2007

Abstract of the Dissertation

Controls on marine community respiration

by

Jesse Mac Wilson

Doctor of Philosophy, Environmental Systems Program
University of California, Merced 2017
Dr. J. Michael Beman, Graduate Advisor
Dr. Michael Dawson, Chair

Microorganisms engineer their surroundings through their metabolisms, and some of the most important metabolic reactions for multicellular life involve oxygen. The supply and removal of oxygen in aquatic systems depends on many physical, chemical, and biological processes, but controls on the biological processes involving oxygen (particularly respiration) are the least well understood. Different communities of microorganisms may produce and consume oxygen at different rates, but chemical and physical conditions also affect microbial activity. An understanding of all the factors affecting respiration is paramount during the era of climate change as the carbon dioxide produced during respiration can serve as a positive feedback. In this work, I sought to better understand the controls on marine community respiration (CR) using a range of study sites and methods across the Pacific Ocean. Each location was selected based on its ability to help untangle some of the possible variables that affect CR. First, I examined how CR varied with coincident measurements of temperature, turbidity, and chlorophyll concentrations (a proxy for phytoplankton biomass) across the entire Pacific Ocean using data collected by wave gliders (drones) that left from San Francisco, CA and arrived in Australia and Japan. CR was weakly related to different explanatory variables across the Pacific, but more strongly related to particular variables in different biogeographical areas. The results indicate that CR is not a simple linear function of chlorophyll or temperature, and that at the scale of the Pacific, the coupling between primary production, ocean warming, and CR is complex and variable as nutrients and the microbial community change. To further understand the contribution of the microbial community to CR I measured the community, changes in CR, and several environmental variables throughout the upwelling season in Monterey Bay, CA—a dynamic nearshore environment. CR varied significantly over time as a function of temperature, dissolved oxygen (DO), upwelling, and chlorophyll—but also varied with a subnetwork of the microbial community. One subnetwork was associated with higher CR and warmer temperatures, while another was associated with lower CR and DO. Although some microbial taxa were represented in both subnetworks (e.g. Flavobacteriaceae), there were also taxa unique to each network—including the Arctic97B-4 marine group and SAR324 clade (in the subnetwork that was negatively correlated with CR) and *Planktomarina* and eukaryotic phytoplankton (in the subnetwork positively correlated with CR). The results indicate that multiple microbial interactions regulate CR and carbon cycling in the coastal ocean, and that the presence of particular eukaryotic phytoplankton contribute to CR. Finally, to understand the contribution of

nutrients and photosynthesis to CR I conducted a series of experiments in the marine lakes of Palau. The lakes served as natural mesocosms, each with slightly different communities and physical and chemical properties. By experimentally adding nitrogen, a labile carbon source, and transplanting bottles to manipulate light and temperature I was able to tease apart which environmental factors were the most important in determining GPP and CR in different types of systems (lakes) in addition to how the two rates are related across systems. While nutrient rich lakes had higher GPP, this was not the case for CR, showing decoupling between the two rates. However, CR spiked when both nitrogen and labile organic matter were added, shifting the metabolic balance of the community from autotrophic to heterotrophic. Together, these results show that both the heterotrophic microbial community and the photosynthetic community are major contributing factors to CR, so models projecting future rates of CR in a changing world should start to include changes in the microbial community in addition to changes in temperature and nutrients.

1 Introduction

1.1 Background

Oxygen is a limiting feature in many ecosystems and microbes play a key role in determining its availability. Outnumbering any other organism on the planet, microorganisms are responsible for half of global primary production (and almost all of photosynthesis in the ocean) (Field et al. 1998) but also have the potential to consume massive quantities of oxygen during the oxidation of organic matter and other reduced chemical compounds in order to gain energy and build biomass, thus regulating fluxes of carbon, oxygen, nutrients and energy throughout the ocean (Falkowski et al., 2008). In certain areas of the ocean, microbial induced oxygen deficiency shifts energy away from macro-organisms towards microorganisms (Diaz & Rosenberg 2008; Wright et al. 2012). Their ability to shape ecosystems collectively makes microorganisms a type of ecosystem engineer (Breitburg et al., 2010). Moreover, as environmental conditions change, so does the community of microorganisms. (e.g. as oxygen decreases below certain thresholds; Beman & Carolan, 2013).

Dissolved oxygen (DO) concentration in water is controlled by a combination of physical, chemical, and biological processes. Atmospheric diffusion, physical mixing of water masses, and oxygenic photosynthesis are responsible for increasing the supply of oxygen in water; while outward flux, aerobic respiration, the biological oxidation of reduced compounds (e.g. hydrogen sulfide, methane, and ammonia), and the abiotic autooxidation of certain reduced gases (e.g. hydrogen sulfide) decrease the amount of oxygen in water. Therefore, the organisms that produce and consume oxygen also affect DO, leading to a chicken and egg scenario in which the cause and effect can be difficult to separate.

In terms of the biological controls on DO, both multicellular organisms and microorganisms (unicellular microscopic organisms) are responsible for the production and consumption of DO in the ocean—however, the activities of microorganisms are more widespread and contribute to a larger fraction—in spite of their small size—due to their ubiquitous nature and staggering number in the world's oceans (Whitman et al., 1998). It is safe to assume that microorganisms would continue to thrive in the world's ocean without the presence of multicellular organisms—much as they did for millions of years—while a significant portion of multicelluar life is dependent on the oxygen produced by unicellular photoautotrophs in order to oxidize reduced carbon to obtain energy (Falkowski et al., 2008).

Despite the important role of microorganisms as planetary engineers, we do not fully understand what factors control microbial oxygen cycling. Studies measuring rates of photosynthesis and respiration in the ocean are often concentrated in a few areas so that large swaths of ocean have little to no data (Regaudie-de-Gioux & Duarte, 2012; Robinson & Williams, 2005), with significantly fewer studies regarding respiration than photosynthesis, which has contributed to a spirited debate as to the metabolic state of the ocean at large (Duarte et al., 2013; Ducklow & Doney, 2013; Williams et al., 2013). This challenge is made more difficult by the fact that the rates in a specific place and time may not represent the rates in that same place at a different time—a phenomenon that can be due to physical, chemical, and/or biological reasons. Microorganisms have been shown to have seasonal cycles in the ocean that correspond to light

availability and stratification (Giovannoni & Vergin, 2012), meaning that both gross primary productivity (GPP) and community respiration (CR) are also affected by such seasonality.

Both physical and chemical factors influence photosynthesis and respiration as each is a biological reaction that requires specific temperatures, light (in the case of photosynthesis), and compounds to proceed. For example, metabolic theory predicts that both CR and GPP should increase as temperature increases (Brown et al., 2004), though CR has been observed to be more sensitive (Pomeroy & Deibel, 1986; López-Urrutia et al., 2006; Kirchman et al., 2009; Riebesell et al., 2009; Wohler et al., 2009; Regaudie-de-Gioux & Duarte, 2012). However, experimental manipulations of possible causative factors that affect rates are less common than purely observational measurements or inferences based on transects, and the role of the microbial community (measures of diversity or the presence of specific microorganisms) on rates of respiration are rarely considered.

Additionally, understanding microbial ecology and its implications for ecosystems is still in its infancy. Some work has applied classic ecological principles to microbial ecology; for example, the relationship between diversity and the amount of energy available in a system has been tested in microbial systems with conflicting results and elusive governing mechanisms (Kassen et al., 2000; Travisano & Rainey, 2000; Horner-Devine et al., 2003). A hump-shaped relationship, in which maximum diversity is achieved at intermediate levels of productivity, has been demonstrated in several situations (Kassen et al., 2000; Horner-Devine et al., 2003). Bell et al. (2005) showed that ecosystem function—as measured by the mean daily rate of bacterial respiration—increased with increasing bacterial species richness in a decelerating manner for cultured tree-hole bacteria. Ecologists have shown that an "insurance hypothesis" serves to stabilize plant communities over time (Tilman et al., 2006) through a combination of functional redundancy and different individual responses to events like warming (Chapin et al., 1996) and grazing (Walker et al., 1999), which can provide long-term resilience to anthropogenic perturbations (Diaz & Cabido, 2001), and a few studies have extended the “insurance hypothesis,” to microbes. In aquatic microcosms with multiple trophic levels, more diverse microbial communities tend to have more predictable biomass and density (Naeem & Li, 1997), undergo less variation in CO_2 flux, and are more resistant to invasion by exotic species (McGrady-Steed et al., 1997) than less diverse communities. These studies were a good foundation, but linking changes in microbial composition to changes in ecosystem function—which will aid in understanding how microorganisms ‘engineer’ their surroundings—is an ongoing effort (Fuhrman, 2009; Graham et al., 2016). Current work is beginning to link specific (sub)communities of microorganisms to ecosystem functions using network analysis and bioinformatics, and has shown that changes in the microbial community and its functional genes can predict changes in ecosystem function, such as bacterial production and carbon export (Guidi et al., 2016; Bowman et al., 2017).

Knowledge about the link between oxygen cycling and community structure is essential given the accelerated rate at which global climate change is occurring, but this also makes study design more challenging (given that the functioning of today may not be the functioning of tomorrow). Climate change stands to change global surface temperatures and thus nutrient regimes and community structure through increased stratification, all of which could impact oxygen cycling rates. Because carbon dioxide is produced and consumed as oxygen is consumed and produced,

changes in CR and GPP could lead to a positive feedback for climate change, as a larger fraction of primary production might be channeled through the microbial food web and respired (Pomeroy & Deibel, 1986, Riebesell et al., 2009, Wohler et al., 2009).

1.2 Scope of the Dissertation

The overall purpose of this dissertation is to assess biological oxygen cycling in ocean systems, factoring in the above gaps in the literature. I chose to focus on the factors influencing CR because there are relatively fewer studies regarding respiration in the literature and because oxygen consumption can be used as a proxy for ecosystem function, though GPP was also measured and is considered in chapter 4. In order to provide a baseline rate of respiration in many systems and to understand how it may change in future oceans with different temperatures and nutrients I assessed CR in a variety of environments while testing how CR varied with space, time, temperature, the microbial community, nutrients, labile organic matter, and photosynthetic rate (as measured by oxygen production). My study locations ranged from near home in Monterey in California, USA to the other side of the Pacific Ocean in the marine lakes of Palau, while also looking at the entire Pacific Ocean in between. Spatial variation across the Pacific was assessed via sensors on autonomous wave gliders while the relative importance of microbial community composition versus physical and chemical characteristics in shaping oxygenic photosynthesis and how all the above factors affected CR were explored through bottle incubations, reciprocal transplant experiments, and culture independent techniques.

1.3 Organization of the Dissertation

The research conducted for this dissertation has been written as three distinct manuscripts and is thus divided into three self-contained chapters (2, 3, and 4). In chapter two, "Ocean-Scale Patterns in Community Respiration Rates along Continuous Transects across the Pacific Ocean," I assessed spatial variation in CR over an entire ocean basin using data from two wave gliders with sensor packages, thus filling in gaps in existing data regarding CR in a majority of the Pacific Ocean and allowing comparisons between the two wave gliders and an analysis of how CR changed over space, according to latitude, temperature, chlorophyll, and turbidity. 605 independent CR rates were calculated using sensor packages attached to wave gliders that left from San Francisco, CA and arrived in Australia and Japan more than a year later. At the time it was published this work more than tripled the total number of CR measurements made in Earth's largest ocean and identified an area of high variability in the North Pacific Subtropical Ocean. In chapter three, "Microbial community networks associated with variations in community respiration rates during upwelling in nearshore Monterey Bay, California," I measured changes in respiration and the microbial community in addition to several environmental variables throughout the upwelling season in a dynamic nearshore environment. I demonstrated that a subset of the microbial community was correlated with CR, and this subset changed over time independent of upwelling events. In chapter four, "Primary production, community respiration, and net community production along oxygen and nutrient gradients: environmental controls and biogeochemical feedbacks within and across 'marine lakes'," I observed how nutrients, temperature, photosynthesis, and respiration were all related in the marine lakes of Palau. The lakes served as natural mesocosms, each with slightly different communities and physical and chemical properties. By experimentally adding nitrogen, a labile carbon source, and transplanting

bottles to manipulate light and temperature I was able to tease apart which environmental factors were the most important in determining CR. While nutrient rich lakes had higher GPP, this was not the case for CR. However, CR spiked when both nitrogen and labile organic matter were added, shifting the metabolic balance of the community from autotrophic to heterotrophic.

1.4 References

Bell, T., Newman, J. A., Silverman, B. W., Turner, S. L., & Lilley, A. K. (2005) The contribution of species richness and composition to bacterial services. *Nature* **436:** 1157-1160.

Beman, J. M., and Carolan, M. T. (2013). Deoxygenation alters bacterial diversity and community composition in the ocean's largest oxygen minimum zone. *Nat. Commun.* 4:2705. doi: 10.1038/ncomms3705

Bowman, J. S., Amaral-Zettler, L. A., Rich, J. J., Luria, C. M., & Ducklow, H. W. (2017) Bacterial community segmentation facilitates the prediction of ecosystem function along the coast of the western Antarctic Peninsula. *The ISME Journal:* 1-12.

Breitburg, D. L., Crump, B. C., Dabiri, J. O., & Gallegos, C. L. (2010) Ecosystem engineers in the pelagic realm: alteration of habitat by species ranging from microbes to jellyfish. *Integrative and Comparative Biology* **50:** 188-200.

Brown, J.H., Gillooly, J.F., Allen, A.P., Savage, A.V.M., & West, G.B. (2004) Toward a metabolic theory of ecology. *Ecology* **7:** 1771-1789.

Chapin, F. S., Bret-Harte, M. S., Hobbie, S. E., & Zhong, H. (1996) Plant functional types as predictors of transient responses of arctic vegetation to global change. *Journal of Vegetation Science* **7:** 347-358.

Díaz, S., & Cabido, M. (2001) Vive la différence: plant functional diversity matters to ecosystem processes. *Trends in Ecology & Evolution* **16:** 646-655.

Diaz, R. J. & Rosenberg, R. (2008) Spreading dead zones and consequences for marine ecosystems. *Science* **321**: 926-929.

Duarte, C. M., Regaudie-de-Gioux, A., Arrieta, J. M., Delgado-Huertas, A., & Agustí, S. (2013) The Oligotrophic Ocean Is Heterotrophic. *Annu Rev Marine Sci* **5:** 551-569.

Ducklow, H. W., & Doney, S. C. (2013) What Is the Metabolic State of the Oligotrophic Ocean? A Debate. *Annu Rev Marine Sci* **5:** 525-533.

Falkowski, P. G., Fenchel, T., & Delong, E. F. (2008) The microbial engines that drive Earth's biogeochemical cycles. *Science* **320:** 1034-1039.

Field, C. B., Behrenfeld, M. J., Randerson, J. T., & Falkowski, P. (1998) Primary Production of the Biosphere: Integrating Terrestrial and Oceanic Components. *Science* **281:** 237-240.

Fuhrman, J. A. (2009) Microbial community structure and its functional implications. *Nature* **459:** 193-199.

Giovannoni, S. J., & Vergin, K. L. (2012) Seasonality in ocean microbial communities. *Science* **335:** 671-676.

Graham, E. B. et al. (2016) Microbes as engines of ecosystem function: when does community structure enhance predictions of ecosystem processes? *Frontiers in Microbiology: Terrestrial Microbiology* **7:** doi.org/10.3389/fmicb.2016.00214.

Guidi, L., et al. (2016) Plankton networks driving carbon export in the oligotrophic ocean. *Nature* **532:** 465-470.

Horner-Devine, M. C. et al. (2003) Bacterial diversity patterns along a gradient of primary productivity. *Ecology* **6:** 613-622.

Kassen, R., Buckling, A., Bell, G., & Rainey, P. (2000) Diversity peaks at intermediate productivity in laboratory microcosm. *Nature* **406:** 508-512.

Kirchman, D. L., Moran, X. A., Ducklow, H. W. (2009) Microbial growth in the polar oceans-role of temperature and potential impact of climate change. *Nature Reviews Microbiology* **7:** 451-459.

López-Urrutia, Á., San Martin E, Harris R. P., Irigoien X. (2006) Scaling the metabolic balance of the oceans. *PNAS* **103:** 8739-8744.

McGrady-Steed, J., Harris, P. M., & Morin, P. J. (1997) Biodiversity regulates ecosystem predictability. *Nature* **390:** 162-165.

Naeem, S., & Li, S. (1997) Biodiversity enhances ecosystem reliability. *Nature* **390:** 507-509.

Pomeroy, L. R., & Deibel, D. (1986) Temperature regulation of bacterial activity during the Spring Bloom in Newfoundland coastal Waters. *Science* **233:** 359-361.

Regaudie-de-Gioux, A., Duarte, C. M. (2012) Temperature dependence of planktonic metabolism in the ocean. *Global Biogeochem Cycles* 26: n/a-n/a. 10.1029/2010GB003907.

Riebesell, U., Kortzinger, A., & Oschlies, A. (2009) Sensitivities of marine carbon fluxes to ocean change. *PNAS* **106:** 20602-20609.

Robinson, C., & Williams, P. l. B. (2005) Respiration and its measurement in surface marine waters. *Respiration in aquatic ecosystems* Oxford University Press, NY. p147-180.

Tilman, D., Reich, P. B., & Knops, J. M. H. (2006) Biodiversity and ecosystem stability in a decade-long grassland experiment. *Nature* **441:** 629-632.

Travisano, M., & Rainey, P. B. (2000) Studies of adaptive radiation using model microbial systems. *The American Naturalist* **156:** S35-S44.

Walker, B., Kinzig, A., & Langridge, J. (1999) Plant attribute diversity, resilience and ecosystem function: the nature and significance of dominant and minor species. *Ecosystems* **2:** 95-113.

Whitman, W., Coleman, D., & William, J. (1998) Prokaryotes: the unseen majority. *PNAS* **95:** 6578-6583.

Wohlers, J., et al. (2009) Changes in biogenic carbon flow in response to sea surface warming. *PNAS* **106:** 7067-7072.

Williams, P. J. l. B., Quay, P. D., Westberry, T. K., & Behrenfeld, M. J. (2013) The Oligotrophic Ocean Is Autotrophic. *Annu Rev Marine Sci* **5:** 535-549.

Wright, J. J., Konwar, K. M., & Hallam, S. J. (2012) Microbial ecology of expanding oxygen minimum zones. *Nature Reviews Microbiology* **10:** 381-394.

2 Ocean-scale patterns in community respiration rates along continuous transects across the Pacific Ocean

2.1 Abstract

Community respiration (CR) of organic material to carbon dioxide plays a fundamental role in ecosystems and ocean biogeochemical cycles, as it dictates the amount of production available to higher trophic levels and for export to the deep ocean. Yet how CR varies across large oceanographic gradients is not well-known: CR is measured infrequently and cannot be easily sensed from space. We used continuous oxygen measurements collected by autonomous gliders to quantify surface CR rates across the Pacific Ocean. CR rates were calculated from changes in apparent oxygen utilization and six different estimates of oxygen flux based on wind speed. CR showed substantial spatial variation: rates were lowest in ocean gyres (mean of 6.93 mmol m^{-3} d^{-1} ± 8.0 mmol m^{-3} d^{-1} standard deviation in the North Pacific Subtropical Gyre) and were more rapid and more variable near the equator (8.69 mmol m^{-3} d^{-1} ± 7.32 mmol m^{-3} d^{-1} between 10ºN and 10ºS) and near shore (e.g., 5.62 mmol m^{-3} d^{-1} ± 45.6 mmol m^{-3} d^{-1} between the coast of California and 124ºW, and 17.0 mmol m^{-3} d^{-1} ± 13.9 mmol m^{-3} d^{-1} between 156ºE and the Australian coast). We examined how CR varied with coincident measurements of temperature, turbidity, and chlorophyll concentrations (a proxy for phytoplankton biomass), and found that CR was weakly related to different explanatory variables across the Pacific, but more strongly related to particular variables in different biogeographical areas. Our results indicate that CR is not a simple linear function of chlorophyll or temperature, and that at the scale of the Pacific, the coupling between primary production, ocean warming, and CR is complex and variable. We suggest that this stems from substantial spatial variation in CR captured by high-resolution autonomous measurements.

2.2 Introduction

Microorganisms have profound effects on their surrounding environment, chemically modifying habitat and affecting other organisms through their biogeochemical activity (Breitburg et al., 2009; Breitburg et al., 2010; Wright et al., 2012). Some of the most fundamental metabolic functions—in terms of both cell function and environmental importance—involve the production and consumption of oxygen. Oxygenic photosynthesis and aerobic respiration are basic measures of ecosystem function because the production, respiration, cycling, and overall availability of carbon affects everything from the number of trophic levels, to the types of organisms present (Odum, 1956). Oxygenic photosynthesis dictates the amount of oxygen available for aerobic organisms (including both microbes and larger organisms), and photosynthesis in the ocean is almost exclusively microbial, accounting for approximately half of global oxygenic photosynthesis (Falkowski, 1994). The subsequent oxidation of organic carbon with oxygen yields tremendous amounts of free energy, making aerobic respiration a preferred method of obtaining energy, and an indication of the total amount of production and activity in an ecosystem.

In many open ocean systems, photosynthesis and aerobic respiration rates tend to be tightly coupled and close to balanced (Spitzer & Jenkins, 1989; Williams & Purdie, 1991; González et

al., 2002; Hamme & Emerson, 2006; Marañón et al., 2007; Luz & Barkan, 2009). However, the biological carbon pump depends in part on decoupling between photosynthesis and the respiration of organic carbon, leading to net export of carbon in areas where gross primary production (GPP) ultimately exceeds community respiration (CR). Importantly, GPP and CR are expected to differ in their sensitivity to ocean warming: metabolic theory predicts that both CR and GPP will increase as global temperatures rise (Brown et al., 2004), but that CR should increase more rapidly than GPP (Pomeroy & Deibel, 1986; López-Urrutia et al., 2006; Kirchman et al., 2009; Riebesell et al., 2009; Wohlers et al., 2009; Regaudie-de-Gioux & Duarte, 2012). This scenario leads to a positive feedback for climate change, as a larger fraction of primary production would be channeled through the microbial food web and respired to carbon dioxide (Pomeroy & Deibel, 1986; Riebesell et al., 2009; Wohlers et al., 2009). Because this has global implications for marine ecosystems and biogeochemical cycles, understanding how CR is affected by temperature and other environmental variables is critical for our understanding of oceanic carbon cycling.

Recent results indicate that CR does scale with temperature, but the majority of these measurements have been collected in the Mediterranean Sea, and Arctic, Atlantic, Indian, and Southern Oceans (Robinson & Williams, 2005; Regaudie-de-Gioux & Duarte, 2012). Most of the limited Pacific Ocean measurements are restricted to the vicinity of station ALOHA north of the Hawaiian Islands (Serret et al., 2002; Quay & Stutsman, 2003; Williams et al., 2004; Viviani et al., 2011; Williams et al., 2013). While these data are a powerful tool for understanding open ocean processes in the North Pacific Subtropical Gyre (NPSG), microbial community composition and nutrient and carbon sources differ significantly between different open-ocean and nearshore sites, such that relationships between GPP and CR are inconstant (Serret et al., 2002). The Pacific also covers a substantially greater area than the Atlantic, and CR in the Pacific Ocean consequently may have a greater influence on global carbon cycling. However, the general lack of information regarding variations in CR across the Pacific means that this is essentially unknown. Of particular interest is how CR varies with natural oceanographic features (like the California Current and Equatorial Upwelling) and proxies for production (such as chlorophyll *a*) compared with temperature-driven changes in CR; understanding and quantifying this variability will lead to a better understanding of the factors driving CR in different regions of the ocean (Kirchman et al., 2009), and how they may change. Finally, most of our understanding of large-scale patterns in CR is drawn from syntheses of existing datasets (e.g., Robinson & Williams, 2005)—systematic investigations of CR are extremely rare.

We used data continuously collected by autonomous Wave Gliders™ (Liquid Robotics, 2012) to assess how CR changes according to latitude, temperature, phytoplankton biomass (chlorophyll *a*), and turbidity across the Pacific Ocean. Quantifying how CR varies across Earth's largest ocean will further our understanding of how climate change may affect CR and ocean carbon cycling in the near future, and we focus on CR alone because of the general disagreement concerning the ideal method for also calculating GPP and net community production (NCP; see below). Our approach dramatically expands the number of CR measurements from the Pacific, and our findings indicate that CR rates are driven by different processes in different regions of the Pacific Ocean.

2.3 Materials and Methods

2.3.1 Autonomous sampling and data

The *Piccard Maru* and *Benjamin* Wave Gliders were deployed by Liquid Robotics (2012) on November 17th, 2011 off the coast of San Francisco, California as part of the Pacific Crossing or 'PacX.' *Benjamin* traveled to Hawaii and turned south, crossing the equator on August 3rd, 2012 and arriving in Brisbane, Australia on February 14th, 2013 (Figure 2-1). *Piccard Maru* also traveled to Hawaii and then continued west towards Japan. The glider did not complete the journey to Japan and contact was lost in the Western Pacific. These two datasets are the most spatially- and temporally-extensive of the datasets collected during PacX.

Conductivity, dissolved oxygen concentration (mL L^{-1}), oxygen solubility (mL L^{-1}), salinity (psu), water temperature (°C), air temperature (°C), average wind speed (knots), chlorophyll *a* (mg m^{-3}), and turbidity (NTU) were recorded by the wave gliders using a Glider Payload CTD, SBE 43F DO sensor, PB200 WeatherStation and C3 submersible fluorometer; data were obtained from the PacX data retrieval site (http://data.liquidr.com/fetch/). Oxygen, salinity, and water temperature were measured by the CTD at 10 seconds intervals, while chlorophyll and turbidity were measured every 2 minutes, and wind speed and air temperature were measured every 10 minutes. Underwater data were collected just below the sea surface (~0.2 m) while wind speed was measured 1 m above the sea surface. Only data from days when both CTD and weather data are available were used when calculating CR, such that the flux of oxygen from the atmosphere to the ocean or from the ocean to the atmosphere could be accounted for based on wind speed.

2.3.2 Respiration rate calculations

To quantify respiration rates, we adapted the approach of Needoba, Peterson, & Johnson (2012) and calculated (1) the nighttime drawdown of oxygen, as well as (2) the expected flux of oxygen into or out of the mixed layer. We directly followed the Needoba et al. (2012) approach for one set of calculations; in these calculations, 'biological demand of oxygen' (BDO) is calculated as the difference in oxygen concentrations between any two consecutive time points, and then all of these BDO values are summed over each dark period. We performed additional calculations where we modified this approach in two ways. First, in addition to summing changes in dissolved oxygen (DO) over time, we calculated nighttime drawdown of DO based on regressions between apparent oxygen utilization (AOU) and time (AOU slope approach). Second, we used more than one relationship with wind speed to calculate oxygen flux; this allowed us to account for a variety of physical processes that affect dissolved oxygen concentrations, including breaking waves and bubble entrainment (Wanninkhof et al., 2009; see below). We applied all of these wind speed relationships to both the BDO approach of Needoba et al. (2012) and to our AOU slope approach.

For the first part of these calculations, DO and oxygen solubility (OS) were used to compute AOU as the difference between OS and DO for ten minute averages of high frequency measurements. AOU measures the cumulative effects of biological activity that have occurred in a water sample and is negative when oxygen is supersaturated, and positive when oxygen is

undersaturated (due to consumption of DO). DO drawdown was calculated during nighttime (when incoming solar radiation was zero) based on regressions between AOU and time, which were tested for significance. Nighttime DO drawdown may differ significantly from daytime DO drawdown (Teira et al., 2010), meaning that nighttime CR rates may differ slightly from actual rates. This is an unavoidable limitation of using autonomously collected DO data to calculate CR.

We calculated gas exchange based on the air-sea concentration gradient and established parameterizations based on wind speed, where the diffusive flux (F) of oxygen equals the difference between the observed oxygen concentration of surface water and expected saturation oxygen concentration (which depends on temperature and salinity), multiplied by the gas transfer velocity (or coefficient of gas exchange; k_{O2}) for oxygen at a given temperature (eq. 1) (Liss & Slater, 1974; Wanninkhof, 1992; MacIntyre et al., 1995).

$$F = k_{O2}\left(\left[DO\right] - \left[OS\right]\right)\Delta time \qquad \text{(eq. 1)}$$

Oxygen is transferred from the water to the atmosphere when F (umol cm^{-2}) is positive, while oxygen is transferred from the atmosphere into the water when F is negative. Flux was calculated every ten minutes based on the measured wind speed, and was integrated over the dark period to obtain the total nighttime flux for each night. Nighttime integrated flux was subtracted from the entire nighttime AOU respiration estimate while each ten minute flux estimate was accounted for at each interval calculated following Needoba et al. (2012).

k_{O2} was obtained by first computing k_{660} (cm hr^{-1}) based on wind speed: this is the k value for CO_2 at 20°C and has been measured empirically for various wind speeds in the ocean. There are multiple mathematical equations relating wind speed to k_{660} and we used six relationships to ultimately calculate oxygen flux and CR; these equations vary in the formulation of k as function of wind speed, especially whether relationships are linear (Crusius & Wanninkhof 2003), quadratic (Wanninkhof, 1992; Nightingale et al., 2000), cubic (Wanninkhof & McGillis, 1999) or power functions Crusius & Wanninkhof, 2003). Needoba et al. (2012) recommend using CR1, while CR2 and CR3 explicitly consider the higher *k* values resulting from breaking waves and bubble entrainment (Wanninkhof & McGillis, 1999; Nightingale et al., 2000; Wanninkhof et al., 2009). CR4-CR6 were specifically designed to capture lower wind speeds. We include all six approaches given the wide variation in environmental conditions across the Pacific and to provide broader context. All of the equations were originally derived using chemical tracers such as sulfur hexafluoride.

CR1) $$k_{660} = 0.31\left(U_{10}\right)^2$$ (eq. 2) (Wanninkhof, 1992)

CR2) $$k_{660} = 0.0283\left(U_{10}\right)^3$$ (eq. 3) (Wanninkhof & McGillis, 1999)

CR3) $$k_{660} = 0.222\left(U_{10}\right)^2 + 0.333\left(U_{10}\right)$$ (eq. 4) (Nightingale et al., 2000)

CR4) $k_{660} = 0.72(U_{10})$ *for* $U_{10} < 3.7\ m\ s^{-1}$ (eq. 5) (Crusius & Wanninkhof, 2003)

$k_{660} = 4.33(U_{10})$ *for* $U_{10} \geq 3.7$

CR5) $k_{660} = 0.228(U_{10})^{2.2} + 0.168\ cm\ hr^{-1}$ (eq. 6) (Crusius & Wanninkhof, 2003)

CR6) $k_{660} = 1.0\ cm\ hr^{-1}$ *for* $U_{10} < 3.7\ m\ s^{-1}$ (eq. 7) (Crusius & Wanninkhof, 2003)

$k_{660} = 5.41(U_{10}) - 17.9\ cm\ hr^{-1}$ *for* $U_{10} \geq 3.7\ m\ s^{-1}$

In all of these equations, wind speed (U_{10}) is measured in m s^{-1} at 10 m above the water's surface whereas our data were collected at 1 m; wind speeds were therefore scaled to 10 m (eq. 8) (Donelan, 1990):

$$U_{10} = U_z\left[1+\left[\left(C_{d10}{}^{0.5}\right)/K\right]ln(10/z)\right] \quad \text{(eq. 8)}$$

Where C_{d10}—the surface drag coefficient for wind above water at 10 m—is 1.3 x 10^{-3} (Stauffer, 1980), K refers to the von Karman constant of 0.41 (Engle & Melack, 2000), and z is the height above the sea surface where wind speed was measured. The Crusius & Wanninkhof (2003) relationships were specifically developed for low wind speeds that may periodically occur over the ocean. In our data, wind speed was greater than 3.7 m s^{-1} 96.5% of the time.

Schmidt numbers (Sc) were used to covert from the modeled k_{660} value in equations 2-6 to a k_{O2} at each recorded surface temperature. A Schmidt number is a dimensionless number that characterizes fluid flow, is unique for each dissolved gas, and is defined as the kinematic viscosity of water divided by the diffusion coefficient of the gas at a given temperature. The Schmidt number for O_2 in saltwater can be calculated with the following equation, in which T is temperature in Celsius (eq. 9) (Wanninkhof, 1992):

$$Sc_{O2} = 1953.4 - 128T + 3.9918T^2 - 0.050091T^3 \quad \text{(eq. 9)}$$

The ratio of k values (for each CO_2 and O_2) equals the ratio of Schmidt numbers raised to negative n (eq. 10) (Homén & Liss, 1984):

$$k_{gas1}/k_{gas2} = \left(Sc_{gas1}/Sc_{gas2}\right)^{-n} \quad \text{(eq. 10)}$$

n depends on the processes that dominate gas transfer including the friction velocity and the mean square slope of the waves (Jahne et al. 1987). Based on the laboratory experiments of Jahne et al. (1987;1989), we set n to 2/3 when $U_{10} < 2$ m s^{-1} and n at 1/2 when $U_{10} \geq 2$ m s^{-1}.

Computed oxygen fluxes were then divided by the mixed layer depth, and subtracted from the nighttime slopes of AOU versus time to obtain respiration rates. (Note that fluxes are defined relative to the atmosphere, and a negative flux represents transfer of oxygen into the ocean from

the atmosphere.) Positive CR values indicate a higher rate of respiration while a 'negative' CR value indicates that DO increased during nighttime hours. Negative CR can be explained by daytime primary production exceeding and masking the amount of nighttime CR that occurred, with isopycnal mixing also potentially playing a role, as these measurements were only made at the surface, whereas photosynthesis and respiration likely varied with depth throughout the mixed layer.

2.3.3 Data analysis

Two outliers (3-9-2012, and 12-31-2012) were removed from the California to Australia dataset due to extremely high calculated respiration values (> 2 standard deviations from the mean). One outlier was removed from the California to Japan dataset (3-6-2012) due to extremely high chl *a* and turbidity values (> 2 standard deviations from the means).

Relationships between respiration, latitude, temperature, chl *a*, and turbidity were explored using multiple regression analysis in R. Regression analysis was completed for all data, for each individual glider, and for latitudinal and longitudinal zones for the California to Australia dataset. These zones follow Longhurst's biogeographical zones (Longhurst 1995; 2010) and ranged from 20°N to 38°N (California Current province), 10°N to 20°N (North Pacific [Sub]Tropical Gyre province), 0°N to 10°N (North Pacific Equatorial Countercurrent province), 15°S to 0°S (Pacific Equatorial Divergence province), and 23°S to 15°S (South Pacific Subtropical Gyre province). The natural log was taken of chlorophyll and turbidity in order to correct slight non-linearity. Due to several slightly 'negative' values (see Discussion for an explanation), turbidity was offset by 1.38 so that the minimum value was 1 before transformation.

2.4 Results

2.4.1 Pacific-scale patterns in CR

Data from autonomous gliders provide ocean-scale patterns in temperature, chlorophyll, turbidity, and respiration; all showed substantial variation across the Pacific Ocean. For the California to Australia transect, water temperature increased as latitude decreased, and was warmest just south of the equator (29.3°C) (Figures 2-1, 2-2A and 2-2B). Water temperatures increased from the eastern to western Pacific along the transect from California to Japan. Chlorophyll concentrations were greatest off coastal California (above 30°N latitude) and were generally low in the open Pacific, with the exception of the elevated levels observed near the equator (Figures 2-2E and 2-2F). Chlorophyll also increased near 18-19°N in the West Pacific, and turbidity was extremely variable throughout the Pacific (Figure 2-2). Several of these variables were correlated with one another across the Pacific, along the different transects, or within different biogeographical zones (Table 2-1).

In total, we generated 341 independent measurements of CR from California to Australia and 264 independent measurements from California to Japan. All of our computational approaches demonstrated that respiration rates were variable across the Pacific. The different windspeed-based approaches used to calculate CR showed strong agreement, with r^2 values ranging from

0.810-0.999 (all $P<0.001$) between different CR datasets within a given method for calculating respiration (AOU change over time, or summed changes in DO based on Needoba et al. (2012) (Tables 2-2 and 2-3). Independent of the wind speed-based flux estimates, the AOU and BDO approaches for estimating oxygen consumption were significantly correlated ($P<0.001$) for each transect, but the California to Japan dataset had an r^2 value of 0.701 while the California to Australia dataset had an r^2 value of 0.3. The BDO approach typically generated more instances of negative CR rates (Figure 2-3)—most likely due to summing many small changes in DO—and so our analysis is focused on the AOU slope approach. These six CR datasets varied slightly in terms of maximum, minimum, mean, and median values (Figures 2-4 and 2-5) but were generally comparable: for example, CR1 rates ranged from -88.9 to 75.4 mmol m^{-3} d^{-1}, CR2 ranged from -88.6 to 77.2 mmol m^{-3} $d^{-1,}$ CR3 ranged from -89.0 to 75.0 mmol m^{-3} d^{-1}, CR4 ranged from -89.2 to 74.7 mmol m^{-3} d^{-1}, CR5 ranged from -88.8 to 76.0 mmol m^{-3} d^{-1}, and CR6 rates ranged from -89.1 to 74.9 mmol m^{-3} d^{-1} for the California to Australia dataset. We focus on CR2 because it considers breaking waves and bubble entrainment, the method used to obtain this relationship utilizes long-standing protocols, and it performs better statistically (see below). CR2 ranged from -120 to 84.4 mmol m^{-3} d^{-1} from California to Japan using our AOU slope approach (for CR2; Figure 2-4), while using Needoba et al.'s BDO approach, CR2 ranged from -58.9 to 61.9 mmol m^{-3} d^{-1} for the California to Australia dataset, and from -84.8 to 93.9 mmol m^{-3} d^{-1} for the California to Japan dataset.

The gliders traveled nearly identical paths from California to the Hawaiian Islands over slightly different time periods, yet they showed highly similar patterns in CR: both were variable and reached maximum and minimum values near the California Coast, and each was more consistent beyond 128ºW. Several local maxima were recorded at various points within the northeastern portion of the North Pacific Gyre, particularly near 150ºW. This included high CR rates measured at 148.7ºW on 2012-02-09 and 156.2ºW on 2012-03-13 for the California to Australia transect, and at 151ºW on 2012-02-19 and 153.1ºW 2012-03-09 for the California to Japan transect (for CR2). These local maxima were slightly greater for the California to Japan transect (39.7 mmol m^{-3} d^{-1} and 37.2 mmol m^{-3} d^{-1}) than the California to Australia transect (35.3 mmol m^{-3} d^{-1} and 17.9 mmol m^{-3} d^{-1}).

The east-to-west, California to Japan transect then crossed a large swath of the oligotrophic North Pacific Subtropical Gyre (NPSG), whereas the northeast-to-southwest, California to Australia transect crossed multiple ocean provinces (Figures 2-4 and 2-5). We expected that the east-west transect would therefore show relatively low rates and little variation, but this was not the case: CR2 averaged 8.38 mmol m^{-3} d^{-1} with a standard deviation of 8.44 mmol m^{-3} d^{-1}. Many of the high CR rates were observed within the NPSG—particularly in the central Pacific to the west of Hawaii—as well as closer to mainland Asia. The overall range of CR values was similar for the California to Australia transect, and also showed substantial spatial variability. CR above 20ºN latitude was variable between days, latitude, and longitude with no obvious increasing or decreasing trends, but became less variable after 128ºW longitude and remained below 10 mmol m^{-3} d^{-1} on all but 6 occasions after leaving the California Coast. CR rates were generally low from Hawaii to the equator, but a small peak in CR occurred near 10ºN latitude. CR rates exhibited several obvious peaks below the equator and were consistently elevated from the equator to 10ºS. CR2 averaged 6.49 mmol m^{-3} d^{-1} with a standard deviation of 11.0 mmol m^{-3} d^{-1} for the entire transect, but reached 26.2 mmol m^{-3} d^{-1} at 6.36ºS latitude; CR was generally

elevated within several degrees of latitude of this peak. CR again increased around 18-19ºS, and the greatest values south of the equator were observed near the coast of Australia (46.5 mmol m^{-3} d^{-1} at 22.5ºS latitude).

2.4.2 Relationships to environmental data

We used several statistical approaches to analyze relationships between possible explanatory variables and CR. No approach to calculating CR was uniformly most significantly related to environmental data, however CR2 generally outperformed the other approaches for both datasets, and for both univariate and multiple linear regression by producing more significant relationships and stronger significant relationships. Most of our analysis therefore focuses on CR2, however all of the CR datasets were correlated and yielded similar results despite differences in their underlying assumptions. For these analyses, we examined both transects together as well as separately, and also analyzed the California to Australia dataset based on multiple latitudinal zones. This stems from the large expected and observed differences in oceanographic conditions across these regions, as well as the fact that datasets from different latitudes exhibit different relationships between temperature and CR (e.g., Kirchman et al., 2009).

Across the long oceanographic transects, CR2 varied significantly with turbidity from California to Australia (r^2=0.085 and P<0.001), and increasing the number of possible explanatory variables in stepwise multiple linear regression did not increase the predictive strength of the model. For the California to Japan data, CR again varied most strongly with turbidity (r^2=0.112, P<0.001); the most descriptive multiple regression model included chlorophyll and turbidity as explanatory variables (r^2=0.167 and P<0.001) using CR2. When California to Australia data were assessed according to latitudinal zones, different explanatory variables were important in different areas. From north to south, no significant relationships were observed from 20°N to 38°N, 10°N to 20°N, and 0°N to 10°N, whereas chlorophyll was most significantly related to CR from 15°S to 0°S (r^2=0.166, P<0.001 using CR2), and turbidity was the best predictor from 23°S to 15°S (r^2=0.325, P<0.001 using CR2). Multiple linear regression did not yield any significant relationships north of the equator, and only increased the explanatory power of the model from 23°S to 15°S slightly, such that water temperature and turbidity explained 37.3% of the variation in CR (P<0.001).

Chlorophyll and turbidity were also log-transformed to fix slight non-linearity but produced highly similar results (Figure 2-6): CR2 had the most significant models; no significant relationships occurred north of the equator; chlorophyll was the best predictor from 15°S to 0°S (r^2 = 0.165, P<0.001); and water temperature and turbidity were collectively the best predictors from 15°S to 23°S (r^2 = 0.347, P<0.001). Allowing second or third order interactions to the log-transformed variable models for CR2 increased the explanatory power of all the models except from 20°N to 38°N (Figure 2-6). For example, there were no significant relationships between CR and any of the variables between 10°N to 20°N, but adding an interaction between chlorophyll and turbidity resulted in a significant relationship (r^2 = 0.391, P<0.001). Adding a third order interaction between water temperature, chlorophyll, and turbidity strengthened this relationship (r^2 = 0.518, P<0.001).

All data were ultimately pooled together to analyze cross-Pacific patterns in respiration as a function of chlorophyll, turbidity, and temperature. Across the dataset, the strongest relationship was between the natural log of turbidity and CR2 ($r^2 = 0.036$, $P<0.001$). Using multiple explanatory variables only incrementally increased the amount of variation explained, with the natural logs of chlorophyll and turbidity producing the best model ($r^2 = 0.043$, $P<0.01$ for CR2). Allowing interactions between explanatory variables likewise incrementally increased the explanatory power of the models (e.g., $r^2 = 0.077$, $P<0.001$ for CR2 allowing interactions between temperature, chlorophyll, and turbidity). A third order interaction term between water temperature, the natural log of chlorophyll, and the natural log of turbidity only explained 8.54% of the data ($P<0.001$ for CR2). We also used multivariate adaptive regression splines (MARS) (Friedman, 1991) to model CR; this approach includes interactions among variables, and identifies regions of the dataset where different basis functions may be applied. The MARS model explained 7.5% of the variation in CR across the Pacific ($P<0.001$) as a function of temperature, chlorophyll, and turbidity.

For these pooled data, we found stronger relationships within the NPSG than across the entire Pacific. The NPSG is Earth's largest ecosystem (Sverdrup et al., 1946; Karl, 1999) and different regions of the NPSG were covered extensively by the two gliders. The natural log of turbidity was the most significant explanatory variable for 4 of the 6 methods of calculating CR ($r^2 = 0.110$, $P<0.001$ for CR2), with water temperature being more strongly correlated with CR4 ($r^2 = 0.041$, $P<0.002$) and CR6 ($r^2 = 0.033$, $P<0.005$), from 10°N to 20°N in the NPSG. Including both of these variables in multiple regression ($r^2 = 0.202$, $P<0.001$ for CR2) and their interactions ($r^2 = 0.245$, $P<0.001$ for CR2) produced stronger relationships.

2.5 Discussion

The CR rate data presented here are unique in both spatial coverage and the frequency with which measurements were taken, as no previous study has calculated CR continuously across an entire ocean basin. While CR has been measured across a few latitudinal and longitudinal transects, these consist largely of discrete measurements made at a limited number of locations (Serret et al., 2002; Viviani et al., 2011; Williams et al., 2013). Our data also provide a large number of measurements from the undersampled Pacific Ocean: in the most recent compilation of CR measurements, Regaudie-de-Gioux and Duarte (2013) report 3854 measurements, with only 296 made in the Pacific Ocean (some of which are unpublished). We report 341 measurements from north to south, and 264 measurements from east to west, across the Pacific, more than tripling the total number of CR measurements made in Earth's largest ocean. Our data and findings are in broad agreement with the limited information available from the Pacific and other large-scale studies, display several interesting spatial patterns, and provide new insight into the environmental drivers of CR.

Most measurements of CR in the Pacific Ocean have been conducted at Station ALOHA (A Long Term Oligotrophic Habitat Assessment) of the Hawaii Ocean Time-series (HOT) program, and both gliders were in the vicinity of Station ALOHA for several days—approaching from the east and passing to the south (Figure 2-1). This allows for comparison of CR between the glider dataset and the extensive HOT dataset. In a year-long study at ALOHA from 2001-2002, Williams et al. (2004) found that surface CR at station ALOHA ranged from 0.63 to 1.15 mmol

O_2 m^{-3} d^{-1}; unpublished CMORE data from more recent HOT cruises show that surface respiration varies from 0.18 to 2.8 mmol O_2 m^{-3} d^{-1} (Regaudie-de-Gioux & Duarte, 2013), [http://cmore.soest.hawaii.edu/cmoredata/Church/GPP_NCP_R_results_summary.xls]. These data illustrate the fact that even stratified, oligotrophic, open ocean sites exhibit order-of-magnitude variations in CR over time (Williams et al., 2004). For the gliders, mean CR values ranged from 2.38-4.64 mmol m^{-3} d^{-1} near station ALOHA. These values overlap the upper end of CR rates from dark bottle incubations conducted at station ALOHA.

Glider-based CR data are also consistent with other datasets collected in the equatorial Pacific. Viviani et al. (2011) measured CR, GPP, and NCP along a transect from 14.3°S, 169.2°W to Station ALOHA that lies to the west of our CA-Australia transect; they observed increased CR near the equator, with a maximum around 10°S. In our data, CR varied widely near the equator and in association with high chlorophyll and turbidity that are likely indicative of a phytoplankton bloom; CR appears to have responded by increasing between the equator and 10ºS latitude. NCP and GPP also varied substantially over relatively short distances (~50 km) along the equator in the Western Equatorial Pacific (Stanley et al., 2010). While Stanley et al.'s data were primarily collected along an east-west transect, and they did not report volumetric CR rates, they followed 170°W for ±2 degrees north and south of the equator. NCP decreased from north to south along 170°W, which could reflect decreased GPP, increased CR, or both. In our data, the glider *Benjamin* detected an increase in CR from north to south also while tracking 170°W, which is consistent with but not directly comparable to Stanley et al. (2010).

As a whole, our datasets substantially increase the number of CR measurements available for the Pacific, and our approach may be useful in constraining the metabolic balance of the oligotrophic ocean (Duarte et al., 1999; Williams & Bowers, 1999; del Giorgio & Duarte, 2002; Karl et al., 2003; Duarte et al., 2013; Williams et al., 2013). *In situ* studies of oxygen production and consumption tend to indicate that the open ocean is net autotrophic while *in vitro* studies indicate net heterotrophy (see Williams et al., 2013). Setting aside issues regarding the depth of integration, the discrepancies most likely have to do with an underestimation/overestimation of photosynthesis rather than mistakes calculating respiration (Westberry et al., 2012; Williams et al., 2013). This view is supported by comparisons of in vitro and *in situ* data from HOT, which found general agreement between respiratory rates for the two approaches (Williams et al., 2004; Quay et al., 2010; Westberry et al., 2012). While most of the global CR database is comprised of light-dark bottle measurements (Robinson & Williams, 2005; Regaudie-de-Gioux & Duarte, 2013), our data represent a large collection of *in situ* measurements that provide a useful point of comparison. Clearly some uncertainty lies in gas exchange, which leads to variations in absolute magnitudes among our CR datasets—however the variation in gas exchange as a function of windspeed (typical r^2 values of 0.8±0.1) is a long-running issue without clear resolution (reviewed by Wanninkhof et al., 2009). Regardless of the approach we used to calculate CR, the majority of the data fell within observations reported elsewhere in the ocean (Robinson & Williams, 2005), with >90% falling within the range of surface CR rates reported in Regaudie-de-Gioux and Duarte's 2013 dataset. The remaining values are almost entirely 'negative' CR rates. Our approach could therefore be adapted to daytime increases in oxygen and used to calculate patterns in surface NCP across the Pacific.

Based on these data we observed several large-scale patterns in CR across the Pacific Ocean, including high CR rates near the equator and the coast of Australia, and surprising variation in CR within the NPSG. While rates were low throughout much of the NPSG, high CR rates may occur at least transiently in portions of the NPSG west of Hawaii. CR was also highly variable in the South Pacific, exhibiting a wide range of values and sharp changes within zones. These data represent the first extensive series of measurements made in the highly undersampled South Pacific Subtropical Gyre (Robinson & Williams, 2005; Longhurst, 2010; Regaudie-de-Gioux & Duarte, 2013) and indicate that large gradients in CR may occur in this ocean. For the most part, these variations were not explained by coincident turbidity, temperature, and chlorophyll measurements made by the gliders. Previous work in the Atlantic Ocean has shown significant relationships with beam attenuation (Robinson et al., 2002), which is consistent with the presence of particles and aggregates in the water column that may be subsequently remineralized and respired. Turbidity was frequently related with CR, including significant relationships across the whole dataset and for each transect. However, there are two main issues with the turbidity data collected by the PacX gliders. First, there were many low, but negative, turbidity values that likely reflect sensor drift over the extended deployment at sea (Figure 2-2C). Second, microbubbles can potentially interfere with the turbidity sensor: as outlined by Villareal and Wilson (2014), this likely explains the highly elevated turbidity values observed south of 18°S, as the glider *Benjamin* traversed Tropical Storm Freda and may have had bubbles entrained in the sensor. While the significant relationships observed in other biogeographic regions and for the other glider correspond with much lower turbidity values, we cannot exclude the possibility that these stem from artifacts present in the data.

Temperature was generally weakly correlated with CR—if at all—and was only a significant predictor in multiple linear regression. The slopes of these relationships were variable, ranging from negative to positive. This contrasts with some previous work (Robinson & Williams, 2005; Regaudie-de-Gioux & Duarte, 2012), but supports the idea that temperature has mixed effects on CR in different regions of the ocean, and specifically the idea that temperature effects are weak outside of high latitude regions (Kirchman et al., 2009). Kirchman et al. (2009) convincingly argue that temperature is not a strong regulating factor in other parts of the ocean because the availability of organic C substrates and nutrients is more important. This likely applies to much of our dataset, as outside of the region that extends from California to 20°N, temperatures fell between a relatively narrow range of 23-30°C (representing >84% of the temperature data). No significant relationship between CR and temperature was observed from 20°-38°N—despite a wider range of temperatures—but no significant relationships were observed between CR and any of the *in situ* measurements in this region. This is due to the localized hotpots in CR observed near 150°W and 25°N, which are not associated with distinct changes in turbidity, temperature, or chlorophyll.

Compilations of CR datasets have also shown that CR can be positively correlated with chlorophyll concentrations (Robinson & Williams, 2005; Regaudie-de-Gioux & Duarte, 2012&2013). Production ultimately sets the pace for CR rates, and it seems likely that coupling between CR and either the biomass (chlorophyll) or photosynthetic activity (GPP) of phytoplankton would co-vary across the ocean and through time. For example, several studies have found that chlorophyll consistently explains ca. 30% of the variance in CR—whether in estuaries, throughout the Atlantic Ocean, or across oceans (Robinson & Williams, 2005;

Robinson et al., 2002; Pérez et al., 2005; Hopkinson & Smith, 2005). However, Regaudie-de-Gioux and Duarte (2013) found that both net community metabolism and CR were each only weakly correlated with chlorophyll while 30% of the variability in GPP was explained by chlorophyll. Robinson and Williams (2005) showed that, overall, CR is not strongly correlated with chlorophyll concentrations, while stronger relationships are observed in regions of the ocean with sharp chlorophyll and CR gradients. Our data from the region south of the equator in the Pacific are consistent with this: high CR rates observed south of the equator correspond with high chlorophyll concentrations (Figure 2-2E). These latter data capture a phytoplankton bloom associated with equatorial upwelling, and CR was significantly related to chlorophyll in the latitudinal band just south of the equator for all CR datasets (Figure 2-6). An increase in CR near the equator appears to be a general feature in the Atlantic Ocean (Robinson et al., 2002; Serret et al., 2002; Pérez et al., 2005) that was also observed by Viviani et al. (2011) in Pacific Ocean, and our data extend these observations. These variations in CR are likely driven by upwelling in the equatorial oceans—either by directly affecting CR through nutrient supply, or by fueling GPP and increasing the supply of organic C to CR.

We also observed high CR rates where chlorophyll showed little change—especially high CR rates in the oligotrophic NPSG west of Hawaii—and low CR rates where chlorophyll was elevated near the International Date Line. Chlorophyll and CR were in fact inversely related along the California to Japan transect. This reflects decoupling between phytoplankton biomass and CR and is in line with the intensive measurements made by Williams et al. (2004) at Station ALOHA: they argue that primary production occurs in intermittent bursts—which they may not have detected even with comprehensive sampling—whereas CR is less variable, and more integrative, over time. Our cross-Pacific data suggest that another distinguishing feature of different oceanic provinces may be differences in the coupling between primary production and CR, with strong coupling in productive provinces, and decoupling in less productive regions. Sampling discrete stations may obscure this pattern, because our data demonstrate that isolated hot spots or moments of CR occur in oligotrophic regions. This finding has implications for understanding carbon and metabolic balance in the sea, as it reinforces the importance of integrating CR over time and depth, but also lateral space.

The net effects of ocean warming and other forms of global change on CR will ultimately depend on a complex series of responses among communities of phytoplankton and heterotrophic microbes in different ocean provinces. For the first time, we provide basin-scale measurements of CR conducted at high spatial and temporal resolution. Like previous CR datasets, our data capture patterns over limited periods of time, and temporal variation may be intertwined with spatial differences. Unlike primary production, CR has not been measured regularly or systematically and cannot be easily sensed from space. Instead, use of spatially-distributed, high-quality, *in situ* biogeochemical measurements made at high frequency by autonomous gliders, floats, and moorings seems a promising approach for regular measurements of CR across the ocean. Our work provides CR data that are consistent in magnitude and pattern with previous data, demonstrating the feasibility of using autonomous platforms to measure CR over large scales. Such data allow us to identify broad biogeographic and biogeochemical patterns that are otherwise undetectable by isolated measurements. This reveals a more nuanced view of the environmental controls on CR, highlighting weak temperature effects in warm waters of the Pacific, and the coupling and decoupling between phytoplankton biomass and CR in different

regions. Of particular relevance are hot spots and moments of CR, which may affect carbon flux estimates and represent interesting oceanographic and ecological phenomena. The novel dataset and approach provides hundreds of new measurements from the under-sampled Pacific, yielding new insight into variation in CR across the world's largest ocean.

2.6 References

Breitburg, D. L., Hondorp, D. W., Davias, L. A., & Diaz, R. J. (2009) Hypoxia, nitrogen, and fisheries: Integrating effects across local and global landscapes. *Marine Science* **1:** 349.

Breitburg, D. L., Crump, B. C., Dabiri, J. O., & Gallegos, C. L. (2010) Ecosystem engineers in the pelagic realm: Alteration of habitat by species ranging from microbes to jellyfish. *Integrative and Comparative Biology* **50:** 188-200.

Brown, J. H., Gillooly, J. F., Allen, A. P., Savage, V. M., & West, G. B. (2004) Toward a metabolic theory of ecology. *Ecology* **85:** 1771-1789.

Crusius, J., & Wanninkhof, R. (2003) Gas transfer velocities measured at low wind speed over a lake. *Limnol Oceanogr*: 1010-1017.

del Giorgio, P. A., & Duarte, C. M. (2002) Respiration in the open ocean. *Nature* **420:** 379-384.

Donelan M. (1990) Air-sea interaction. *The sea* **9:** 239-292.

Duarte, C. M., Agustí, S., del Giorgio, P. A., & Cole, J. J. (1999) Regional carbon imbalances in the oceans. *Science* **284:** 1735.

Duarte, C. M., Regaudie-de-Gioux, A., Arrieta, J. M., Delgado-Huertas, A., & Agustí, S. (2013) The oligotrophic ocean is heterotrophic. *Annu Rev Marine Sci* **5:** 551-569. 10.1146/annurev-marine-121211-172337. http://dx.doi.org/10.1146/annurev-marine-121211-172337

Engle, D., & Melack, J. M. (2000) Methane emissions from an amazon floodplain lake: Enhanced release during episodic mixing and during falling water. *Biogeochemistry* **51:** 71-90.

Falkowski, P. G. (1994) The role of phytoplankton photosynthesis in global biogeochemical cycles. *Photosynthesis Research* **39:** 235-258.

Friedman, J. H. (1991) Multivariate adaptive regression splines. *The annals of statistics*, 1-67.

González, N., Anadón, R., & Marañón, E. (2002) Large-scale variability of planktonic net community metabolism in the atlantic ocean: Importance of temporal changes in oligotrophic subtropical waters. *Mar Ecol Prog Ser* **233:** 21-30.

Hamme, R. C., & Emerson, S. R. (2006) Constraining bubble dynamics and mixing with dissolved gases: Implications for productivity measurements by oxygen mass balance. *J Mar Res* **64:** 73-95.

Holmén, K., & Liss, P. (1984) Models for air–water gas transfer: An experimental investigation. *Tellus B* **36:** 92-100.

Hopkinson Jr., C. S., & Smith, E. M. (2005) Estuarine respiration:An overview of benthic pelagic, and whole system respiration. *Respiration in aquatic ecosystems*, Oxford University Press: 122-146.

Jähne, B., Münnich, K. O., Dutzi, R. B. A., Huber, W., & Libner, P. (1987) On the parameters influencing air-water gas exchange. *Journal of Geophysical research* **92:** 1937-1949.

Jähne, B., Libner, P., Fischer, R., Billen, T., & Plate, E. (1989) Investigating the transfer processes across the free aqueous viscous boundary layer by the controlled flux method. *Tellus B* **41:** 177-195.

Karl, D. M. (1999) A sea of change: Biogeochemical variability in the North Pacific Subtropical gyre. *Ecosystems* **2:** 181-214.

Karl, D. M., Laws, E. A., Morris, P., Williams, P., & Emerson, S. (2003) Metabolic balance of the open sea. *Nature* **426:** 32.

Kirchman, D. L., Moran, X. A., & Ducklow, H. W. (2009) Microbial growth in the polar oceans-role of temperature and potential impact of climate change. *Nature Reviews Microbiology* **7:** 451-459.

Liquid Robotics I. (2012). PacX. http://liquidr.com/. Accessed 1 February 2013.

Liss, P. S., & Slater, P. G. (1974) Flux of gases across the air-sea interface. *Nature* **247:** 181-184.

Longhurst, A. (1995) Seasonal cycles of pelagic production and consumption. *Prog. Oceanogr.* **36:** 77-167.

Longhurst, A. (2010) *Ecological Geography of the Sea*. Academic Press.

López-Urrutia, Á., San Martin, E., Harris, R. P., & Irigoien, X. (2006) Scaling the metabolic balance of the oceans. *PNAS* **103:** 8739-8744.

Luz, B., & Barkan, E. (2009) Net and gross oxygen production from O 2/Ar, 17 O/16 O and 18 O/16 O ratios. *Aquat Microb Ecol* **56:** 133-145.

MacIntyre, S., Wanninkhof, R., & Chanton, J. (1995) Trace gas exchange across the air-water interface in freshwater and coastal marine environments. Biogenic trace gases: Measuring emissions from soil and water. *Methods in Ecology*. Blackwell: 52-97.

Marañón, E., et al. (2007) Planktonic carbon budget in the eastern subtropical north Atlantic. *Aquat Microb Ecol* **48:** 261-275.

Needoba, J. A., Peterson, T. D., & Johnson, K. S. (2012) Method for the quantification of aquatic primary production and net ecosystem metabolism using in situ dissolved oxygen sensors. In: *Anonymous Molecular Biological Technologies for Ocean Sensing*. Springer. pp. 73-101.

Nightingale, P. D., et al. (2000) In situ evaluation of air-sea gas exchange parameterizations using novel conservative and volatile tracers. *Global Biogeochem Cycles* **14:** 373-387.

Odum, H. T. (1956) Primary production in flowing waters. *Limnology and Oceanography* **1:** 103-117.

Pérez, V., et al. (2005) Latitudinal distribution of microbial plankton abundance, production, and respiration in the equatorial atlantic in autumn 2000. *Deep Sea Research Part I: Oceanographic Research Papers* **52:** 861-880.

Pomeroy, L. R., & Deibel, D. (1986) Temperature regulation of bacterial activity during the spring bloom in newfoundland coastal waters. *Science* **233:** 359-361.

Quay, P. D., Peacock, C., Björkman, K., & Karl, D. M. (2010) Measuring primary production rates in the ocean: Enigmatic results between incubation and non-incubation methods at station ALOHA. *Global Biogeochem Cycles* **24:** 10.1029/2009GB003665.

Quay, P., & Stutsman, J. (2003) Surface layer carbon budget for the subtropical N. Pacific: Δ13C constraints at station ALOHA. *Deep Sea Research Part I: Oceanographic Research Papers* **50:** 1045-1061. 10.1016/S0967-0637(03)00116-X.

Regaudie-de-Gioux, A., & Duarte, C. M. (2012) Temperature dependence of planktonic metabolism in the ocean. *Global Biogeochem Cycles* **26:** 10.1029/2010GB003907.

Regaudie-de-Gioux, A., & Duarte, C. M. (2013) Global patterns in oceanic planktonic metabolism. *Limnol Oceanogr* **58:** 977-986.

Riebesell, U., Körtzinger, A., & Oschlies, A. (2009) Sensitivities of marine carbon fluxes to ocean change. *PNAS* **106:** 20602-20609.

Robinson, C., et al. (2002) Plankton respiration in the eastern Atlantic Ocean. *Deep Sea Research Part I: Oceanographic Research Papers* **49:** 787-813.

Robinson, C., & Williams, P. l. B. (2005) Respiration and its measurement in surface marine waters. *Respiration in aquatic ecosystems* Oxford University Press, NY. p147-180.

Schlitzer, R. (2013) Ocean Data View. http://odv.awi.de.

Serret, P., Fernández, E., & Robinson, C. (2002) Biogeographic differences in the net ecosystem metabolism of the open ocean. *Ecology* **83:** 3225-3234.

Spitzer, W. S., & Jenkins, W. J. (1989) Rates of vertical mixing, gas exchange and new production: Estimates from seasonal gas cycles in the upper ocean near Bermuda. *J Mar Res* **47:** 169-196.

Stanley, R. H., Kirkpatrick, J. B., Cassar, N., Barnett, B. A., & Bender, M. L. (2010) Net community production and gross primary production rates in the western equatorial Pacific. *Global Biogeochem Cycles* **24:** GB4001.

Stauffer, R. E. (1980) Windpower time series above a temperate lake. *Limnol Oceanogr*: 513-528.

Sverdrup, H. U., Johnson, M. W., & Fleming, R. H. (1946) *The oceans, their physics, chemistry and general biology*. New York: Prentice-Hall.

Teira, E., Martínez-García, S., Fernández, E., Calvo-Díaz, A., & Morán, X. A. G. (2010) Lagrangian study of microbial plankton respiration in the subtropical North Atlantic Ocean: bacterial contribution and short-term temporal variability. *Aquat Microb Ecol* **61:** 31−43.

Villareal, T. A., & Wilson, C. (2014) A comparison of the Pac-X trans-pacific wave glider data and satellite data (MODIS, aquarius, TRMM and VIIRS). *PloS one* **9:** e92280.

Viviani, D. A., Björkman, K. M., Karl, D. M., & Church, M. J. (2011) Plankton metabolism in surface waters of the tropical and subtropical Pacific Ocean. *Aquat Microb Ecol* **62:** 1-12.

Wanninkhof, R. (1992) Relationship between wind speed and gas exchange over the ocean. *Journal of Geophysical Research: Oceans (1978–2012)* **97:** 7373-7382.

Wanninkhof, R., Asher, W. E., Ho, D. T., Sweeney, C., & McGillis, W. R. (2009) Advances in quantifying air-sea gas exchange and environmental forcing. *Marine Science* **1**.

Wanninkhof, R., & McGillis, W. R. (1999) A cubic relationship between air-sea CO2 exchange and wind speed. *Geophys Res Lett* **26:** 1889-1892.

Westberry, T. K., Williams, P., & Behrenfeld, M. J. (2012) Global net community production and the putative net heterotrophy of the oligotrophic oceans. *Global Biogeochem Cycles* **26:** 10.1029/2011GB004094.

Williams, P., & Bowers, D. G. (1999) Regional carbon imbalances in the oceans. *Science* **284:** 1735-1735. 10.1126/science.284.5421.1735b.

Williams, P. J., Morris, P. J., & Karl, D. M. (2004) Net community production and metabolic balance at the oligotrophic ocean site, station ALOHA. *Deep Sea Research Part I: Oceanographic Research Papers* **51:** 1563-1578. 10.1016/j.dsr.2004.07.001.

Williams, P., & Purdie, D. (1991) *In vitro* and *in situ* derived rates of gross production, net community production and respiration of oxygen in the oligotrophic subtropical gyre of the north Pacific Ocean. Deep Sea Research Part A. *Oceanographic Research Papers* **38:** 891-910.

Williams, P. J., Quay, P. D., Westberry, T. K., & Behrenfeld, M. J. (2013) The oligotrophic ocean is autotrophic. *Annu Rev Marine Sci* **5:** 535-549. 10.1146/annurev-marine-121211-172335. Available: http://dx.doi.org/10.1146/annurev-marine-121211-172335 via the Internet.

Wohlers, J., et al. (2009) Changes in biogenic carbon flow in response to sea surface warming. *PNAS* **106:** 7067-7072.

Wright, J. J., Konwar, K. M., & Hallam, S. J. (2012) Microbial ecology of expanding oxygen minimum zones. *Nature Reviews Microbiology* **10:** 381-394.

2.7 Tables

Table 2-1 r values for relationships among environmental datasets in different regions of the Pacific.

	Pacific Ocean	**California to Japan**	**California to Australia**	**20 to 38°N**	**10 to 20°N**	**0 to 10°N**	**-15 to 0°S**	**-23 to -15°S**
Chlorophyll and temperature	-0.418	-0.423	-0.410	-0.795	0.341	Not significant	0.592	Not significant
Temperature and turbidity	0.276	0.454	-0.288	Not significant	-0.270	Not significant	0.458	Not significant
Chlorophyll and turbidity	Not significant	Not significant	Not significant	Not significant	Not significant	Not significant	0.639	0.647

Table 2-2 r^2 values for comparisons among different AOU approaches used to calculate CR for the California to Australia (above the diagonal) and California to Japan (below the diagonal datasets). P<0.001 in all instances.

	CR1	**CR2**	**CR3**	**CR4**	**CR5**	**CR6**	**Raw**
CR1		0.905	0.993	0.979	0.986	0.986	0.842
CR2	0.917		0.856	0.810	0.957	0.826	0.601
CR3	0.996	0.881		0.988	0.959	0.994	0.899
CR4	0.985	0.839	0.995		0.940	0.999	0.883
CR5	0.990	0.961	0.973	0.953		0.948	0.750
CR6	0.990	0.853	0.998	0.999	0.961		0.891
Raw	0.921	0.718	0.952	0.965	0.860	0.961	

Table 2-3 r^2 values for comparisons among different BDO approaches used to calculate CR for the California to Australia (above the diagonal) and California to Japan (below the diagonal datasets). P<0.001 in all instances.

	CR1	**CR2**	**CR3**	**CR4**	**CR5**	**CR6**	**Raw**
CR1		0.923	0.993	0.984	0.987	0.989	0.870
CR2	0.914		0.881	0.848	0.968	0.860	0.665
CR3	0.996	0.876		0.990	0.963	0.996	0.919
CR4	0.985	0.834	0.995		0.951	0.999	0.903
CR5	0.990	0.960	0.972	0.952		0.956	0.788
CR6	0.989	0.848	0.998	0.999	0.959		0.911
Raw	0.921	0.712	0.952	0.965	0.859	0.961	

2.8 Figures

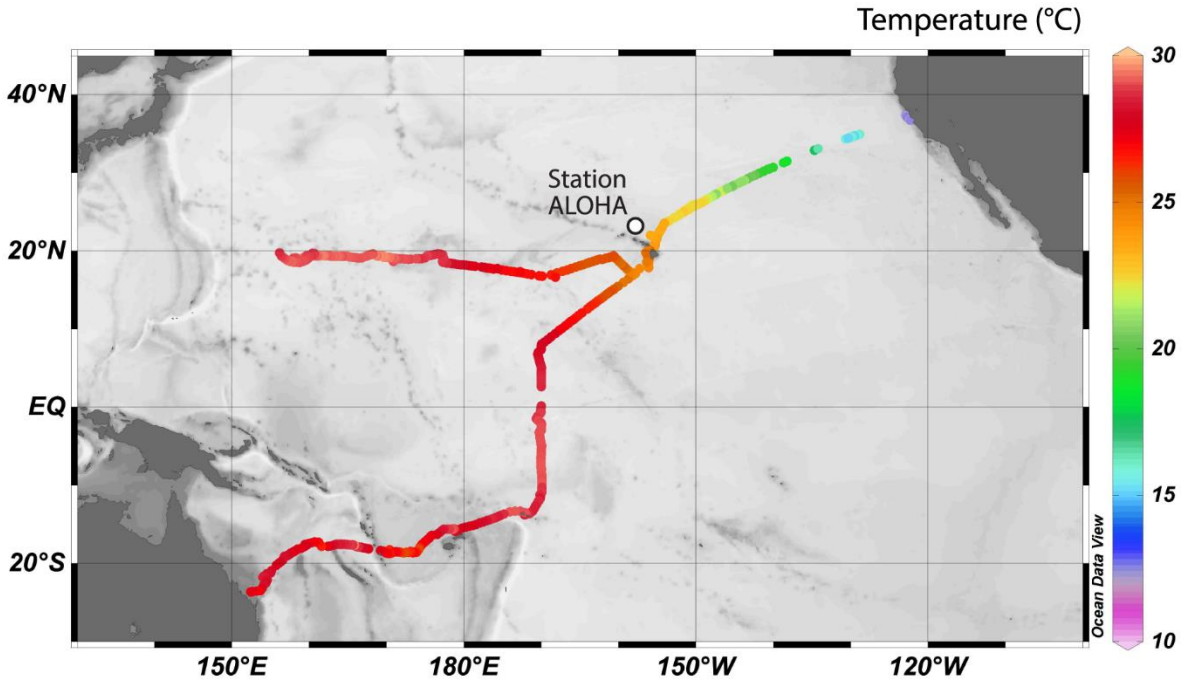


Figure 2-1 Map of the transpacific paths of the California to Australia and the California to Japan gliders and sea surface temperature as measured by the gliders. Eleven datapoints are not displayed due to obvious GPS errors. Ocean Data View (Schlitzer, 2013) was used to plot and visualize data across the Pacific.

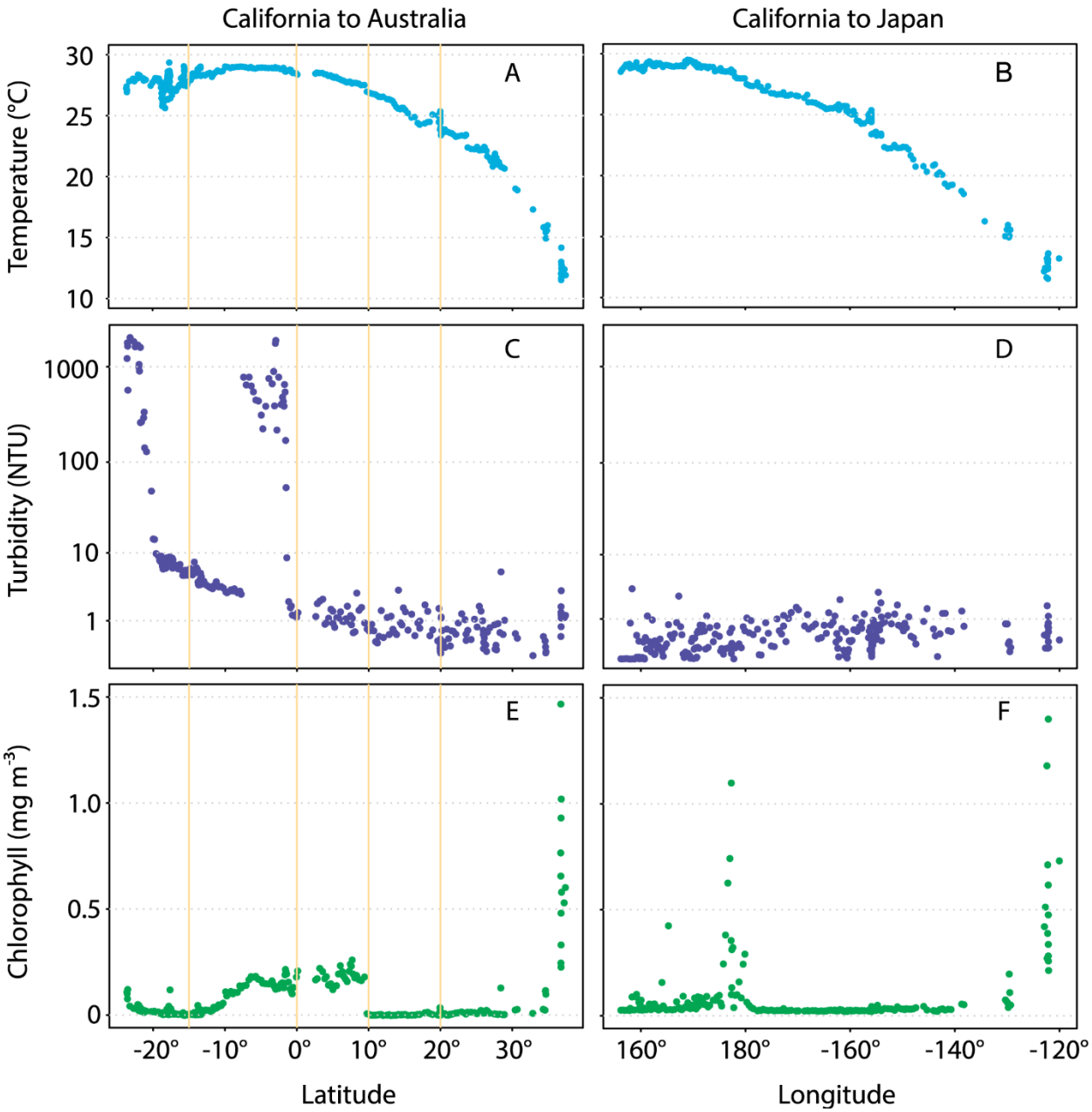


Figure 2-2 Environmental data collected by the gliders along the two transects. Panels depict temperature (°C) according to latitude for California to Australia (A) and according to longitude for California to Japan (B); turbidity (NTU) from California to Australia (C) and California to Japan (D); and Chlorophyll (RFU) from California to Australia (E) and California to Japan (F).

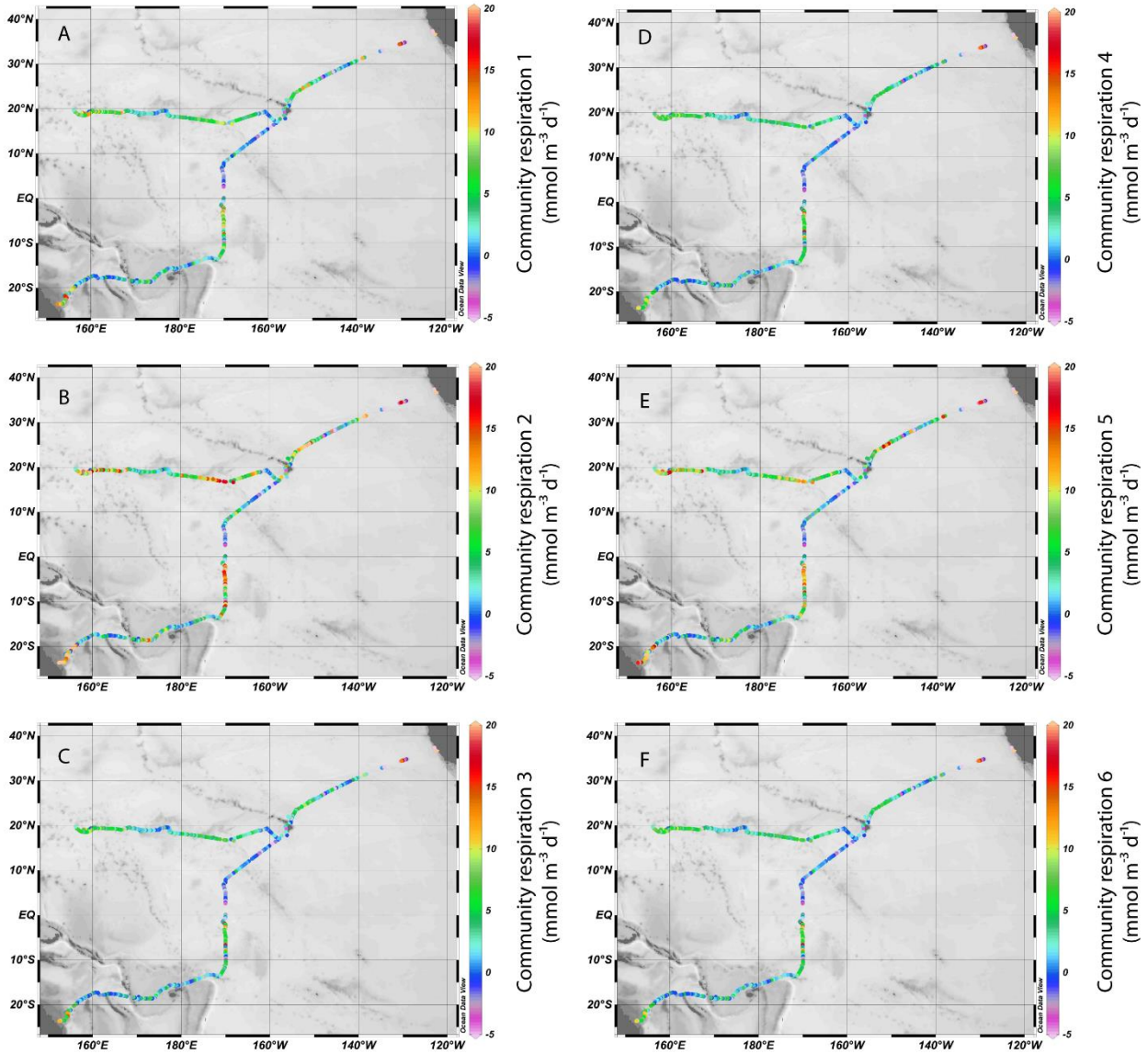


Figure 2-3 BDO computed community respiration rates along the two transects. Color shading shows (A) community respiration 1 (mmol m^{-3} d^{-1}) (B) community respiration 2 (mmol m^{-3} d^{-1}) (C) community respiration 3 (mmol m^{-3} d^{-1}) (D) community respiration 4 (mmol m^{-3} d^{-1}) (E) community respiration 5 (mmol m^{-3} d^{-1}) and (F) community respiration 6 (mmol m^{-3} d^{-1}) across the Pacific Ocean. Data displayed using Ocean Data View (Schlitzer, 2013).

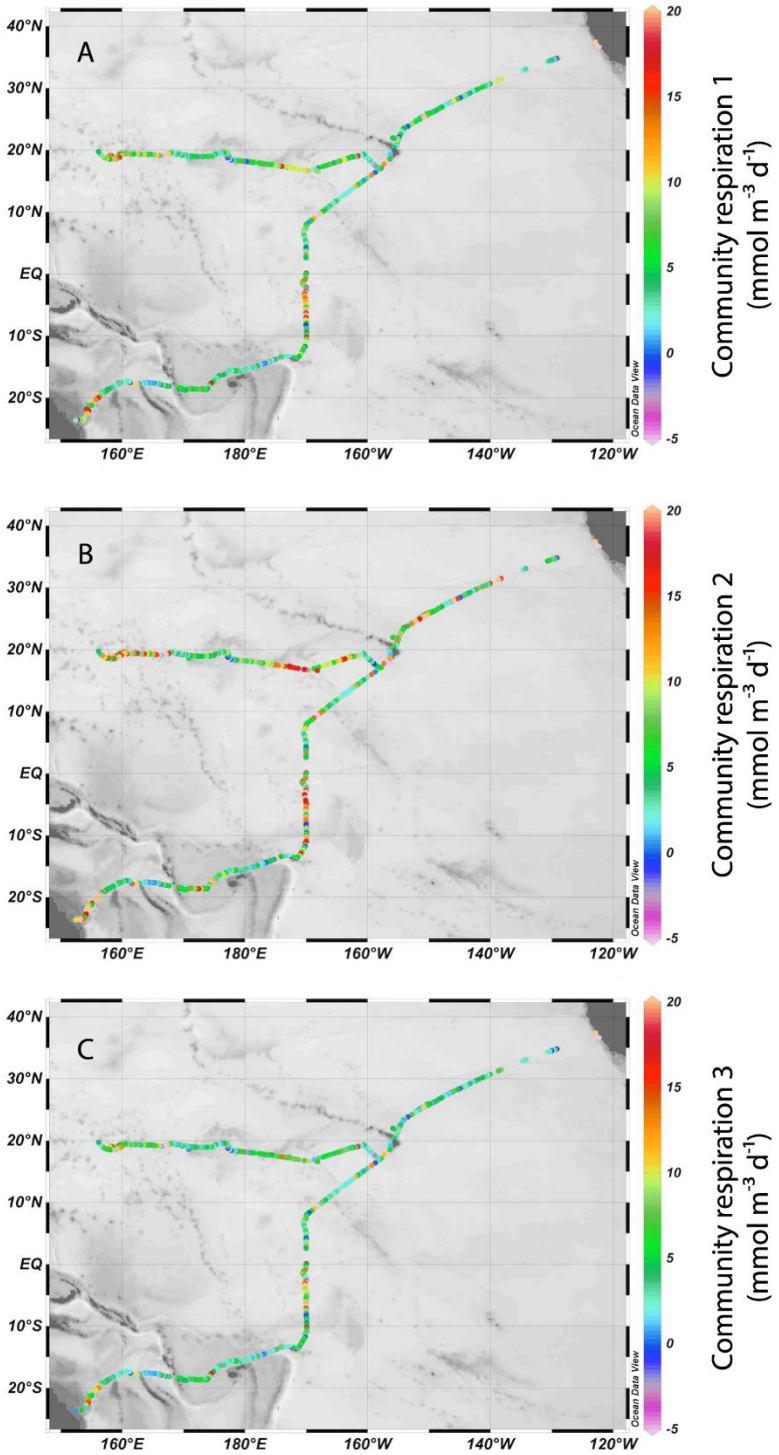


Figure 2-4 Computed community respiration rates along the two transects. Color shading shows (A) community respiration 1 (mmol m^{-3} d^{-1}) (B) community respiration 2 (mmol m^{-3} d^{-1}) and (C) community respiration 3 (mmol m^{-3} d^{-1}) across the Pacific Ocean. 14 datapoints, 24 datapoints, and 15 datapoints exceed 20 mmol m^{-3} $d^{-1}$and appear pink for CR1, CR2, and CR3, respectively; 19 datapoints, 15 datapoints, and 19 datapoints fall below -5 mmol m^{-3} d^{-1} and appear light purple for CR1, CR2, and CR3, respectively. Data displayed using Ocean Data View (Schlitzer, 2013).

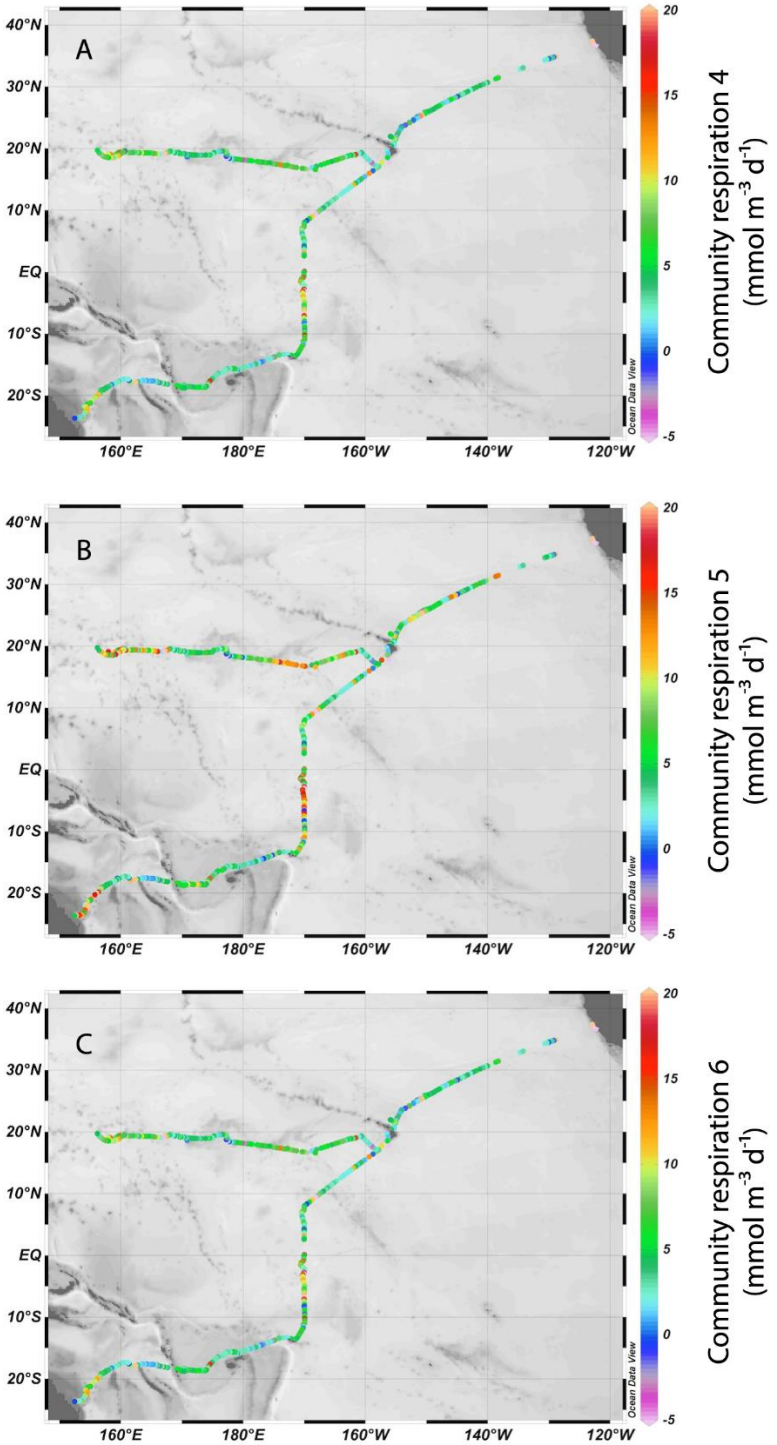


Figure 2-5 Computed community respiration rates along the two transects. Color shading shows (A) community respiration 4 (mmol m^{-3} d^{-1}) (B) community respiration 5 (mmol m^{-3} d^{-1}) and (C) community respiration 6 (mmol m^{-3} d^{-1}) across the Pacific Ocean. 14 datapoints, 16 datapoints, and 39 datapoints exceed 20 mmol m^{-3} $d^{-1}$and appear pink for CR4, CR5, and CR6, respectively; 19 datapoints, 18 datapoints, and 14 datapoints fall below -5 mmol m^{-3} d^{-1} and appear light purple for CR4, CR5, and CR6, respectively. Data displayed using Ocean Data View (Schlitzer, 2013).

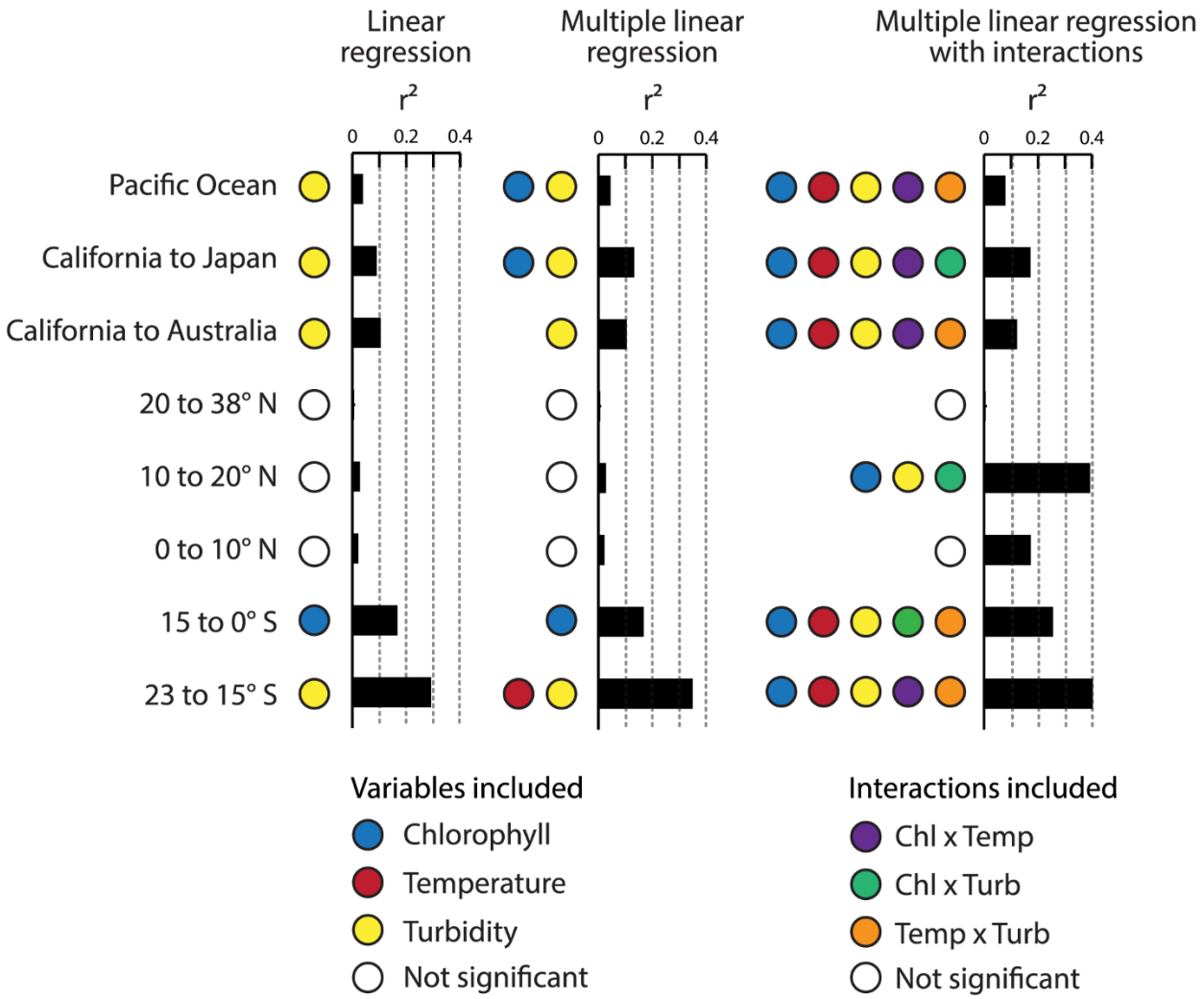


Figure 2-6 Regression statistics for best AIC derived relationships between AOU-slope-based CR2 data and environmental data. Bar graphs show regression r^2 values for univariate linear regression, multiple linear regression, and multiple linear regression with interactions. Color-coded symbols next to the bar graphs indicate which variables or interactions yielded significant relationships; a white circle indicates that no significant relationships were found. These model statistics represent log-transformed turbidity and chlorophyll data.

3 Microbial community networks associated with variations in community respiration rates during upwelling in nearshore Monterey Bay, California

3.1 Abstract

Respiration of organic material is a central process in the global carbon (C) cycle catalyzed by diverse microbial communities. Microbial C cycling is particularly significant in the coastal ocean—where large biogeochemical fluxes drive rapid rates—but is variable in space, time, and in the contributions of different microbial groups to C cycling. We measured rates of community respiration (CR) and analyzed microbial ecology via 16S rRNA gene sequencing to identify how CR and microbial communities vary as a function of upwelling, and each other, in nearshore Monterey Bay, California. CR varied significantly over time as a function of temperature, dissolved oxygen (DO), upwelling, and chlorophyll—but also varied with a subnetwork of the microbial community. One subnetwork was associated with higher CR and warmer temperatures, while another was associated with lower CR and DO. Although some microbial taxa were represented in both subnetworks (e.g. Flavobacteriaceae), there were also taxa unique to each network—including the Arctic97B-4 marine group and SAR324 clade (in the subnetwork that was negatively correlated with CR) and *Planktomarina* and eukaryotic phytoplankton (in the subnetwork positively correlated with CR). Our results indicate that multiple microbial interactions regulate CR and C cycling in the coastal ocean.

3.2 Introduction

Microbial communities regulate fluxes of carbon, oxygen, nutrients, and energy throughout the ocean. The breakdown and respiration of photosynthetically-produced organic carbon (C) is one of the most important processes catalyzed by microbes: community respiration (CR)—which is dominanted by microbes (Williams, 1981)—plays a central role in C and energy flow by remineralizing organic C to carbon dioxide (CO_2), consuming oxygen in the process. CR is indicative of net ecosystem metabolism (Duarte & Agusti, 1998; Serret et al., 2002), and in many open ocean systems, photosynthesis and aerobic CR rates tend to be tightly coupled and close to balanced (Robinson & Williams, 2005). However, in the case of coastal carbon (C) cycling, many fluxes are poorly constrained, and there is no consensus as to whether present-day continental shelves are net autotrophic (production exceeds CR) or heterotrophic (CR exceeds production) (Regnier et al., 2013; Bauer et al., 2013). This remarkable uncertainty stems in part from (1) strong temporal and spatial variation in environmental conditions along the coast (Capone & Hutchins, 2013); (2) a lack of CR measurements compared with primary productivity measurements more commonly made in shelf waters (Bauer et al., 2013); and (3) uncertainties in how diverse microbial and macrobial communities assimilate and respire organic C (Azam, 1998; Carlson et al., 2004).

These issues are particularly salient in coastal upwelling regions. These areas are biogeochemically and ecologically important due to high nutrient flux that drives high primary production rates; however, spatial and temporal variation in upwelling produces substantial heterogeneity (Capone & Hutchins, 2013). In upwelling regions like coastal California, CR rates

are high, but do not typically keep pace with primary production (Bograd et al., 2001; Johnson, 2010; Munro et al., 2013). However, high temporal-resolution data from Johnson (2010) show that CR can periodically match or temporarily exceed production rates in Monterey Bay, California. Similarly, while conducting biweekly bottle incubations along the Iberian coast, Moncoiffé et al. (2000) observed occasional bursts of high CR. Measurements of bacterial production along the California coast also show spatial and temporal variation indicative of hot spots and hot moments (Fuhrman & Azam, 1982; Brown et al., 2005; Steele et al., 2011; Samo et al., 2012)—which Ohman et al. (2013) hypothesize may play a disproportionately greater role in the California Current ecosystem in the future.

How microbial community dynamics influence, or are influenced by these biogeochemical variations in upwelling regions, is not well understood. Bowman et al. (2017) recently demonstrated that the microbial community was a significant factor in explaining variation in bacterial production in the coastal waters of the western Antarctic Peninsula, and that the seasonality of the entire microbial community contributed to changes in bacterial production. Previous work in both freshwater and marine environments have found that the microbial community changes as CR changes (Gattuso et al., 2002; Kalvelage et al., 2015); and while the type of phytoplankton in bloom is certainly connected to C export (Boyd & Newton, 1995; et al., 2009), Guidi et al. (2016) recently showed that the photosynthetic community is only a minority of the planktonic network that is connected to changes in C export—with key nodes including *Synechococcus*, *Cobetia*, *Pseudoalteromonas*, *Idiomarina*, *Vibrio*, and *Arcobacter*. The microbial groups contributing most substantially to CR may be a subset of the whole community (Guidi et al., 2016)—meaning that assessing changes in the whole microbial community may obscure the most biogeochemically relevant microorganisms.

Given the significance of, variability in, and paucity of measurements relating respiration to both environmental and biological factors, we sought to better understand this process in California's nearshore environment. In order to assess the controls on planktonic CR, we regularly measured CR throughout the upwelling season in nearshore Monterey Bay at two sites, while also measuring environmental variables and assessing microbial community dynamics. The two sites were located within and adjacent to the kelp forest ecosystems common along the California coast (and in other upwelling regions), and microbial communities were examined at both the entire community level and by identifying microbial subnetworks that correlated with environmental variables and CR.

3.3 Methods

3.3.1 Sample collection

Sampling took place from small boats directly offshore from Hopkins Marine Station (36.6205° N, 121.9045° W), both inside the kelp forest (approximately 100m offshore) at Station K, and at a site directly outside of the kelp forest at Station O. Our sampling took place in conjunction with the Marine Life Observatory (MLO, http://mlo.stanford.edu/) every two weeks between 6-18-2014 to 8-26-2014, with higher frequency sampling (every 2 days) between 8-10-2014 to 8-14-2014 (though CR rates were only able to be measured from 7-16-2014 through 8-26-2014 due to personnel restraints). Samples were collected at three depths: surface (1m), the transition zone

(which exhibited a relatively sharp change in the temperature and/or oxygen profiles on the day of collection), and approximately 1m above the bottom at Station K (8 to 9m, depending on the tide) and at 14m at Station O (which was a couple meters above the bottom but the maximum depth of our sampling pump). Transition zone depths were based on dissolved oxygen (DO) and temperature profiles taken with a non-consumptive optode (YSI ProODO™, Xylem Inc., Yellow Springs, OH, USA), and changed slightly between time points depending on tide and profile data. Water was collected for analysis using a motorized sampling pump (model P-10500, Proactive Environmental Products, Bradenton, FL, USA) with a Proactive™ Low Flow Sampling Controller (model PA-10750, Proactive Environmental Products, Bradenton, FL, USA) that was run at a low laminar rate to exclude bubbles. Bottles were triple rinsed and then filled to three times overflowing.

3.3.2 CR rate measurements

To assess how planktonic oxygen consumption changed over time in association with various explanatory variables, water samples were collected in triplicate and returned to the lab, where DO and temperature were measured at the initial start time, followed by measurement every 4 to 6 hours for 24 hours, after which point the experiment was terminated. DO was measured using a fiberoptic oxygen optode and optical sensor spots (Fibox 3, PreSens, Regensburg, Germany). Bottles were wrapped in aluminum foil and stored in a dark container with flowing seawater to control temperature; incubation temperature was tracked using a HOBO Pendant datalogger (MicroDAQ, Contoocook, NH, USA) and remained constant throughout the experiments (data not shown). Experiments commenced between 9 and 11 am and were run for 24 hours to integrate and eliminate variations in oxygen consumption over the course of the day (Williams, 2000).

CR rate measurements were calculated by subtracting the initial DO of a bottle from DO at the termination time (24 hours except for unfiltered water at Station O which was 21 hours) and dividing by the time passed. Data from 7-16-2014 were not included in pooled statistical analyses due to slight oxygen accumulation in the bottles—likely due to issues with bottle filling and handling in rough seas (Figure 3-4A&B). Once again, the fact that incubations took place over 24 hours removes bias from slightly different start times as diel variation is integrated over the course of the day (Williams, 2000).

3.3.3 Size fractionation

The microbial contribution to total observed CR was quantified on 8-14-2014 by comparing triplicate samples from the <200 µm size fraction, with triplicate samples from unfiltered samples, in surface and deep samples from each station. Previous research has examined the bacterial respiration of many different size classes (Robinson, 2008), but for our purposes only excluding metazooplankton and larger organisms from filtered samples was necessary. We did not conduct additional size fractionation experiments owing to the fact that sample manipulation can introduce artifacts. Unpaired t-tests demonstrated that initial sample DO was not significantly different for either size fraction at either depth sampled at Station K (1m and 8m). However, the two size factions showed significant differences in initial DO at both depths

sampled at O (1m and 14m, P=0.026 and P=0.040, respectfully), most likely due to sample manipulation.

3.3.4 Environmental Data

Initial temperature and DO were obtained from the YSI profiles on all days except 7-16-2014 when the YSI instrument was not available. Upwelling index was obtained from the NOAA Pacific Fisheries Environmental Laboratory website (http://www.pfel.noaa.gov/products/PFEL/ accessed Sept. 16, 2016), which calculates upwelling index based on Ekman's theory of mass transport due to wind stress, and correspond to the location of two buoys: located in an area North of the study sites (39°N 125°W) and an area South of the study sites (36°N 122°W). We used the index for the exact date of interest for each site (Upwelling-N and Upwelling-S) in addition to the mean for the three days prior to the date of interest (Preupwelling-N and Preupwelling-S).

Phosphate (PO_4^{3-}) and salinity were measured for the surface and deep of Station K and Station O by HMS Marine Life Observatory. PO_4^{3-} was measured colormetrically at semiregular intervals of which several were close to the dates of rate measurements/microbial collection (on 7-03-2014, 7-16-2014, 7-30-2016, 8-14-2016, 8-27-2016; allowing for a pairing of those dates). Mid depths and dates that were not within one day of sampling dates had no PO_4^{3-} or salinity value associated with it.

Finally, chlorophyll *a* (chl-*a*) was measured by HMS Marine Life Observatories and Karina Nelson using a WET Labs ECO FL fluorometer (Sea-Bird Scientific, Philomath, OR, USA). The fluorometer had excitation/emission wavelengths of 470/695nm, a sensitivity of 0.02 µg/l, and a range of 0-125 µg/l. The fluorometer was installed in the mid-intertidal zone (~0-0.3 m above mean lower low water) at Hopkins Marine Station. Observations were logged every 15 minutes and the sensor face was cleaned every 1-2 weeks. The WET Labs' chl-*a* equivalent concentration scale factor was used to convert raw fluorescence to chl-*a* and double checked every two weeks by extracting and measuring chl-*a* according to the methods of Welshmeyer (1994) utilizing a benchtop fluorometer calibrated to certified standards from Turner Designs (San Jose, CA, USA). The average daily chl-*a* value was calculated and, due to the location of the *in situ* instrument, the same daily chl-*a* value was used for each depth/site for a given date. The validity of using the same chl-*a* measurement for each site/depth was demonstrated by the fact that raw fluorescence from each location (Station K and a few meters away from Station O), which were taken every 15 minutes by HMS Marine Life Observatory, were identical for a given time point. Because we also had raw fluorescence for each site taken every 15 minutes (starting on 7-30-2014) we also applied raw fluorescence at the exact sampling time to each measurement. In sum. PO_4^{3-}, salinity, chl-*a*, and fluorescence data were used in the models but are not otherwise reported here.

3.3.5 Microbial community assessment

The microbial community was assessed by filtering 500 mL of water on to 0.22 µm filters (Millipore, Darmstadt, Germany) using a peristaltic pump from each station, depth, and date. Samples were frozen until DNA was extracted following Beman et al. (2008): 100µL 10%

sodium dodecyl sulfate (SDS) was added to tubes containing STE buffer and filters, samples were bead-beat for 2 minutes (BioSpec Products, Inc., Bartlesville, OK, USA), and incubated for 3 minutes on a dry heat block at 99°C. Following transfer of sample solutions to 1.5 mL LoBind Microcentrifuge tubes (Eppendorf, Hauppauge, NY, USA), 50µL proteinase K (20mg mL^{-1}; Qiagen, Inc., Valencia, CA, USA) was added, and tubes were incubated at 55°C for 3 hours. Lysates were purified using a DNeasy Blood and Tissue Kit according to the manufacturer's protocol (Qiagen, Inc., Valencia, CA, USA). DNA concentrations were measured using the Quant-iT PicoGreen dsDNA Assay Kit and the manufacturer's protocol (Invitrogen Corporation, Carlsbad, CA, USA) on a Stratagene MX 3005P (Agilent Technologies, Inc., Santa Clara, CA, USA).

Following extraction, samples were sent to Argonne National Laboratory (Lemont, IL, USA) for Illumina MiSeq 16S rRNA sequencing using the universal primers 515F-Y (5'-GTGYCAGCMGCCGCGGTAA) and 926R (5'-CCGYCAATTYMTTTRAGTTT) according the Earth Microbiome protocols; these primers have been shown to better estimate marine communities (Parada et al. 2015). We recovered 2,249,597 sequences (from 47 samples) with a median read length of 373 bp. Sequence processing and community analysis was conducted in mothur (http://www.mothur.org/) following the approach of Hayden and Beman (2015) modified from the mothur MiSeq SOP (Kozich et al., 2013; http://www.mothur.org/wiki/MiSeq_SOP accessed Aug. 19, 2016). Additionally, a delta 1 was allowed between quality scores of mismatched bases as contigs were made and, during the screening process, a minimum length of 280 was required (75% of average at the recommendation of the Earth Microbiome Project), a maximum length of 385 was required, and up to 3 ambiguous bases were allowed during the screening process.

The remaining 2,141,177 16S rRNA sequences (with individual sample library sizes ranging from 7,515-92,576 sequences, mean 45,557±24,904) were aligned to the SILVA SEED database (version 119). Kunin et al. (2010) raised the issue of sequencing errors inflating diversity estimates, and Huse et al. (2010) proposed a pseudo-single linkage 'preclustering' algorithm as a means of reducing these errors; we used this approach as implemented in mothur to remove sequences that may be affected by sequencing errors. Chimeras were removed using uchime in mothur.

All samples were subsampled to 7,515 reads (the minimum library size) and we calculated beta diversity across these normalized sample libraries using multiple indices (abundance-based Sørensen, Bray-Curtis, θ). Each index gave similar results, and we chose to focus on the Sørensen index, calculating Analysis of Molecular Variance (AMOVA) in mothur. Taxonomy was determined by classifying the 16S rRNA sequences based on the SILVA (version 123) database in mothur. Unclassified cyanobacterial chloroplasts were identified using BLASTn (https://blast.ncbi.nlm.nih.gov/Blast.cgi?PAGE_TYPE=BlastSearch). We reported cultured organisms when possible. Finally, we define the microbial community as the absence, presence, and relative abundance of particular operational taxonomic units (OTUs) within sequence libraries.

3.3.6 Statistical analyses

Both CR and the microbial community varied significantly with date (see below), and various methods were used to assess the relationships between variables to explain the significant variation we observed over time. Analysis of Variance (ANOVA) with Tukey Honestly Significant Difference (HSD), multivariate regression, and linear regression (using the general linear model) in R were utilized to examine relationships between environmental variables with CR. CR rates were analyzed within and across stations according to temperature, initial DO, upwelling index, PO_4^{3-} concentration, chl-*a* concentration, and fluorometric measurements using linear regression. All unfiltered CR data was pooled (minus 7-16-2014) and analyzed using multivariate regression and the environmental variables above; AIC was used to determine the best multivariate regression models.

Variation in the entire microbial community with environmental data and CR was analyzed using a combination of methods. Multiple Regression on Matrices (MRM; using the R ecodist package) was used to test correlations between changes in environmental variables and a microbial community distance matrix (measured via abundance-based Sørensen). 1,000 permutations were utilized for each MRM analysis. Redundancy Analysis (RDA; using the R vegan package) was used to analyze multivariate relationships between the community (for which a Hellinger transformed OTU abundance matrix was used) and explanatory variables. We also used emergent self-organizing maps (ESOMs; using the R kohonen package; Wehren & Buydens, 2007), a neural network algorithm that has recently been applied to analysis of complex microbial communities in a time-series (Bowman et al. 2017). ESOM reduces the dimensionality of the community from each sample to a single variable using Euclidean distance. Sample similarity is represented with topography and by relating community types (made up of similar samples) to environmental variables and CR we were able to see how entire community types changed in relation to these traits. A Hellinger transformed OTU abundance matrix of the 750 most abundant OTUs was used. The grid to which samples were assigned was a series of 3x4 circular nodes in a hexagonal grid with a three-dimensional edgeless toroidal configuration. 100 iterations were run with an alpha from 0.05 to 0.01. Clusters of nodes were identified using k-means clusters, with k=5 selected via evaluation of a scree plot of within-clusters sum of squares against different k values and finding the inflection point.

Weighted Gene Correlation Network Analysis (WGCNA; using the R WGCNA package) was used to identify subnetworks of microorganisms that correlated with CR and environmental variables based on their relative abundances with each environmental feature. WGCNA is a network analysis tool originally created to find and summarize clusters of highly correlated genes, and then relate clusters to one another and external traits (Langfelder & Horvath, 2007 & 2008). This graph-based approach can be used on sequence data by using a relative abundance matrix in which nodes represent operational taxonomic units (OTUs), and edges represent significant co-occurrence. These co-occurrence scores are created by way of an adjacency function that 1) factors in the degree of shared neighbors between two nodes and 2) is magnified by a power-law function so that the topology of the graph becomes scale-free. OTUs are sorted into modules (or subnetworks) and the co-occurrence profiles for each profile are represented by an “eigengene”. By correlating a module’s eigengene with an environmental variable we can find significant correlations between subnetworks and environmental traits of interest. This package

and has recently been used to find subnetworks of microbial communities (Duran-Pinedo et al., 2011; Aylward et al., 2015; Guidi et al., 2016) and the authors of the package provide advice for data analysis (https://labs.genetics.ucla.edu/horvath/CoexpressionNetwork/Rpackages/WGCNA/faq.html). We used a Hellinger transformed prokaryotic abundance matrix which was limited to the 750 most common OTUs (after 750 the frequency of OTUs in any sample was likely to be zero). A signed adjacency measure was calculated for each pair of OTUs by raising the value of a function involving their Pearson correlation coefficient to the soft thresholding value of 10 (the power that the co-occurrence adjacency score is raised to that is derived to optimize a scale-free topological overlap measure, or TOM, that considers each pair of OTU's weighted pairwise correlation and weighted correlations with other OTUs in the network).

3.4 Results

3.4.1 Temperature, oxygen, and upwelling

Temperature and dissolved oxygen (DO) YSI profiles were very similar between the two stations; each decreased with depth, and the two measurements were significantly correlated ($P<0.001$, $r^2=0.118$; Figure 3-2A,B,C,&D). There was also variation over time for each measurement, with 7-02-2014 possessing the coldest surface water at both stations, while 8-10-2014 possessed the lowest surface DO values at both stations. Upwelling occurred throughout the summer—as indicated by the significantly positive upwelling indexes (Figure 3-3A,B,C&D)—and the strongest current upwelling index at both the N and S site corresponded to the day of coolest temperatures, while the lowest DO value corresponded with the strongest Preupwelling-N.

3.4.2 Community respiration

We found that CR varied with depth and date, but not station (proximity to kelp), throughout our sampling. Overall, date explained 56% of the variation in respiration ($P<0.001$) and, according to Tukey HSD Tests, there were significant differences in CR for surface and deep samples ($P=0.015$), between 7-30-14 with each of the other dates for surface samples ($P<0.001$-0.02), and between 8-10-14 and each of the other dates for mid and deep samples ($P<0.001$-0.021). On 8-14-2014—when size fractionated studies took place—CR did not vary significantly with depth when compared within a size class, but did vary with size fractionation in one case (discussed below).

All unfiltered respiration rate data were pooled and triplicate values averaged so that various factors—DO, temperature, upwelling index, previous upwelling, salinity, fluorescence, chlorophyll *a* (chl-*a*), and phosphate (PO_4^{3-})—could be tested independently and together using multivariate regression. Initial DO (taken from starting profiles) alone explained 31.3% of the variation in respiration ($P=0.002$) while initial temperature (taken from starting profiles) explained 25.2% of the variation in respiration ($P=0.006$). There was a positive relationship between initial DO and respiration and between initial temperature and CR, meaning that higher respiration rates occurred when either initial DO or temperature were higher.

The most obvious explanation for changes in temperature and oxygen in Monterey Bay is upwelling. We observed significant upwelling over the course of this experiment (Figure 3-3A,B,C,&D), with the maximum current upwelling index at both areas (Upwelling-N and Upwelling-S) occurring on 7-2-2014, though upwelling index when averaged over the previous three days was above 250 on 6-18-2014 and 8-10-2014 for the Northern buoy (Preupwelling-N) and on 6-18-2014 for the Southern buoy (Preupwelling-S). While upwelling during the period of time that CR was quantified (7-30-2014 through 8-26-2014) was not typically as strong as the earlier portion of the summer (Figure 3-3A,B,C&D), the upwelling signal that was encountered during our sampling time period correlated with CR. Mean CR correlated with Preupwelling-S ($P<0.001$, $r^2=0.414$) and Preupwelling-N ($P=0.006$, $r^2=0.25$), but not with either current upwelling measurement. Initial DO (taken from the YSI) was also correlated with Preupwelling-S ($P<0.001$, $r^2=0.219$) and Preupwelling-N ($P<0.001$, $r^2=0.286$), but not current upwelling while the initial temperature (taken from the YSI) was weakly correlated with Upwelling-N ($P=0.028$, $r^2=0.058$) and with Preupwelling-S ($P=0.006$, $r^2=0.090$). Chl-*a* explained 37.2% of the variation in CR ($P=0.001$) and was also significantly correlated with Preupwelling-S ($P=0.050$, $r^2=0.772$).

Finally, CR was not significantly correlated with salinity, fluorescence, or PO_4^{3-}. Using the Step function in R, the best model to predict CR used DO, Preupwelling-S, and Preupwelling-N as explanatory variables ($P<0.001$, $r^2=0.606$). When interactions were introduced, the best model included the previous three variables in addition to Chl-*a* and interactions between DO and each of the three other variables individually and between Preupwelling-S and Preupwelling-N ($P<0.001$, $r^2=0.736$). In the size-fractionation experiments, CR only significantly correlated with treatment (unfiltered or <200µm) at the surface at K ($P=0.044$; Figure 3-4)—the other depths at station K, and all depths at station O, were not significantly different.

3.4.3 Microbial community dynamics

Microbial communities were dominated by Flavobacteria (45.5%), Rhodobacteraceae (24.2%), Oceanospiralles (6.6%; mostly SAR86), various chloroplasts (6.5%) and SAR11 (4%). However, the proportions of these different groups varied over time and space, with high variation seen in all of the above groups, as well as the Acidimicrobiales, Alteromonadales, Chellvibrionales, Rickettsiales, Sphingobacteriales, Thermoplasmatales, Puniceicoccales, and Verrucomicrobiales. Community turnover (beta diversity as measured by the Sørensen Index) was strongly related to date, with AMOVA (calculated based on the Sørensen Index) demonstrating that the community significantly varied between each sampling date except between 8-10-2014 and 8-12-2014, and 8-10-2014 and 8-14-2014 ($P<0.001$-0.04).

We used four approaches to relate changes in the microbial community to environmental variation and CR—multiple regression on matrices (MRM), redundancy analysis (RDA), emergent self-organizing maps (ESOM), and weighted gene correlation network analysis (WGCNA). First, MRM showed that changes in the microbial community correlated with changes in certain environmental variables, and with changes in CR. Changes in the microbial community were significantly correlated with changes in DO, CR, temperature, Preupwelling at both sites, Upwelling-N, and Chl-*a* ($P=0.001$-0.023 for Sørensen Index), with changes in CR and changes in the community correlating most strongly ($r^2=0.102$). When the significant environmental distance matrices were combined and correlated to the Sørensen based distance

matrix, 23.4% of the variation in the microbial community was explained by environmental variation (P=0.001). Of note is that the relevant explanatory variables that correlated with changes in the microbial community were similar to those that predicted variation of CR using linear and multiple regression. We also ran MRM using a distance matrix of CR as the dependent variable, in order to assess how it compared to the results of linear and multiple regression. We found the same explanatory distance matrices (DO, temperature, Preupwelling-N, Preupwelling-S, and chl-*a*; P=0.002-0.015) correlated with changes in CR as when explanatory variables were related to CR using linear regression. Of these correlations, Preupwelling-S had the highest r^2 of 0.109.

RDA was used to further analyze multivariate relationships between the microbial community and various explanatory variables. Sampling date accounted for 41.5% of the variation over the entire time period that the microbial community was sampled, and the six most significant variables for the subset of time period that CR was measured (CR, DO, temperature, Preupwelling-N, Upwelling-S, and chl-*a*) explained 35.3% of the variation in the microbial community (Figure 3-5). Only 6.5% of the variation in the whole community was explained by variation in CR, while DO explained 5.3% of the variation, temperature explained 9.2% of the variation, and the various upwelling indexes explained 5.8% to 10.9% of the variation in the entire community (with Preupwelling-S and Upwelling-N becoming more important than the other two indexes when all the dates were included).

ESOM was also used to assess how different segments of the microbial community (identified by the algorithm) varied with different environmental variables and CR. The five community types that were identified by ESOM (Figure 3-6A,B,&C) correlated with date (P<0.001; Figure 3-6D), CR (P=0.023; Figure 3-6E), DO (P=0.003; Figure 3-6F), temperature (P=0.042; figure 5G), salinity (P=0.005; Figure 3-6H) and each measure of upwelling (P<0.001 for each, Figures 3-6I,J,K,&L). For example, community type 2 was associated with the highest rate of CR, moderate Preupwelling-N, and the highest temperatures. This community was also observed in a majority of samples throughout the 7-16-2014 and 7-30-2014 sampling dates.

Finally, WGCNA was used to assess how subnetworks responded to environmental variation and CR. WGCNA finds clusters of highly correlated taxa across samples and then relates those clusters to one another and external traits (Langfelder & Horvath, 2007 & 2008). Seven major modules (or subnetworks) based on the co-occurrence of operational taxonomic units (OTUs) (hereafter referred to as Modules 1-7) were identified. Several modules significantly correlated with environmental variables, including depth, both current and previous upwelling, CR, temperature, DO, salinity, PO_4^{3-} concentration, chl-*a*, and fluorescence (Table 3-1A). Within each module, by correlating the Pearson correlation coefficient for OTU module membership with the Pearson correlation coefficient for each trait (e.g. depth, CR, etc.) we identified OTUs that were the most important (central nodes whose presence correlated with a change in an environmental trait) to each subnetwork (Table 3-1B), allowing us to refine which modules we assessed (Table 3-1C).

While several modules and their members correlated strongly with the different upwelling indices, and even more correlated strongly with temperature, we were ultimately interested in the two modules that varied significantly with CR: Module 2, which consisted 64 OTUs (Pearson

cor.=-0.53, $P=1e^{-04}$), and Module 6, which consisted 135 OTUs (Pearson cor.=0.43, P=0.003). Module 2 was inversely related to CR and DO, while positively related to depth. Module 6 was positively related to CR and temperature, while negatively related to depth. For these modules, we summed the Hellinger transformed abundances of the OTUs (calculated for each sample) so that each sample had a different abundance sum depending on the relative amount of important OTUs present, and regressed the resulting values with the corresponding CR, DO, temperature, and depth values; we found that the relationships that WGCNA found to be significant were also significant using the general linear model in R (Figure 3-7A,B,C,D,E&F; Table 3-2A). Finally, we sorted the OTUs of each module by the WGCNA Pearson correlation coefficient for CR and found that summing the 7 Hellinger transformed abundances of OTUs with the highest CR Pearson correlation coefficients in Module 2, and the 12 Hellinger transformed abundances of OTUs with the highest CR Pearson correlation coefficients in Module 6, explained most of the variation in CR (Table 3-2B; Table 3-3).

After classifying the bacterial and archaeal OTUs to 97% similarity and identifying chloroplasts using BLASTn, we identified the taxa represented by these OTUs that are most strongly related to variations in CR in each network (Table 3-3). The 7 most important OTUs in Module 2 corresponded to 1 archeon and 6 different bacterial groups (one of which was not able to be identified; OTU 290), while the 12 most important OTUs in Module 6 corresponded to 5 different bacteria and to 4 chloroplasts. *Owenweeska* made up 11.7% of total reads and was a member of both Modules (though it was not important enough to make it in the top 12 OTUs for Module 6). However, the NS9 marine group in Flavobacteriales that made up 1.72% of total reads was an important member of both Module 2 and 6. Meanwhile, Flavobacteriaceae in Module 6 made up 30.4% of the total reads. Flavobacteriales in general made up 45.5% of the total reads, 23.4% of Module 2, and 37.8% of Module 6.

3.5 Discussion

CR has been understudied in nearshore environments (Bauer et al., 2013), despite the fact that it is a proxy for microbial ecosystem functioning in oxygenated environments, and has the potential to change rapidly in dynamic coastal environments—as planktonic CR can remineralize both local, advected, and terrestrial C. Our results demonstrate that CR is variable with depth, temperature, DO, and specific segments of the microbial community. Both environmental conditions and microbial community dynamics appear to play a role in determining CR, suggesting they interact to control CR and the cycling of C, oxygen, and energy in this nearshore environment.

3.5.1 Spatial and temporal variation

CR varied significantly over time, as sampling date was the most significant factor in explaining variation in CR (r^2=0.56). Spring and summertime environmental variation in Monterey Bay can be due to a number of changes that occur with upwelling, including (but not limited to) changes in DO, temperature, nutrients, and labile organic matter (Pennington et al., 2000). Upwelling significantly explained a large amount of the variation in CR when averaged over the previous three days. This means that there is a lag period between CR response and the introduction of factors affecting CR that change with upwelling. Preupwelling measured at the Southern buoy

explained more of the variation in CR than Preupwelling measured at the Northern buoy (41.4% versus 25%), likely due to the fact that the Northern buoy is located much further offshore than the Southern buoy. The Southern buoy appears to better represent water conditions in nearshore Monterey Bay where our sampling was conducted.

We expected to observe differences in CR with depth as many of the factors that affect CR also vary with depth. DO varies with depth even over short distances, for instance, and this study was no exception (Figure 3-2). Initial DO alone predicted 31.3% of the variation in CR in this study, suggesting that a large portion of the variation in CR with depth is related to variations in oxygen with depth. DO is affected by biological activity, equilibration with the atmosphere, and hydrography. Intense, low-DO upwelling events have been identified in nearshore Monterey Bay (Booth et al., 2012), for instance, but the oxygen concentrations found in this study were similar to those observed when upwelling was more moderate (e.g., DeGrandpre et al., 1998). One explanation for the observed relationship between DO and CR is that high oxygen concentrations reflect elevated rates of photosynthesis (by kelp or phytoplankton) that 'prime' the water column for respiration by providing organic C and oxygen—similar to how the introduction of fresh, liable soil organic matter increases soil microbial remineralization rates leading to oxidation of a portion of the recalcitrant organic matter (Dalenberg & Jager, 1989; Kuzyakov & Bol, 2006). Indeed, Guenet et al. (2010) reviewed several instances in which the priming effect may contribute to respiration in marine systems, and hypothesize that the priming effect may be important to the remineralization of recalcitrant organic matter much more frequently than has been reported.

We observed a significant change in DO between stations but we did not observe any change in CR with station. The difference in DO could have been due to the presence of kelp as the site in the kelp forest tended to have slightly higher DO, however, the change in DO was not significant enough to affect CR (which was positively correlated with DO). To our knowledge, our study is the first to assess how planktonic CR is affected by the presence of large macrophytes such as kelp. Previous studies within kelp forests have focused primarily on respiration of kelp itself (Gerard, 1986; Abdullah & Fredriksen, 2004), its biofilm (Bengtsson et al., 2012), or did not compare planktonic CR inside versus outside the kelp forest (Delille et al. 1997). It is reasonable to assume that the presence of kelp or other macrophytes would affect microbial respiration given their substantial physical and biogeochemical influence. Kelp provides three-dimensional habitat, dampens waves, influences water flow and coastal erosion, reduces light levels, and provides C and nutrients that can be consumed and respired (Santelices & Ojeda, 1984; Duggins et al., 1990; Mann, 2009; Steneck et al., 2002). However, our results showed that the station (proximity to kelp) did not affect CR. These results indicate that free-floating heterotrophic bacteria are not as strongly stimulated by the presence of kelp as previously observed for biofilm bacteria (Bengtsson et al., 2012). However, the possibility that CR may vary significantly within and outside a kelp forest may still hold true with greater distance from the kelp forest as Station O, while outside the kelp forest, was close enough that advection could have created very similar amounts of kelp derived organic matter for microorganisms to consume.

The variation in CR with size fractionation is an indication of the relative contributions of the microbial community, versus larger organisms, to overall CR rates. Respiration varied between unfiltered and filtered samples only at the surface at K, and was otherwise indistinguishable

among treatments. This suggests that microbes are the primary contributors to CR—a result consistent with previous work in marine systems (Robinson & Williams, 2005)—and implies that microbial function is the dominant form of ecosystem function. In the lone instance where respiration for unfiltered samples was significantly higher than filtered samples was at the surface at Station K, meaning that larger size classes significantly contributed to CR. One explanation for this pattern is that the structure of the kelp provides refuge for larger size class organisms near the surface, while shading from kelp fronds may reduce planktonic primary production at deeper depths; this would reduce the supply of labile organic matter to zooplankton, reducing their respiratory activity, and produce similar CR values between unfiltered and filtered samples.

3.5.2 Microbial community dynamics and CR

The composition of our sequence libraries was similar to previous studies that have examined microbial communities along the coast of California using a mix of methodologies (Suzuki et al., 2004; Rich et al., 2011; Michelou et al., 2013). At the class level, communities were dominated by Flavobacteria (45.5%), Alphaproteobacteria (29.8%), and Gammaproteobacteria (12.4%). However, within these broad classes, many different groups contributed to the overall percentages, and these different groups varied in abundance over time. For example, seven Flavobacterial groups varied between 0.1% to 10% of sequence libraries (Polaribacter, NS4 marine group, NS5 marine group, NS9 marine group, Formosa, Tenacibaculum, and Ulvibacter), SAR11 varied from 0.03 to 19.4%, and SAR86 varied from 0.19 to 14.9%. Many of these bacterial clades are known to play important roles in the degradation of organic carbon (Cottrell and Kirchman, 2000; Bauer et al., 2006; Gonzalez et al., 2008; Kirchman 2008), and different OTUs drawn from these groups co-occur at different times off the coast of Southern California (Beman et al., 2011).

We used several different approaches to examine microbial community dynamics in conjunction with variations in CR. ESOM identified variations in five major community types (Figure 3-6D), along with several of the other factors that changed over time, including CR (Figure 3-6E). This is not surprising given that microbial communities have been observed to undergo seasonal cycles and change with environmental forcing (Giovannoni et al., 2012; Campbell et al., 1997; Gilbert et al., 2012), while Bowman et al. (2017) recently showed that shifts in the entire community correlated with microbial functioning. However, RDA (Figure 3-5) and MRM showed that the entire microbial community explained a relatively modest fraction of the variation in CR during the upwelling season in Monterey Bay (6.5% for RDA and 10.2% for MRM). We therefore sought to explain the specific subnetworks of microorganisms whose abundances correlated with CR using WGCNA; we found that the abundances of particular combinations of OTUs were significant predictors of CR. These OTUs also correlated with specific environmental variables. For example, if a sample had a high concentration of Flavobacteriaceae or *Planktomarina*, then it likely had high CR, and came from warmer water at a shallower depth. On the other hand, if Arctic97B-4 or *Nitrosopumilus* ammonia-oxidizing archaea (AOA) from the Marine Group 1 *Thaumarchaeota* were present in a sample, then it likely had low CR and DO.

Within Modules 2 and 6, OTUs that had the highest magnitude Pearson correlation coefficients also correlated with module membership—meaning that these particular OTUs appear to be important in contributing to overall CR, while also representing OTUs that are centralized nodes to each subnetwork. The most important OTUs to Module 2 (the module negatively correlated with CR) were identified as Arctic97B-4 of the Verrucomicrobia, Marine Group 1 *Thaumarchaeota*, and SAR324/Marine Group B of the Deltaproteobacteria. SAR324/Marine Group B was originally described by Fuhrman & Davis (1997) and Wright et al. (1997), but has since been observed to be a prevalent member of the upper water column (Treusch et al., 2009) with significant metabolic flexibility (Sheik et al., 2013; Haroon et al., 2016). The marine *Thaumarchaeota* are abundant throughout the mesopelagic zone (Karner et al., 2001), but transiently and dramatically increase in abundance in Monterey Bay (Robidart et al., 2012). Our data capture similar variations in nearshore Monterey Bay, and we found that CR rates are typically lower at these times.

In contrast, the most important OTU to Module 6 (the module positively correlated with CR) was identified as *Planktomarina*, while Flavobacterial OTUs were the second and third most important. *Planktomarina* is a monotypic genus of the Roseobacter clade that was originally isolated in the German Wadden Sea (Giebel et al., 2013); consisting of temperate, sub-polar, and polar planktonic clades, it has also been identified off the coast of California (Mayali et al., 2008). Members of Roseobacter have been seen post diatom blooms (Riemann et al., 2000) and have also been identified to live in the phycosphere of dinoflagellates (Lafay et al., 1995)—notably, chloroplasts from dinoflagellates were identified as important members of Module 6 using BLASTn.

Many of these bacterial groups are similar to those identified by Teeling et al. (2012), in which the heterotrophic response to a diatom bloom in the German Bight displayed a distinct successional pattern among taxa belonging to *Bacteroidetes*, *Gammaproteobacteria*, and *Alphaproteobacteria* (each with specialized transporters). For instance, the first successional phase following the introduction of algal derived organic matter included the Flavobacteria: *Ulvibacter* (in Module 6 in this study) and *Formosa* (in Module 2 and 6 in this study), though many different types of Bacteroidetes were found in both modules. Bacteroidetes are thought to respond rapidly to organic matter introduction following phytoplankton blooms (Cottrell & Kirchman, 2000; Bauer et al., 2006; Gonzalez et al., 2008; Kirchman, 2008) and both Module 2 and 6 included chloroplast sequences from several types of eukaryotic phytoplankton—though only Module 6 had several that were extremely important to the module (Table 3-1).

The photosynthetic organisms in Module 6 likely provided organic matter to support CR, and the fact that only eukaryotic chloroplasts made it into the top 12 most important OTUs in Module 6 suggests that CR in upwelling systems largely depends on photosynthetic eukaryotes. Microorganisms have long been observed to be significant consumers of eukaryotic photosynthetic products (Vargas et al., 2007), with many microorganisms (e.g. Bacteroidetes) found attached to sinking particulate organic matter (DeLong et al., 1993; Woebken et al., 2007). While the spring/summer upwelling season tends to favor diatoms in Monterey Bay (Chavez, 1996), the most important eukaryotic OTUs that were positively correlated with CR were revealed by BLASTn to include coccolithophores, dinoflagellates, and chlorophytes. Dinoflagellates tend to be much more abundant in the fall/winter, when the upwelling conditions

relax, or during periods of anomalously high sea surface temperatures that lead to stratification (Chavez, 2006). Our data indicate that while summer phytoplankton blooms may be dominated by diatoms, changes in other types of phytoplankton correlate more strongly with changes in CR. This may reflect differences in the types of organic material produced by different phytoplankton, which in turns affects overall CR rates.

We focused on the OTUs in each subnetwork that showed exceptionally strong correlations with CR (either positive or negative depending on the subnetwork) to infer which microbes may be most important to CR; but the results also imply ecological interactions among microorganisms in each subnetwork. Each subnetwork was made up of many OTUs that showed various correlation strengths with CR—each OTU had associated with it 1) a Pearson correlation coefficient for module membership (how well it correlated with that subnetwork) and 2) a Pearson correlation coefficient for CR. For each of the subnetworks that correlated with CR, a few OTUs had high module membership (meaning that the tended to co-occur with the other OTUs in that subnetwork) but were not well correlated with CR (data not shown). While untestable with the frequency at which this dataset was collected, such OTUs may represent taxa that are interacting with microorganisms that are important to CR (but are not directly influencing CR themselves). For example, SAR86 of Oceanospirillales was identified as having high module membership to Module 2 (Pearson cor.=0.640, $P=1.3e^{-06}$) but was not significantly correlated with CR (Pearson cor.=-0.144, P=0.335). It is possible that SAR86 was interacting with one of the microorganisms that was significantly and negatively correlated with CR in Module 2. However, if an interaction involving an important taxon was extremely strong, then the interacting taxa would be expected to have a measurable effect on CR—a Pearson correlation coefficient with the same sign as the important taxon would be expected for positive interactions (e.g. mutualism), while a Pearson correlation coefficient with the opposite sign would be expected for negative interactions (e.g. predation or competition). Because of OTUs indirectly affecting CR via positive interactions (thus having the same signed Pearson correlation coefficient as those microbes that are actually affecting CR), it is not possible to assess which microbes are truly responsible for changes in CR outside of the microorganisms with exceptionally strong Pearson correlation coefficients. Such inquiries would require high frequency sampling and causality tests that assess individual abundances over time. Finally, we would like to point out that certain taxa were assigned to many OTUs and, in some cases, these OTUs were seen across many different modules with varying degrees of importance. For example, OTUs representing NS9 marine group from Flavobacteriales were seen in both Module 2 and 6 with both high and low Pearson correlation coefficients (actually making it into the most important subgroup for each module). Such microbes are either 1) generalists capable of metabolic flexibility given different environments conditions, 2) different microbes that were not able to differentiated via 16s rRNA identification, or 3) interacting (both positively and negatively given the range of Pearson correlation coefficients) with microbes responsible for changes in CR in each module.

It is telling that although several microbial subnetworks (and the entire community, based on ESOM) correlated strongly with upwelling, the two modules that correlated with CR did not directly correlate with upwelling. Upwelling brings high concentrations of nutrients upward, and is associated with a change in community diversity (Allen et al., 2012). Our results suggest that although upwelling typically alters the environmental variables partially responsible for changes

in CR (e.g. temperature and DO), the microbial groups and networks most strongly related to shifts in CR are controlled by other factors—put another way, changes observed in the microbial community during upwelling mostly reflect variations in microbial groups that do not affect CR. However, it is important to point out that upwelling was moderate during the summer of 2014 in Monterey Bay, California and intense upwelling episodes did not occur. These events may have distinct effects on the microbial community that would in turn affect microbial functioning.

Instead, our work indicates that the critically important process of CR is regulated by a combination of variations in the physical and chemical environment, microbial responses to these changes, and ecological and biogeochemical interactions between microbial groups. For example, we found that higher rates of CR correlated with non-diatom eukaryotic phytoplankton, such that regime shifts in the dominant phytoplankton present may affect CR by changing the subset of the microbial community that correlates with CR. These types of phytoplankton regime shifts in Monterey Bay have been observed in the past with both climate change (Zachos et al., 2006) and temporary changes in stratification (Chavez, 2006; Keating, 2013). This highlights the complexity of carbon cycling and microbial dynamics in the coastal ocean, as physical forcing may affect phytoplankton community composition, which in turn affects bacterial communities, and subsequently rates of CR. We also identified subnetworks of microorganisms that change with CR in nearshore Monterey Bay, and many of these groups are widespread and display similar dynamics elsewhere along the coast of California (Beman et al., 2011) and in other coastal areas (Teeling et al., 2012). *Planktomarina* and multiple Flavobacterial groups therefore appear to be important players in coastal marine C cycling deserving of additional study.

3.6 References

Abdullah, M. I., & Fredriksen, S. (2004) Production, respiration and exudation of dissolved organic matter by the kelp Laminaria hyperborea along the west coast of Norway. *Journal of the Marine Biological Association of the UK* **84:** 887-894.

Allen, L. Z., et al. (2012) Influence of nutrients and currents on the genomic composition of microbes across an upwelling mosaic. *The ISME journal* **6:** 1403-1414.

Aylward, F. O., Eppley, J. M., Smith, J. M., Chavez, F. P., Scholin, C. A., & DeLong, E. F. (2015) Microbial community transcriptional networks are conserved in three domains at ocean basin scales. *Proc Natl Acad Sci U S A* **112:** 5443-5448.

Azam, F. (1998) Microbial control of oceanic carbon flux: the plot thickens. *Science* **280:** 694-696.

Bauer, J. E., Cai, W., Raymond, P. A., Bianchi, T. S., Hopkinson, C. S., & Regnier, P. A. (2013) The changing carbon cycle of the coastal ocean. *Nature* **504:** 61-70.

Bauer, M., et al. (2006) Whole genome analysis of the marine Bacteroidetes 'Gramella forsetii'reveals adaptations to degradation of polymeric organic matter. *Environ Microbiol* **8:** 2201-2213.

Beman, J. M., Popp, B. N., & Francis, C. A. (2008) Molecular and biogeochemical evidence for ammonia oxidation by marine Crenarchaeota in the Gulf of California. *The ISME Journal* **2:** 429-441.

Beman, J. M., Steele, J. A., & Fuhrman, J. A. (2011) Co-occurrence patterns for abundant marine archaeal and bacterial lineages in the deep chlorophyll maximum of coastal California. *The ISME Journal* **5:** 1077-1085.

Bengtsson, M. M., Sjøtun, K., Lanzén, A., & Øvreås, L. (2012) Bacterial diversity in relation to secondary production and succession on surfaces of the kelp Laminaria hyperborea. *The ISME journal* **6:** 2188-2198.

Bograd, S. J., & Lynn, R. J. (2001) Physical-biological coupling in the California Current during the 1997–99 El Niño-La Niña Cycle. *Geophys Res Lett* **28:** 275-278.

Booth, J. A. T., et al. (2012) Natural intrusions of hypoxic, low pH water into nearshore marine environments on the California coast. *Cont Shelf Res* **45:** 108-115.

Bowman, J. S., Amaral-Zettler, L. A., Rich, J. J., Luria, C. M., & Ducklow, H. W. (2017) Bacterial community segmentation facilitates the prediction of ecosystem function along the coast of the western Antarctic Peninsula. *The ISME Journal* 1-12.

Boyd, P., & Newton, P. (1995) Evidence of the potential influence of planktonic community structure on the interannual variability of particulate organic carbon flux. *Deep Sea Research Part I: Oceanographic Research Papers* **42:** 619-639.

Brown, M. V., Schwalbach, M. S., Hewson, I., & Fuhrman, J. A. (2005) Coupling 16S-ITS rDNA clone libraries and automated ribosomal intergenic spacer analysis to show marine microbial diversity: development and application to a time series. *Environ Microbiol* **7:** 1466-1479.

Campbell, L., Liu, H., Nolla, H. A., & Vaulot, D. (1997) Annual variability of phytoplankton and bacteria in the subtropical North Pacific Ocean at Station ALOHA during the 1991–1994 ENSO event. *Deep Sea Research Part I: Oceanographic Research Papers* **44:** 167-192.

Capone, D. G., & Hutchins, D. A. (2013) Microbial biogeochemistry of coastal upwelling regimes in a changing ocean. *Nature Geoscience* **6:** 711-717.

Carlson, C. A., Giovannoni, S. J., Hansell, D. A., Goldberg, S. J., Parsons, R., & Vergin, K. (2004) Interactions among dissolved organic carbon, microbial processes, and community structure in the mesopelagic zone of the northwestern Sargasso Sea. *Limnol Oceanogr* **49:** 1073-1083.

Chavez, F. P. (1996) Forcing and biological impact of onset of the 1992 El Niño in central California. *Geophys Res Lett* **23:** 265-268.

Chavez, G. P. (2006) Seeing the future in the stratified sea. *2006 MBARI Annual Report*: 16-18.

Cottrell, M. T., & Kirchman, D. L. (2000) Natural assemblages of marine proteobacteria and members of the Cytophaga-Flavobacter cluster consuming low- and high-molecular-weight dissolved organic matter. *Appl Environ Microbiol* **66:** 1692-1697.

Dalenberg, J., & Jager, G. (1989) Priming effect of some organic additions to 14C-labelled soil. *Soil Biol Biochem* **21:** 443-448.

DeGrandpre, M., Hammar, T., & Wirick, C. (1998) Short-term pCO 2 and O 2 dynamics in California coastal waters. *Deep Sea Research Part II: Topical Studies in Oceanography* **45:** 1557-1575.

Delille, D., Marty, G., Cansemi-Soullard, M., & Frankignoulle, M. (1997) Influence of subantarctic Macrocystis bed metabolism in diel changes of marine bacterioplankton and CO2 fluxes. *J Plankton Res* **19:** 1251-1264.

DeLong, E. F., Franks, D. G., & Alldredge, A. L. (1993) Phylogenetic diversity of aggregate-attached vs. free-living marine bacterial assemblages. *Limnol Oceanogr* **38:** 924-934.

Duarte, C. M., & Agusti, S. (1998) The CO2 balance of unproductive aquatic ecosystems. *Science* **281:** 234-236.

Duggins, D. O., Eckman, J. E., & Sewell, A. T. (1990) Ecology of understory kelp environments. II. Effects of kelps on recruitment of benthic invertebrates. *J Exp Mar Biol Ecol* **143:** 27-45.

Duran-Pinedo, A. E., Paster, B., Teles, R., & Frias-Lopez, J. (2011) Correlation network analysis applied to complex biofilm communities. *PLoS One* **6:** e28438.

Fuhrman, J., & Azam, F. (1982) Thymidine incorporation as a measure of heterotrophic bacterioplankton production in marine surface waters: evaluation and field results. *Mar Biol* **66:** 109-120.

Fuhrman, J., & Davis, A. (1997) Widespread Archaea and novel Bacteria from the deep sea as shown by 16S rRNA gene sequences. *Mar Ecol Prog Ser* **150:** 275-285.

Gattuso, J., Peduzzi, S., Pizay, M., & Tonolla, M. (2002) Changes in freshwater bacterial community composition during measurements of microbial and community respiration. *J Plankton Res* **24:** 1197-1206.

Gerard, V. (1986) Photosynthetic characteristics of giant kelp (Macrocystis pyrifera) determined in situ. *Mar Biol* **90:** 473-482.

Giebel, H., al. (2013) Planktomarina temperata gen. nov., sp. nov., belonging to the globally distributed RCA cluster of the marine Roseobacter clade, isolated from the Gilbert, J. A.,

Steele, J. A., Caporaso, J. G., Steinbrück, L., Reeder, J., Temperton, B. et al. (2012) Defining seasonal marine microbial community dynamics. *The ISME journal* **6:** 298-308.

Giovannoni, S. J., & Vergin, K. L. (2012) Seasonality in Ocean Microbial Communities. *Science* **335:** 671-676.

Gonzalez, J. M., et al. (2008) Genome analysis of the proteorhodopsin-containing marine bacterium Polaribacter sp. MED152 (Flavobacteria). *Proc Natl Acad Sci U S A* **105:** 8724-8729.

Guenet, B., Danger, M., Abbadie, L., & Lacroix, G. (2010) Priming effect: bridging the gap between terrestrial and aquatic ecology. *Ecology* **91:** 2850-2861.

Guidi, L., et al. (2009) Effects of phytoplankton community on production, size, and export of large aggregates: A world-ocean analysis. *Limnol Oceanogr* **54:** 1951-1963.

Guidi, L., et al. (2016) Plankton networks driving carbon export in the oligotrophic ocean. *Nature* **532**: 465-470.

Haroon, M. F., Thompson, L. R., & Sting, U. (2016) Draft genome sequence of uncultured SAR324 bacterium lautmerah10, Binned from a Red Sea metagenome. *Genome Announc* **4:** e01711-15.

Hayden, C. J., & Beman, J. M. (2014) High abundances of potentially active ammonia-oxidizing bacteria and archaea in oligotrophic, high-altitude lakes of the Sierra Nevada, California, USA. *PLoS one* **9:** e111560.

Huse, S. M., Welch, D. M., Morrison, H. G., & Sogin, M. L. (2010) Ironing out the wrinkles in the rare biosphere through improved OTU clustering. *Environ Microbiol* **12:** 1889-1898.

Johnson, K. S. (2010) Simultaneous measurements of nitrate, oxygen, and carbon dioxide on oceanographic moorings: Observing the Redfield ratio in real time. *Limnol Oceanogr* **55:** 615-627.

Kalvelage, T., al. (2015) Aerobic microbial respiration in oceanic oxygen minimum zones. *PloS one* **10:** e0133526.

Karner, M. B., DeLong, E. F., & Karl, D. M. (2001) Archaeal dominance in the mesopelagic zone of the Pacific Ocean. *Nature* **409:** 507-510.

Keating, K. (2013) Seasonal variation of diatoms and dinoflagellates in Monterey Bay, CA determined by CHEMTAX analysis of HPLC pigment data. Master's Thesis.

Kirchman, D. L. (2008) New light on an important microbe in the ocean. *Proc Natl Acad Sci U S A* **105:** 8487-8488.

Kozich, J. J., Westcott, S. L., Baxter, N. T., Highlander, S. K., & Schloss, P. D. (2013) Development of a dual-index sequencing strategy and curation pipeline for analyzing amplicon sequence data on the MiSeq Illumina sequencing platform. *Appl Environ Microbiol* **79:** 5112-5120.

Kunin, V., Engelbrektson, A., Ochman, H., & Hugenholtz, P. (2010) Wrinkles in the rare biosphere: pyrosequencing errors can lead to artificial inflation of diversity estimates. *Environmental microbiology* **12:** 118-123.

Kuzyakov, Y., & Bol, R. (2006) Sources and mechanisms of priming effect induced in two grassland soils amended with slurry and sugar. *Soil Biol Biochem* **38:** 747-758.

Lafay, B., Ruimy, R., De Traubenberg, C. R., Breittmayer, V., Gauthier, M. J., & Christen, R. (1995) Roseobacter algicola sp. nov., a new marine bacterium isolated from the phycosphere of the toxin-producing dinoflagellate Prorocentrum lima. *Int J Syst Evol Microbiol* **45:** 290-296.

Langfelder, P., & Horvath, S. (2008) WGCNA: an R package for weighted correlation network analysis. *BMC Bioinformatics* **9:** 559.

Langfelder, P., & Horvath, S. (2007) Eigengene networks for studying the relationships between co-expression modules. *BMC systems biology* **1:** 54.

Mann, K. H. (2009) *Ecology of coastal waters: with implications for management.* 2nd Ed. John Wiley & Sons, Hoboken, NJ. 432p.

Mayali, X., Franks, P. J., & Azam, F. (2008) Cultivation and ecosystem role of a marine roseobacter clade-affiliated cluster bacterium. *Appl Environ Microbiol* **74:** 2595-2603.

Michelou, V. K., Caporaso, J. G., Knight, R., & Palumbi, S. R. (2013) The ecology of microbial communities associated with Macrocystis pyrifera. *PLoS One* **8:** e67480.

Moncoiffé, G., Alvarez-Salgado, X. A., Figueiras, F. G., & Savidge, G. (2000) Seasonal and short-time-scale dynamics of microplankton community production and respiration in an inshore upwelling system. *Mar Ecol Prog Ser* **196:** 111-126.

Munro, D. R., Quay, P. D., Juranek, L. W., & Goericke, R. (2013) Biological production rates off the Southern California coast estimated from triple O2 isotopes and O2: Ar gas ratios. *Limnol Oceanogr* **58:** 1312-1328.

NOAA Pacific Fisheries Environmental Laboratory http://www.pfel.noaa.gov/products/PFEL/ Accessed Sept. 16, 2016.

Ohman, M. D., Barbeau, K., Franks, P. J., Goericke, R., Landry, M. R., & Miller, A. J. (2013) Ecological transitions in a coastal upwelling ecosystem. *Oceanography* **26:** 210-219.

Parada, A. E., Needham, D. M., & Fuhrman, J. A. (2015) Every base matters: assessing small subunit rRNA primers for marine microbiomes with mock communities, time series and global field samples. *Environ Microbiol* **18:** 1403-1414.

Pennington, J. T., & Chavez, F. P. (2000) Seasonal fluctuations of temperature, salinity, nitrate, chlorophyll and primary production at station H3/M1 over 1989–1996 in Monterey Bay, California. *Deep Sea Research Part II: Topical Studies in Oceanography* **47:** 947-973.

Regnier, P., et al. (2013) Anthropogenic perturbation of the carbon fluxes from land to ocean. *Nature geoscience* **6:** 597-607.

Riemann, L., Steward, G. F., & Azam, F. (2000) Dynamics of bacterial community composition and activity during a mesocosm diatom bloom. *Appl Environ Microbiol* **66:** 578-587.

Rich, V. I., Pham, V. D., Eppley, J., Shi, Y., & DeLong, E. F. (2011) Time-series analyses of Monterey Bay coastal microbial picoplankton using a 'genome proxy'microarray. *Environ Microbiol* **13:** 116-134.

Robidart, J. C., et al. Seasonal *Synechococcus* and *Thaumarchaeal* population dynamics examined with high resolution with remote *in situ* instrumentation. *The ISME Journal* **6:** 513-523.

Robinson, C., & Williams, P. l. B. (2005) Respiration and its measurement in surface marine waters. *Respiration in aquatic ecosystems* Oxford University Press, NY. p147-180.

Samo, T. J., et al. (2012) Microbial distribution and activity across a water mass frontal zone in the California Current Ecosystem. *J Plankton Res* fbs048.

Santelices, B., & Ojeda, F. (1984) Effects of canopy removal on the understory algal community structure of coastal forests of Macrocystis pyrifera from southern South America. *Marine ecology progress series.* **14:** 165-173.

Serret, P., Fernández, E., & Robinson, C. (2002) Biogeographic differences in the net ecosystem metabolism of the open ocean. *Ecology* **83:** 3225-3234.

Sheik, C. S., Jain, S., & Dick, G. J. (2013) Metabolic flexibility of enigmatic SAR324 revealed through metagenomics and metatranscriptomics. *Environ Microbiol* **16:** 304-317.

Steele, J. A., et al. (2011) Marine bacterial, archaeal and protistan association networks reveal ecological linkages. *The ISME journal* **5:** 1414-1425.

Steneck, R. S., Graham, M. H., Bourque, B. J., Corbett, D., Erlandson, J. M., Estes, J. A., & Tegner, M. J. (2002) Kelp forest ecosystems: biodiversity, stability, resilience and future. *Environ Conserv* **29:** 436-459.

Suzuki, M., Preston, C., Beja, O., De La Torre, J., Steward, G., & DeLong, E. (2004) Phylogenetic screening of ribosomal RNA gene-containing clones in bacterial artificial chromosome (BAC) libraries from different depths in Monterey Bay. *Microb Ecol* **48:** 473-488.

Teeling, H., et al. (2012) Substrate-controlled succession of marine bacterioplankton populations induced by a phytoplankton bloom. *Science* **336:** 608-611.

Treusch, A. H., Vergin, K. L., Finlay, L. A., Donatz, M. G., Burton, R. M., Carlson, C. A., & Giovannoni, S. J. (2009) Seasonality and vertical structure of microbial communities in an ocean gyre. *The ISME journal* **3:** 1148-1163.

Vargas, C. A., et al. (2007) The relative importance of microbial and classical food webs in a highly productive coastal upwelling area. *Limnol Oceanogr* **52:** 1495-1510.

Wehrens, R., & Buydens, L. M. (2007) Self-and super-organizing maps in R: the Kohonen package. *J Stat Softw* **21:** 1-19.

Welschmeyer, N. A. (1994) Fluorometric analysis of chlorophyll a in the presence of chlorophyll b and pheopigments. *Limnol Oceanogr* **39:** 1985-1992.

Williams, P. l. B. (2000) Net production, gross production and respiration: what are the interconnections and what controls what. *The Changing Ocean Carbon Cycle: A Midterm Synthesis of the Joint Global Ocean Flux Study.* Cambridge University Press, Cambridge 37-60.

Williams, P. (1981) Microbial contribution to overall marine plankton metabolism-direct measurements of respiration. *Oceanol Acta* **4:** 359-364.

Woebken, D., Fuchs, B. M., Kuypers, M. M., & Amann, R. (2007) Potential interactions of particle-associated anammox bacteria with bacterial and archaeal partners in the Namibian upwelling system. *Appl Environ Microbiol* **73:** 4648-4657.

Wright, T. D., Vergin, K. L., Boyd, P. W., & Giovannoni, S. J. (1997) A novel delta-subdivision proteobacterial lineage from the lower ocean surface layer. *Appl Environ Microbiol* **63:** 1441-1448.

Zachos, J. C., Dickens, G. R., & Zeebe, R. E. (2008) An early Cenozoic perspective on greenhouse warming and carbon-cycle dynamics. *Nature* **451:** 279-283.

3.7 Tables

Table 3-1 Weighted gene correlation network analysis identified seven modules (or subnetworks), based on the co-occurrence of OTUs. Table 3-1A shows the Pearson correlation coefficient of each module with environmental variables or CR when P<0.05. Table 3-1B identifies modules from Table 3-1A for which OTU module membership significantly correlated with the OTU Pearson correlation for each environmental variables or CR using linear regression. Table 3-1C is a refined version of Table 3-1A after taking into account the results from Table 1B, allowing us to refine which modules we assessed.

A

Module	Depth	UpwellingS	UpwellingN	PreUpwellingS	PreUpwellingN	CR	Oxygen	Temperature	Salinity	PO_4^{3-}	Chl	Fluor
1		0.58	0.58	0.51	0.5			-0.65	0.6			
2	0.52					-0.53	-0.65	-0.31		0.41		
3		-0.5	-0.57	-0.52	-0.54			0.48	-0.35	-0.4	-0.4	
4			-0.37	-0.43	-0.51			0.41		-0.32		0.69
5				-0.44	-0.32							
6	-0.3					0.43		0.56				
7								0.38				

B

1		Yes	Yes	Yes	Yes			Yes	Yes			
2	Yes					Yes	Yes	No		No		
3		Yes	Yes	Yes	Yes			Yes	No	Yes	Yes	
4			Yes	Yes	Yes			Yes		No		Yes
5				Yes	Yes							
6	Yes					Yes		Yes				
7								Yes				

C

1		0.58	0.58	0.51	0.5			-0.65	0.6			
2	0.52					-0.53	-0.65					
3		-0.5	-0.57	-0.52	-0.54			0.48		-0.4	-0.4	
4			-0.37	-0.43	-0.51			0.41				0.69
5				-0.44	-0.32							
6	-0.3					0.43		0.56				
7								0.38				

Table 3-2 Linear regression results relating the sum of the Hellinger transformed OTU abundances for the two modules that significantly correlated with CR to each environmental variable that was also significantly correlated with said module. Table 3-2A relates the sum of the Hellinger transformed OTU abundances of the entire module (64 OTUs for Module 2 and 135 OTUs for Module 6) to each variable while Table 3-2B relates the OTUs with the most significant OTU Pearson's correlation coefficients for CR to each variable (the top 7 OTUs for Module 2 and the top 12 OTUs for Module 12).

	Module	Dependent Variable	r^2	p-val
A	2	CR	0.283	0.003
	6	CR	0.262	0.005
	2	Oxygen	0.477	<0.001
	6	Temperature	0.343	<0.001
	2	Depth	0.301	<0.001
	6	Depth	0.163	0.005
B	2	CR	0.391	<0.001
	6	CR	0.493	<0.001
	2	Oxygen	0.36	<0.001
	6	Temperature	0.158	0.011
	2	Depth	0.182	0.0003
	6	Depth	0.116	0.019

Table 3-3 Taxa identification for top 7 OTUs in Module 2 and top 12 OTUs in Module 6, as identified by WGCNA. Additionally, each OTU's Pearson Correlation to CR, the p-value for that relationship, and each OTU's module membership is reported. Taxonomy was determined by classifying the 16S rRNA sequences based on the SILVA (version 123) database in mothur. Unclassified cyanobacterial chloroplasts were identified using BLASTn (https://blast.ncbi.nlm.nih.gov/Blast.cgi?PAGE_TYPE=BlastSearch). We reported cultured organisms when possible.

OTU	Taxa Identification	OTU Pearson Correlation to CR	OTU p-val for correlation to CR	Module Membership Pearson Correlation	p-val for Module Membership
Module 2					
200	Verrucomicrobia;Arctic97B-4_marine_group;Arctic97B-4_marine_group_unclassified;Arctic97B-4_marine_group_unclassified	-0.5473	6.86E-05	0.763333	4.41E-10
197	Thaumarchaeota;Marine_Group_I;Unknown_Order;Unknown_Family;Candidatus_Nitrosopumilus	-0.53674	0.000101	0.820468	1.69E-12
430	ProteoDeltaproteoSAR324_clade(Marine_group_B);SAR324_clade(Marine_group_B)_unclassified	-0.51873	0.000187	0.771926	2.12E-10
421	Bacteroidetes;Flavobacteriia;Flavobacteriales;Cryomorphaceae;Owenweeksia	-0.49682	0.000382	0.764498	4.00E-10
369	Bacteroidetes;Flavobacteriia;Flavobacteriales;NS9_marine_group	-0.49569	0.000396	0.642571	1.12E-06
290	Bacteria_unclassified;Bacteria_unclassified;Bacteria_unclassified;Bacteria_unclassified	-0.48804	0.000501	0.68958	8.29E-08
287	ProteoGammaproteoOceanospirillales;OM182_clade	-0.46545	0.000978	0.647944	8.50E-07
Module 6					
545	ProteoAlphaproteoRhodobacterales;Rhodobacteraceae;Planktomarina	0.647465	8.71E-07	0.13347	0.37111
667	Bacteroidetes;Flavobacteriia;Flavobacteriales;Flavobacteriaceae	0.629011	2.19E-06	0.446814	0.001641
5	Bacteroidetes;Flavobacteriia;Flavobacteriales;Flavobacteriaceae	0.614087	4.41E-06	0.192862	0.194005
145	CyanoChloroplast;Chloroplast_unclassified;Chloroplast_unclassified Top 3 Blasts: Uncultured *Emiliania*, *Teleaulax amphioxea*, *Dinophysis acuminata*	0.601355	7.81E-06	0.779616	1.07E-10
393	Bacteroidetes;Flavobacteriia;Flavobacteriales;Flavobacteriaceae	0.600253	8.20E-06	0.509956	0.000251
60	ProteoAlphaproteoRhodobacterales;Rhodobacteraceae;Lentibacter	0.584385	1.61E-05	0.51325	0.000225
77	CyanoChloroplast;Chloroplast_unclassified;Chloroplast_unclassified Top 3 Blasts: *Haptolina hirta*, *Prymnesium kappa*, *Haptolina*	0.575328	2.33E-05	0.52488	0.000152
299	Bacteroidetes;Flavobacteriia;Flavobacteriales;NS9_marine_group	0.516648	0.000201	0.67569	1.88E-07
556	Bacteroidetes;Flavobacteriia;Flavobacteriales;Cryomorphaceae;Crocinitomix	0.505308	0.000292	0.267835	0.068735
190	CyanoChloroplast;Chloroplast_unclassified;Chloroplast_unclassified Top 2 Blasts: *Teleaulax acuta*, *Dinophysis acuminata*	0.495852	0.000394	0.76922	2.68E-10
111	CyanoChloroplast;Chloroplast_unclassified;Chloroplast_unclassified Top 3 Blasts: *Pyramimonas disomata*, *Pyramimonas sp. Pyramimonas sp.*	0.476597	0.000707	0.745276	1.87E-09
210	CyanoChloroplast;Chloroplast_unclassified;Chloroplast_unclassified Top 3 Blasts: Uncultured *cryptophyte*, Uncultured *Emiliania*	0.47538	0.000733	0.776158	1.46E-10

3.8 Figures



Figure 3-1 Station locations in Monterey Bay, California: one inside the kelp forest (Station K) and one outside the kelp forest (Station O).

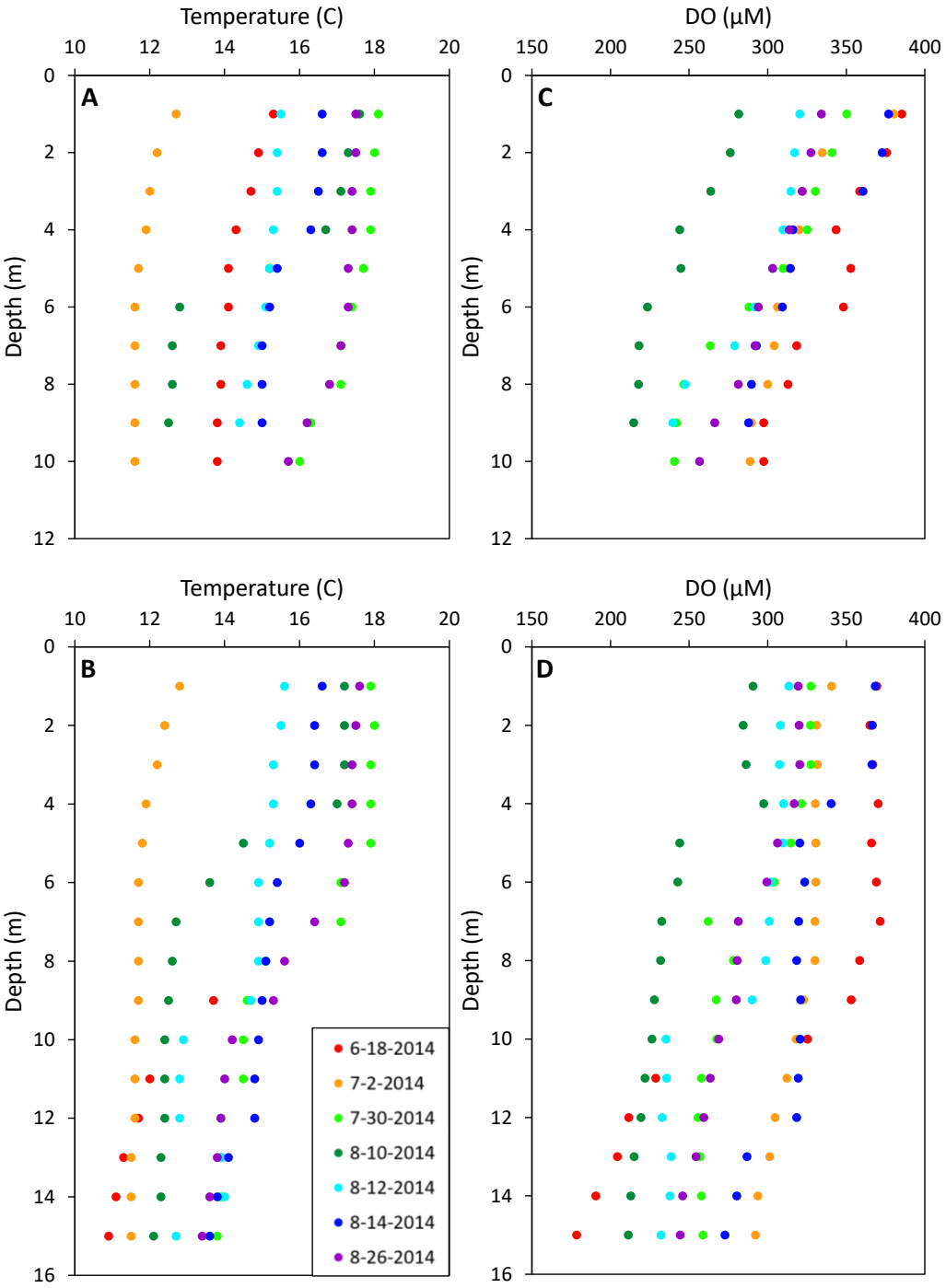


Figure 3-2 Temperature profiles for A) Station K and B) Station O. Oxygen profiles for C) Station K and D) Station O. Colors depict different sampling dates. Total sampling depth was 1m above the bottom at Station K (which changed depending on the tide). Sampling depth was 15m at Station O.

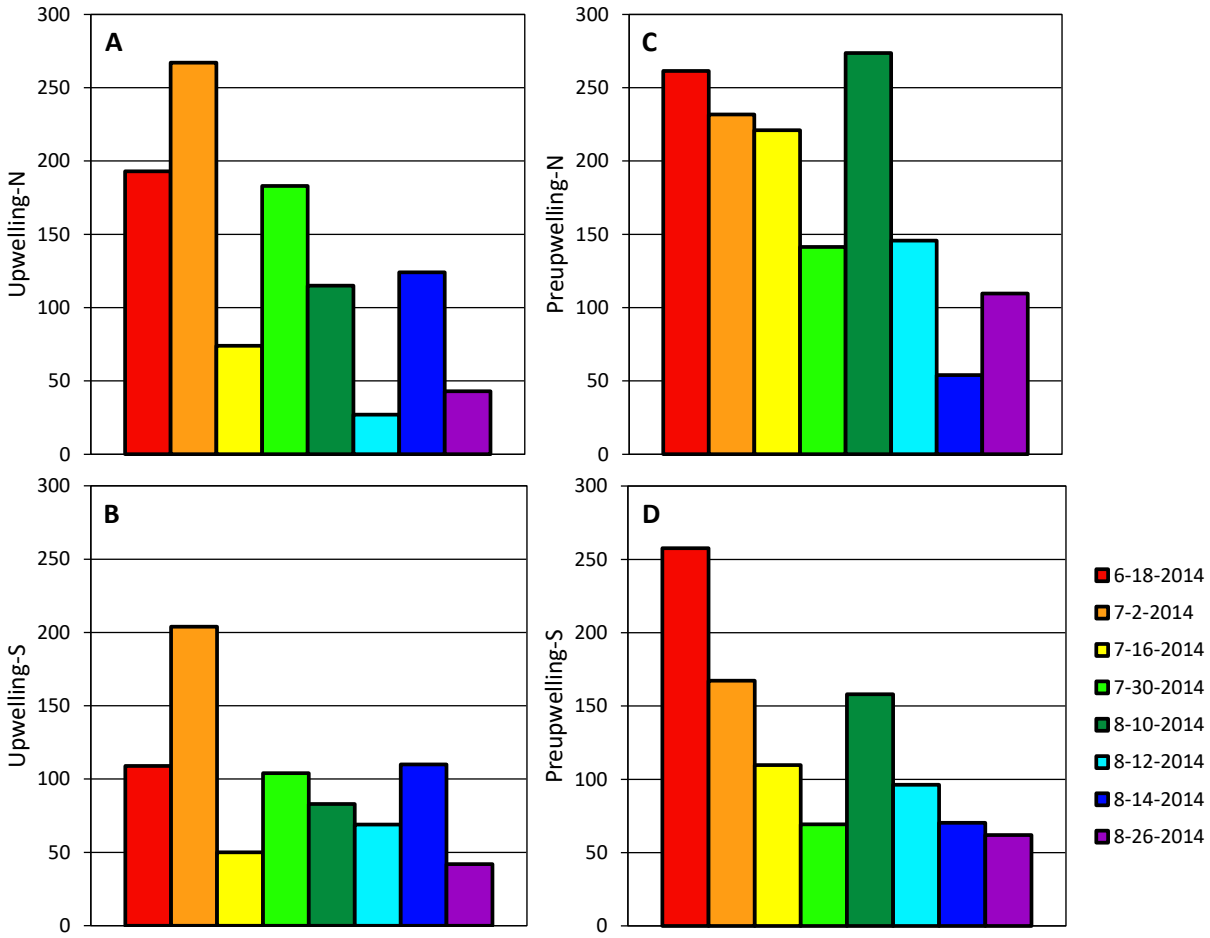


Figure 3-3 Upwelling Indexes from NOAA Pacific Fisheries Environmental Laboratory website (http://www.pfel.noaa.gov/products/PFEL/) for A) the date of interest at an area North of the two stations (39°N 125°W) termed Upwelling-N, B) for the date of interest at an area South of the two stations (36°N 122°W) termed Upwelling-S, C) a mean value for the three days leading up to the date of interest at the Northern site termed Preupwelling-N, and D) a mean value for the three days leading up to the date of interest at the Southern site termed Preupwelling-S.

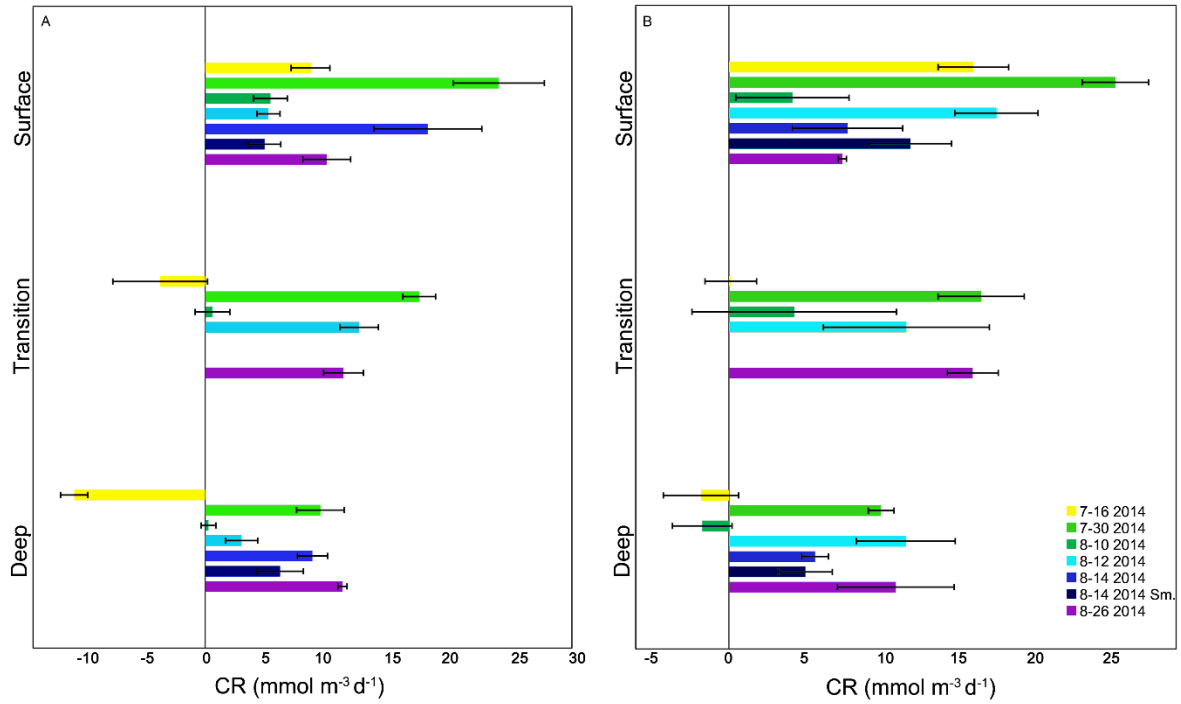


Figure 3-4 Community respiration (CR) for A) Station K and B) Station O according to date (color). Bars represent standard error.

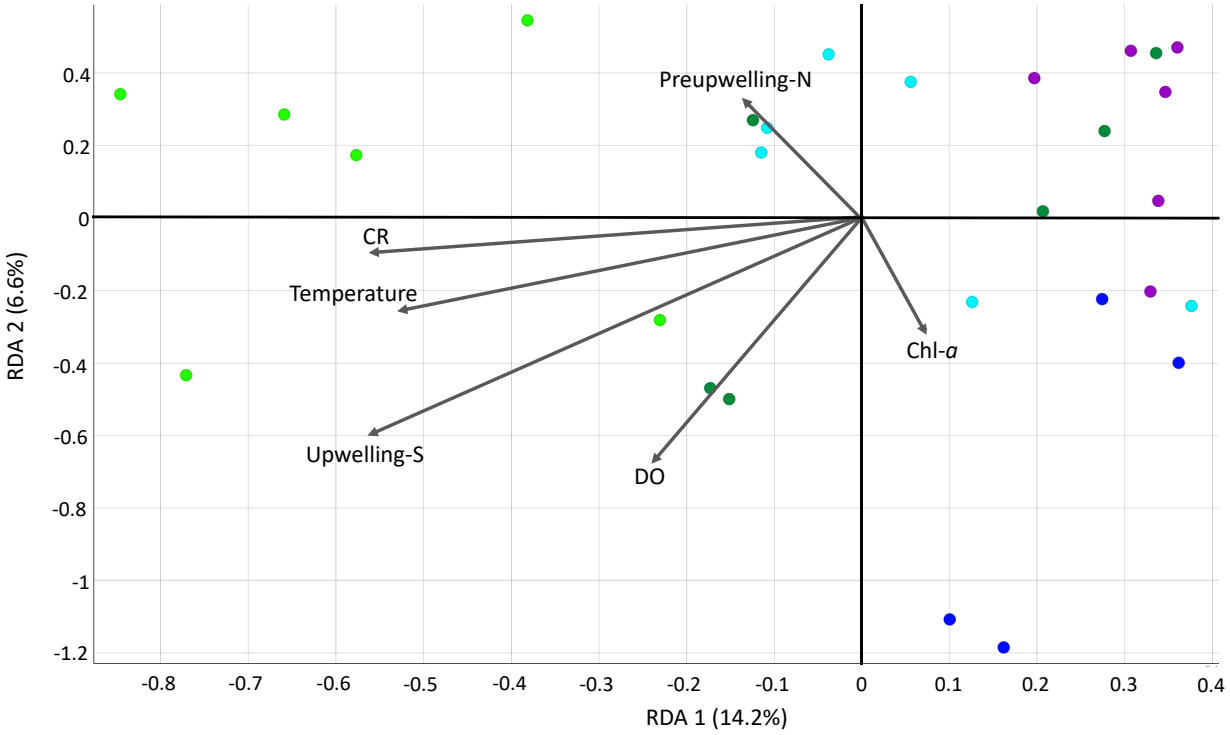


Figure 3-5 Redundancy Analysis of Hellinger transformed OTU abundance matrix for the subsampled microbial community (carried out with the vegan package in R). Dots represent sample scores (weighted sums of OTU scores for each sample) and vectors correspond to the amount of variation explained by each variable. Color depicts sampling date.

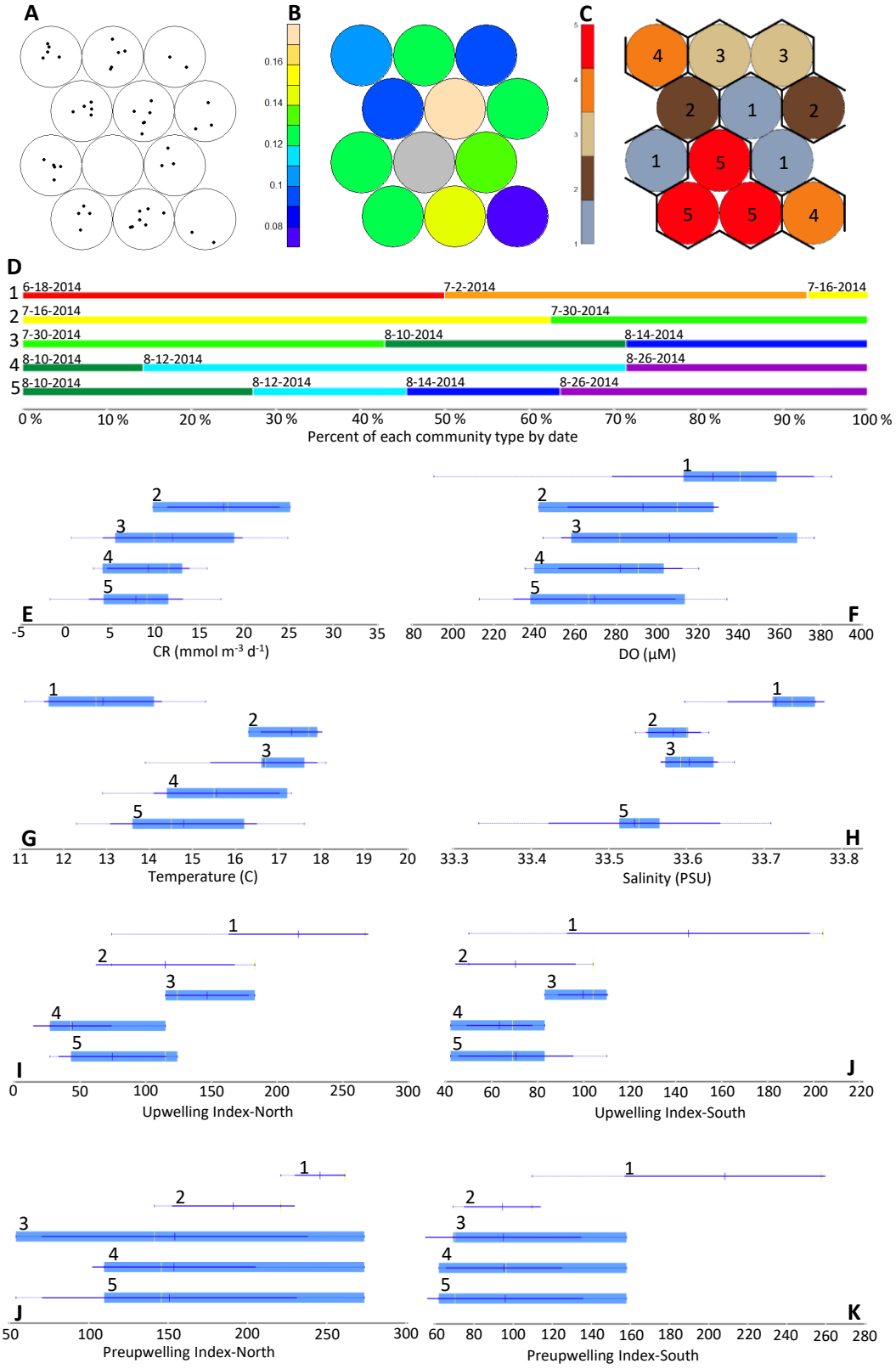

A
B
C
D
1 6-18-2014 7-2-2014 7-16-2014
2 7-16-2014 7-30-2014
3 7-30-2014 8-10-2014 8-14-2014
4 8-10-2014 8-12-2014 8-26-2014
5 8-10-2014 8-12-2014 8-14-2014 8-26-2014
0 % 10 % 20 % 30 % 40 % 50 % 60 % 70 % 80 % 90 % 100 %
Percent of each community type by date
E
CR (mmol m-3 d-1)
F
DO (µM)
G
Temperature (C)
H
Salinity (PSU)
I
Upwelling Index-North
J
Upwelling Index-South
J
Preupwelling Index-North
K
Preupwelling Index-South

Figure 3-6 ESOM identified five main microbial community types. Initial sequence sorting allowed for A) a mapping plot to be made in which each dot corresponds to a different sample and the similarity of samples is represented by the distance to other dots. Similar samples (closely clustered) are assigned to a circular node in a hexagonal grid and the two-dimensional map represents a three-dimensional edgeless toroidal configuration. B) Next a distance plot was made in which the color depicts the similarity of each map unit to the samples within in it—a shorter distance between map unit and samples means that the samples are better defined by the map. C) The mapping plot was clustered allowing for five community types, with community type (1-5) color coded and the lines dividing the circular nodes visible (this map represents a three-dimensional edgeless toroid). Finally, community types were plotted according to D) date, E) CR, F) DO, G) temperature, H) salinity, and I-L) each measure of upwelling.

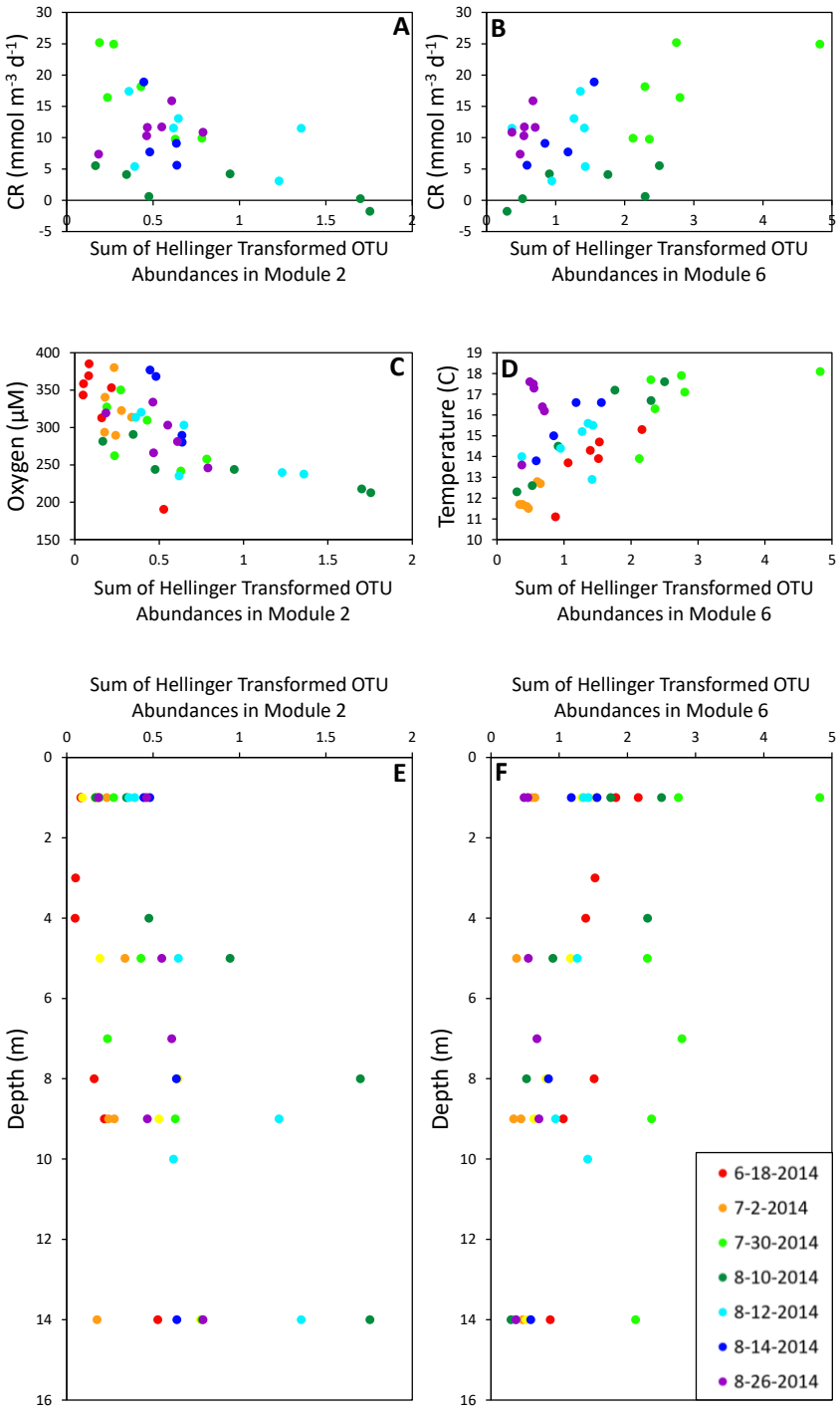


Figure 3-7 The sum of the Hellinger transformed abundances of A) Module 2 OTUs (64 OTUs in all) versus CR, B) the sum of Hellinger transformed abundances of Module 6 OTUs (135 OTUs in all) versus CR, C) the sum of Hellinger transformed abundances of Module 2 OTUs versus DO, D) the sum of Hellinger transformed abundances of Module 6 OTUs versus DO, E) the sum of Hellinger transformed abundances of Module 2 OTUs versus depth, and F) the sum of Hellinger transformed abundances of Module 6 OTUs versus depth. Color denotes date (see legend).

4 Primary production, community respiration, and net community production along oxygen and nutrient gradients: environmental controls and biogeochemical feedbacks within and across 'marine lakes'

4.1 Abstract

Declining ocean oxygen content driven by anthropogenic climate change has wide ranging ramifications for marine ecosystems. These effects are significant but complex at the upper margins of expanding oxygen minimum zones (OMZs), where deoxygenation and biogeochemical feedbacks to low dissolved oxygen (DO) are regulated by biological production and consumption of DO via gross primary production (GPP) and community respiration (CR). We used 'marine lakes'—bodies of seawater surrounded by land—as a natural experimental system for examining the environmental factors that dictate coupling and de-coupling between GPP and CR. Distinct gradients in DO (from fully oxygenated to anoxic conditions), temperature, light, quantity and quality of organic matter, presence of key nutrients, and microbial community structure occur across multiple stratified meromictic lakes and well-mixed holomictic marine lakes present in Palau. We found consistently high GPP rates in stratified meromictic lakes (>10 mmol O_2 m^{-3} d^{-1})—especially near the chemocline, where nutrients diffuse upwards from anoxic waters—and a wider range of rates in well-mixed lakes (0.350 to 57.9 mmol O_2 m^{-3} d^{-1}). In contrast to GPP, CR rates were typically lower and less variable across different depths and lakes. Most depths in most lakes were therefore net autotrophic (i.e., net community production [NCP] > 0). However, experimental additions of ammonium (5 μM) and labile organic carbon (100 μM) had strong effects on CR, resulting in (i) several-fold increases in CR, (ii) larger increases in CR in meromictic lakes with chemoclines near the surface, and (iii) the occurrence of net heterotrophy and DO consumption. Our results are indicative of several biogeochemical feedback mechanisms to deoxygenation present at the upper margins of shoaling OMZs that are governed by nutrient turnover. In marine lakes, these feedbacks can have strong effects on nutrient uptake and the production and consumption of oxygen, with implications for carbon, nutrient, and oxygen cycling throughout large areas of the ocean.

4.2 Introduction

The availability of dissolved oxygen (DO) is a fundamental aspect of marine ecosystems that ultimately controls both the chemical compounds and biota present in a given region of the ocean (Ulloa et al., 2012; Wright et al., 2012; Gilly et al., 2013). DO concentrations are governed by the physiochemical properties of seawater, as well as the biological production and consumption of oxygen and organic matter via photosynthesis and respiration. Throughout the ocean, DO and organic matter are produced only in the well-lit upper ocean, but can be consumed throughout the water column. In areas of high surface production and slow resupply of oxygen at depth (compared to the rate it is respired), DO concentrations are reduced to low levels at depth. Low DO concentrations are found in a variety of marine ecosystems, from enclosed bays and basins to large oxygen minimum zones (OMZs; defined by DO of <20 μM; Paulmier & Ruiz-Pino, 2009) located in the Eastern Pacific Ocean and Arabian Sea. In all of these regions, ocean warming has

the potential to drive further deoxygenation and oxygen loss through reduced oxygen solubility and changes in physical mixing (Keeling et al., 2010).

However, fully understanding ocean biogeochemical responses to deoxygenation is challenging owing to multiple biogeochemical feedbacks to low DO that are superimposed on physiochemical changes (Paulmier et al., 2011). In particular, both biological production of DO via gross primary production (GPP), and DO consumption via community respiration (CR), may change as the ocean warms and loses oxygen (Gregg et al., 2005; Behrenfeld et al., 2006; Bakun et al., 2010; Doney et al., 2012; Regaudie-de-Gioux & Duarte, 2012). Quantifying the net balance of these processes—and how they are arrayed along depth gradients of nutrients, light, temperature, and DO itself—is therefore essential. In the waters above OMZs, upwelled and regenerated nutrients stimulate high primary production at the surface, which provides ample organic matter to be respired as it sinks, reinforcing low oxygen waters below. If upwelling increases due to climate change (Bakun et al., 2010; Doney et al., 2012), or low oxygen/high nutrient areas shoal (Stramma et al., 2008; Gilly et al., 2013), then increased GPP could enhance CR and deoxygenation at depth. However, additional changes in nutrient cycling—and particularly the loss of available nitrogen (N) through anaerobic microbial activity in OMZs (Ward et al., 2009; Dalsgaard et al., 2012)—could directly affect rates of GPP and CR by altering the relative availability of nutrients (Elser et al., 2000; Moore et al., 2013). GPP and CR tend to be tightly coupled in many oceanic environments (Bograd & Lynn, 2001; Robinson & Williams, 2005), but GPP is obviously sensitive to light regimes, while both may be directly sensitive to temperature change (López-Urrutia et al., 2006; Regaudie-de-Gioux & Duarte, 2012). All of these issues are compounded by a lack of CR measurements in large portions of the world's oceans (del Giorgio & Williams, 2005; Robinson & Williams, 2008) including areas with naturally low DO conditions.

We used ‘marine lakes’ as a natural experimental system for examining the environmental factors that dictate coupling and de-coupling between GPP and CR. Marine lakes formed as rising sea levels flooded inland basins, creating bodies of seawater surrounded by land (Hamner & Hamner, 1998; Dawson, 2006). Porous karst limestone allows varying connections between each marine lake with the outside sea, and the degree of connectivity is mostly dependent on a lake's distance inland (Hamner & Hamner, 1998; Colin, 2009). This varying level of connectivity, along with a lake's size and depth, dictate its degree of stratification (Hamner & Hamner, 1998). Consequently, marine lakes in Palau range from well-mixed holomictic lakes—which contain marine fauna such as corals, sponges, and sharks—to stratified, meromictic lakes (Colin, 2009). Across these different lakes, distinct gradients in DO (from fully oxygenated to anoxic conditions), temperature, light, the flux of organic material, the presence of key nutrients, and microbial community structure occur (Burnett et al., 1988; Hamner & Hamner, 1998; Meyerhof et al., 2016). In stratified meromictic lakes, the depths at which low DO values occur (6-18 m) are much shallower than in open ocean OMZs, and allow us to sample along oxygen gradients without spanning vast vertical and horizontal areas. This provides a natural, replicated experimental system where it is possible to study biogeochemical processes across multiple environmental gradients.

In Palau, we studied a gradient of sites ranging from a cove that lies within Palau’s barrier reef lagoon; to two lakes that are well-connected to the surrounding ocean/lagoon, are well-mixed

(holomictic), and are typically oligotrophic; to two less-connected holomictic lakes; to three stratified meromictic lakes that vary in the depth of and vertical extent of anoxia (i.e., the depth of chemocline and total depth of lake). Across this cove, four holomictic lakes, and three meromictic lakes (Figure 4-1), we quantified GPP, CR, and net community production (NCP) at multiple depths—allowing us to identify variations in absolute rates and the relative balance of these processes. In order to quantify the effects of individual environmental variables that may be important in regulating GPP, CR, and NCP, two types of experimental manipulations were also conducted:

1) Experimental additions of N and labile organic carbon (C) tested the degree to which GPP, CR, and NCP may be affected by N and C availability. We hypothesized that both GPP and CR may be limited by N to varying degrees, leading to varying effects on NCP. In particular, we hypothesized that N removal in more deoxygenated lakes may lead to stronger N limitation of GPP and possible N limitation of CR, while holomictic lakes may be P-limited and show no response to N additions. We expected that C additions would have no obvious effects on GPP, but would increase CR, particularly in holomictic lakes that lack available C. Finally, we hypothesized co-additions of C and N could produce interactive effects (e.g., through complementarity), leading to strong increases in CR.

2) The effects of light and temperature on GPP, CR, and NCP were evaluated by 'transplanting' bottles to new depths. We expected that changing light regimes would have obvious effects on GPP but little to no effect on CR, whereas CR would be more temperature sensitive than GPP.

Coupled with the natural gradients available in marine lakes, experimental manipulations allowed us to identify existing patterns and variations in GPP, CR, and NCP and the degree to which variations in N, C, light, and temperature may subsequently alter these patterns. We were able to elucidate some of the biogeochemical controls on metabolism in these tropical marine lakes, which may be applicable to other marine ecosystems.

4.3 Methods

4.3.1 Study sites

Figure 4-1 shows the location of sampling sites on a Landsat 8 Operational Land Imager (OLI) Natural Color image collected in June 2016 (https://landsat.usgs.gov/). We examined one protected cove (Risong Cove; RCA) to provide a system that was completely connected to the ocean, for comparison to the marine lakes. Sampled holomictic lakes included Heliofungia (HLO), Mekeald (MLN), Ngeruktabel (NLN), and Uet era Ngchas (ULN). None of these lakes are stratified, but two are well-connected, ocean-like lakes with numerous marine fauna (HLO and MLN; Hamner & Hamner, 1998; Dawson & Hamner, 2005), whereas two are less-connected to the surrounding sea (NLN and ULN). However, surface salinities in all of these holomictic lakes are 32-35 ppt (Hamner & Hamner, 1998; Colin, 2009).

Among meromictic lakes, the depth at which stratification occurs differs between lakes, creating oxyclines of varying intensity (Table 4-1). We examined stratified meromictic lakes with the least extreme oxyclines, including Ngermeuangel Lake (abbreviated NLK), Ongeim'l Tketau

(OTM aka Jellyfish Lake), and T Lake (TLN). Stratification in these lakes is driven by differences in salinity—and therefore density—with depth (Hamner et al., 1982; Hamner & Hamner, 1998). Surface waters are typically 25 ppt in OTM and NLK and increase to 32-33 ppt at depth (Hamner & Hamner, 1998; Meyerhof et al., 2016). T Lake is 'transitional' in that it periodically stratifies but is not permanently meromictic; it was stratified at the time of our sampling. Due to the lack of mixing and oxygen at depth, the concentration of reduced compounds increases greatly with depth in meromictic lakes, with hydrogen sulfide concentrations reaching 2,500 µM below 25 m in OTM (Hamner et al., 1982). However, each of the meromictic lakes possesses a distinct chemocline—an area of sharp increase in reduced compounds as oxygen reaches zero—at a unique depth. Chemocline depths are typically consistent over time in each lake (Hamner & Hamner, 1998).

4.3.2 Temperature, oxygen, and nutrient profiles

Temperature and DO profiles were collected using a YSI ProODO (YSI Incorporated, Yellow Springs, OH, USA). The detection limit for DO was 2.8 µM. Light and temperature were collected for the duration of the incubations by HOBO Dataloggers UA-002-08 (Onset Computer Corporation, Bourne, MA, USA). Dissolved nutrient profiles were collected, and nutrient analyses were conducted both before and after all incubations. For these measurements, water samples were filtered through 0.22 µm Durapore PVDF hydrophilic filters (Millipore, Billerica, MA, USA) and filtrate was collected in high density polyethylene bottles; samples were then frozen and subsequently processed via flow injection analysis at the University of California, Santa Barbara Marine Analytical Laboratory.

Samples were analyzed for ammonium (NH_4^+; UCSB MAL analytical method for NH_4^+, see below; Diamond & Huberty, 1996), nitrite (NO_2^-; Environmental Protection Agency (EPA) Method 353.2; Schroeder, 1997), nitrate+nitrite ($NO_3^- + NO_2^-$; EPA Method 353.2; Diamond, 1997), and phosphate (PO_4^{3-}; EPA Method 365.1; Huberty & Diamond, 1998), on a Lachat QuikChem 8000 Flow Injection Analyzer (Hach Company, Loveland, CO, USA). For all assays, a mid-range check standard took place every 20 samples to verify the accuracy of the measurements, and samples that were detected outside of the standards' range were diluted 1:10 and reanalyzed. Detection limits were 0.10 µM for NH_4^+, 0.10 µM for NO_2^-, 0.20 µM for $NO_3^- + NO_2^-$, and 0.10 µM for PO_4^{3-}. For NH_4^+ measurements, each sample was injected into a flowing carrier stream through an injection valve, and then merged with an alkaline solution stream; the produced NH_3 was diffused through a hydrophobic, gas-permeable membrane into a recipient stream containing a pH indicator. Color change occurs in the indicator solution due to an increase in pH, and the concentration of NH_4^+ was determined spectrophotometrically based on absorption at 570 nm.

N* is a measure of N versus phosphorus (P) availability based on the Redfield ratio (N:P = 16:1; Gruber & Sarmiento, 1997) and was calculated based on nutrient concentrations. The original formulation of N* includes only oxidized dissolved N compounds, as dissolved NH_4^+ is typically found only at low concentrations in the open ocean (Gruber, 2008). However, dissolved NH_4^+ is detectable in Palau's marine lakes and reaches elevated levels below the chemocline in meromictic lakes (see below; Figure 4-3B). We therefore included NH_4^+ in the N pool in our revised N* calculations according to equation 1:

$$N^* = (NO_3^- + NO_2^- + NH_4^+) - 16*PO_4^{3-} \quad \text{(eq. 1)}$$

4.3.3 Production and respiration rate measurements and experiments

Triplicate light and dark bottle incubations were used to measure NCP and CR throughout the oxic zone of holomictic and meromictic lakes, and into the low DO waters found in meromictic lakes, in 2014 and 2015 (Table 4-1). Depth profiles were collected in five out of seven lakes (HLO, NLN, ULN, NLK, and OTM), while measurements were made only in surface waters of MLN, TLN, and RCA. GPP was calculated by adding the mean value of CR to the mean value of NCP (Morán et al., 2004). Measurements were made in 300 mL Wheaton BOD glass bottles filled to at least two times overflowing via slow laminar flow in order to exclude bubbles. For all lakes, bottles were incubated at the desired depth in each lake on a floating array constructed from cable and PVC pipe and attached to a surface buoy. The buoy was tied off to the sides of the lake to prevent drifting so that all incubations took place under *in situ* conditions. For the cove (RCA), it was not possible to anchor the array, and *in situ* incubations were mimicked by incubating bottles in the ocean at Coral Reef Research Foundation laboratory (Koror, Palau). The start time of all experiments was mid to late morning. All incubations were conducted for 24 hours so that changes in CR with time of day would be integrated and eliminated (Williams, 2000).

During 2015, N and labile organic C additions were conducted for six lakes and RCA, while N additions were conducted at two depths in HLO (Table 4-1). All experiments were conducted in triplicate for both light and dark bottles. Water from 1 m depth was incubated at 1 m (*in situ* for lakes, and at the lab for RCA) as a control. Additionally, 3 treatments consisting of NH_4^+ (5 μM NH_4Cl), sucrose (100 μM $C_{12}H_{22}O_{11}$), and both NH_4^+ + sucrose (at the above concentrations) were also incubated at 1 m. At one lake (HLO), experiments were conducted at both 1 m and 10 m, but only with controls and NH_4^+ additions (at the above concentration). NH_4^+ was used as an N source because the regeneration of NH_4^+ supports a large proportion of primary production throughout the ocean, and because several of the marine lakes have high concentrations of NH_4^+ at depth.

Reciprocal depth 'transplants' were conducted for several lakes (HLO, NLN, ULN, OTM) during both 2014 and 2015. Samples from 1 m and the deepest depth sampled in each lake were incubated at the opposite depth to assess the effect of light and temperature on NCP, CR, and GPP (Table 4-1). The deepest depth was near the lake bottom for holomictic lakes, while it was located just above the chemocline for meromictic lakes. All incubations were conducted in triplicate; however, oxygen contamination in two of the bottles from 10 m incubated at 1 m depth in OTM resulted in a single CR measurement for this treatment. It was therefore not possible to calculate standard errors for CR or for GPP.

All rates are reported in terms of mmol of O_2 produced or consumed (rather than converted into g of C) because (1) terrestrial inputs of organic matter may lead to non-Redfieldien consumption of oxygen and carbon, and (2) the amount of oxygen that is evolved during photosynthesis depends on the type of N utilized by phytoplankton, and (3) directly studying the cycling of oxygen is critically important in low-oxygen ecosystems.

4.3.4 Statistical analyses

GPP, CR, and NCP rates from *in situ* measurements, experimental additions, or transplants were assessed via several statistical approaches. Linear and multiple regressions were performed on *in situ* rates with nutrients, the natural log of light, temperature, initial oxygen concentration, and site as explanatory variables (GPP was also used an explanatory variable for variation in CR). ANOVA was used to test the significance of the regressions. Linear regression was appropriate in all instances except for relating initial DO concentrations to CR, in which case a quadratic regression was performed. For experimental additions and transplants, Cohen's *d* effect sizes were calculated for GPP, CR, and NCP. Cohen's *d* demonstrates the strength of an experimental treatment by dividing the mean difference between treatments by the pooled standard deviation of the two means, and therefore shows the relative size and direction of change for each treatment and rate. For experimental additions and transplants, significant differences in NCP and CR were determined using ANOVA, and Tukey honestly significant difference (HSD) post-hoc tests were utilized to show which treatments/controls differed. It should be noted that end oxygen concentrations were analyzed for Tukey HSD tests in order to obtain replicate measurements because triplicate rate measurements were pooled in order to obtain a rate from pooled T0 concentrations. For experimental transplants, linear and multiple regressions were performed relating GPP, CR, and NCP to the natural log of light and to temperature in order to elucidate the effect of each on rates. ANOVA, linear regression, multiple regression, and best-fit models (as defined by the step function, which utilizes the Akaike Information Criterion) were carried out in the R statistical environment (RStudio Version 0.99.467). Figures were made with plot.ly and Adobe Illustrator.

4.4 Results

4.4.1 Oxygen, temperature, nutrient, and N profiles*

DO decreased with depth for all lake types and the cove, but the intensity of these gradients varied across lakes. For the ocean-like holomictic lakes (HLO and MLN) and the cove (RCA), DO decreased only slightly with increasing depth, and DO concentrations always remained above 180-200 μM (Figure 4-2A). In the less-connected holomictic lakes (NLN and ULN), DO decreased more substantially with depth, dipping below 175 μM but remaining above 140 μM. In the three meromictic lakes, DO concentrations decreased to undetectable levels (< 2.8 μM) at 18 m depth in NLK, 12 m in OTM, and 6 m in TLN. Temperature profiles showed that the holomictic lakes and RCA had very similar temperatures over space (depth) and time, while the meromictic lakes showed more variation (Figure 4-2B). The two deep meromictic lakes (NLK and OTM) showed the greatest depth variation in temperature. In NLK, temperature increased significantly with depth above the chemocline, before then decreasing with depth. In OTM, the decline in temperature took place around the depth at which DO reached undetectable levels, while the temperature decline took place several meters above this zone for NLK.

The stratified meromictic lakes also displayed the greatest change in NH_4^+ and PO_4^{3-}, showing substantial increases with depth below the chemocline, whereas mixed homomictic lakes varied only slightly (Figure 4-3A and B; see also Hamner et al., 1982, Landing et al., 1991). In deeper portions of both OTM and NLK, NH_4^+ exceeded 100 μM and PO_4^{3-} exceeded 5 μM. NO_3^- +

NO_2^- was more variable with depth in all the lakes, but tended to be higher in surface samples in meromictic lakes and increased with depth in holomicitc lakes (Figure 4-3C). Regardless of the specific lake or the depth of collection, $NO_3^- + NO_2^-$ was always below 3 μM. N* is a proxy for the degree of N limitation or excess in marine ecosystems, and reflects underlying biogeochemical processes (Gruber & Sarmiento, 1997). In general, low oxygen marine ecosystems tend to be N depauperate (N*<0) because denitrification and anammox can remove fixed forms of N under low oxygen conditions (Lam & Kuypers, 2011). OTM and TLN (meromictic lakes with shallower chemoclines) were typically N-deficient (N*<0) above the chemocline, while NLK (a meromictic lake with a fairly deep chemocline) typically had N* values very close to 0 near the surface (Figure 4-3D). In all meromictic lakes, N* increased with depth and was strongly positive below the chemocline due to the high concentrations of NH_4^+ (included in our formulation of N*). In contrast, NH_4^+ concentrations were relatively constant and low in holomictic lakes. All holomictic lakes tended to have a slight excess of N based on our formulation of N*.

4.4.2 In situ *rates of GPP, CR, and NCP*

Within and across lakes, we quantified GPP, CR, and NCP using *in situ* light/dark bottle incubations. We found high GPP in meromictic lakes, with all but two of the measurements exceeding 10 mmol O_2 m^{-3} d^{-1} (Figure 4-4A). A wider range of rates was observed in holomictic lakes (0.350±0.660 to 57.9±29.5 mmol O_2 m^{-3} d^{-1}), with 60% of measurements lower than 10 mmol O_2 m^{-3} d^{-1}. For holomictic lakes, GPP tended to be higher near the surface, declining by as much as 95.7% with depth (in HLO on Nov. 4, 2015). The more connected, ocean-like holomictic lakes were generally less productive than the more isolated holomictic lakes (ULN and NLN), which showed moderate but consistent decreases in GPP with depth (49.2-86.2%). In contrast to holomictic lakes, GPP was often higher at depth in meromictic lakes, especially near the chemocline. For example, GPP was 60.6±41.4 mmol O_2 m^{-3} d^{-1} at 12 m depth in OTM on Nov. 05, 2014; this represents a 2620% increase from the surface rate and occurred at the approximate depth of the chemocline on that day. While there was variation in GPP within a site over time, this was minor compared to the variation between sites and with depth. Analyzing GPP and environmental data across all sites, dates, and depths, GPP significantly ($P<0.05$) correlated with PO_4^{3-} concentration ($r^2=0.297$), oxygen concentration ($r^2=0.185$; Figure 4-5A), and NH_4^+ concentration ($r^2=0.102$)—with GPP increasing as each of the nutrients increased, and decreasing at higher O_2 concentrations. In multiple regression, the model that best explained variation in GPP was one that accounted for site, temperature, PO_4^{3-} concentration, NO_2^- concentration, and NO_3^- concentration ($r^2=0.782$, $P<0.001$).

In contrast to GPP, CR was typically lower in magnitude and less variable with depth and across lakes (Figure 4-4B). For holomictic lakes, CR ranged from 0.196±2.18 to 26.6±29.5 mmol O_2 m^{-3} d^{-1}, with these values both observed at the surface in ULN. The ocean-like holomicitc lakes (HLO and MLN) tended to have lower CR rates, with 9 of the 14 measurements below 5 mmol m^{-3} d^{-1} (data from MLN not shown). RCA behaved similarly to these lakes in terms of CR, with a rate of 5.24±0.462 mmol O_2 m^{-3} d^{-1} (data not shown). For meromictic lakes, CR ranged from undetectable levels to 53.6±19.3 mmol O_2 m^{-3} d^{-1} and, similar to GPP, rates tended to increase with depth (up to 263% when the deepest depth was compared to the surface). However, the highest CR rates in meromictic lakes were observed a few meters above the chemocline at 7m in

OTM (53.6±19.3 mmol O_2 m^{-3} d^{-1} in 2014 and 48.2±11.2 mmol O_2 m^{-3} d^{-1} in 2015). Like GPP, CR was significantly correlated with oxygen (r^2=0.340); however, this relationship was nonlinear, with highest CR at intermediate oxygen concentrations (Figure 4-5B). When regressed linearly, CR was not significantly correlated with GPP, but was significantly positively correlated with the natural log of light (r^2=0.156). In multiple regression, accounting for site, GPP, the natural log of light, PO_4^{3-} concentration, NO_2^- concentration, and NO_3^- concentration explained the most variation in CR across all sites, dates, and depths (r^2=0.712).

As the data above indicate, most depths in most lakes were net autotrophic (i.e., NCP > 0 mmol O_2 m^{-3} d^{-1}; Figure 4-4C). This was particularly true for surface samples (1 m), which were almost uniformly autotrophic. For the ocean-like holomictic lakes (HLO and MLN), NCP ranged from -5.69±1.98 mmol O_2 m^{-3} d^{-1} (in MLN, data not shown) to 19.9±1.53 mmol O_2 m^{-3} d^{-1}, with both values observed at the surface. NCP in the more productive holomictic lakes (NLN and ULN) ranged from -9.85±1.7 to 31.3±1.15 mmol O_2 m^{-3} d^{-1}. NCP tended to decrease with increasing depth (by as much as 158% in HLO and 163% in ULN), with deeper samples becoming slightly heterotrophic in ULN and in HLO on certain dates. For meromictic lakes, NCP ranged from -54.9±14.6 to 36.5±17.7 mmol O_2 m^{-3} d^{-1}. In both NLK and OTM, the lowest and most heterotrophic NCP was observed several meters above the chemocline, while the depth sampled nearest the chemocline was autotrophic in each case. In both of these lakes, NCP was therefore positive at the surface, negative at mid-depth, and then strongly positive again near the chemocline. Across all lakes, NCP significantly positively correlated with PO_4^{3-} concentration (r^2=0.114) and the natural log of light (r^2=0.141). In multiple regression, variation in NCP was best-explained by site, the natural log of light, PO_4^{3-} concentration, NO_2^- concentration, and NO_3^- concentration (r^2=0.832).

4.4.3 N and C additions

Experimental additions of NH_4^+ (5 μM), labile C (100 μM), and both N and C, had significant effects on GPP, CR, and NCP (Figure 4-6). Responses varied between treatments, sites, and rate, with Cohen's *d* demonstrating the direction and magnitude of each effect. As we hypothesized, C addition alone had very little effect on GPP, with Cohen's *d* only increasing above 2 for RCA (Figure 4-7A). TLN actually had a slightly negative effect size following C addition (-0.409), but all other values were slightly positive. In contrast to C addition, N addition had much larger effects on GPP: Cohen's *d* values that ranged from slightly negative (RCA, HLO, MLN, and TLN) to significantly positive in NLN, ULN, NLK, and OTM. In general, the highest rates of GPP for both controls and following experimental addition were observed where N*<0. Adding both C and N produced the largest change in GPP in RCA, MLN, NLN, and NLK—with NLK showing a Cohen's *d* of 13.5.

CR rates were typically more responsive than GPP to additions (Figures 4-6B and 4-7B). Adding N caused CR to significantly increase in NLN and NLK (P=0.012 and 0.014, respectively) with Cohen's *d* values <4. Labile C additions caused CR to significantly increase in RCA and ULN (P<0.001 and 0.025, respectively), nearly significantly increase in NLN (P=0.056), and significantly decrease in MLN (P=0.003). An effect size larger than 10 was observed from C additions in RCA. C and N co-additions resulted in a significant several-fold increase in CR at all sites (P<0.001-0.048) but MLN, with the highest Cohen's *d* values observed in RCA and

OTM (60.4 and 45.5, respectively; Figure 4-7B). The highest overall values were observed following C and N co-addition in the meromictic lakes—especially those with chemoclines close to the surface (85.3±9.43 mmol O_2 m^{-3} d^{-1} in TLN and 91.5±1.51 mmol O_2 m^{-3} d^{-1} in OTM)—while RCA and the less-connected holomictic lakes (i.e., NLN and ULN) all had CR values above 40 mmol O_2 m^{-3} d^{-1} following C and N addition.

As the results above indicate, co-additions of C and N yielded the greatest overall changes in NCP (Figure 4-6C). NCP frequently switched from net autotrophy to net heterotrophy (NCP < 0 mmol O_2 m^{-3} d^{-1}), with five of the seven treatments that were subjected C and N co-additions becoming heterotrophic, and displaying Cohen's *d* values of -2.02 to -9.03 (Figure 4-7C). The largest changes in metabolic state were observed in OTM and TLN, followed by NLN and ULN. Neither MLN nor NLK changed metabolic state following C and N addition, but each displayed an increase in NCP, with NLK showing a significant increase in NCP. All changes in metabolic state were significant (P<0.001-0.006), except for ULN (P=0.069). C addition alone caused a change in metabolic state on two occasions, with RCA and TLN each switching from net autotrophy to net heterotrophy (P<0.001 and 0.022; Cohen's *d* of -8.76 and -1.87). None of the other lakes had significant changes in NCP following C additions. Adding NH_4^+ alone significantly affected NCP in NLK, producing a significant increase in autotrophy in that layer of the lake (P=0.015) with an effect size of 2.79. Because lakes and depths with lower N* values had the highest CR following C and N addition, these lakes and depths also yielded the most heterotrophic systems following C and N addition.

Nutrient concentration measurements following experimental additions and 24 hour incubations showed relatively few differences—however, this included bottles to which 5 μM NH_4^+ was added, alone or in combination with C (Table 4-2). NH_4^+ concentrations were elevated in dark bottles following N addition (P<0.05), but NH_4^+ concentrations were similar across controls, C additions, and N and C co-additions.

4.4.4 Rate measurements

We also experimentally quantified the effects of light and temperature on GPP, CR, and NCP by incubating bottles at different depths (although the particular lake and nutrient concentrations also played roles in the observed rates). As expected, GPP increased as the water was moved closer to the surface—the rate actually surpassed the *in situ* rates in some cases (e.g., HLO in 2014 and ULN)—and it decreased as water was moved to deeper depths (Figure 4-8A). Following incubation at a new depth (which depended on overall lake depth and whether a chemocline was present), both light and dark bottles tended to remain significantly different from the control groups—i.e., rates incubated at a new depth differed from both the original depth and the depth they were transplanted to. However, almost all the transplanted bottles became more similar (for both light and dark bottles) to the water at the depth they were incubated.

Cohen's *d* values were generally lower for CR rates than for GPP (data not shown), with the greatest changes observed in ULN—as CR increased in surface water that was moved down (*d*= 3.69)—and in HLO—as CR in deep water that was incubated at the surface decreased (*d*=-2.45). NCP also changed the most with transplantation in ULN and in HLO. These transplants modify light and temperature, and GPP was significantly correlated with the natural log of light when

both controls and transplants were assessed together (P=0.031, r^2=0.292). However, the best multiple regression model for predicting GPP accounted for site, temperature, NO_3^- concentration, and NH_4^+ concentration (P=0.090, r^2=0.718). CR did not show strong responses to transplantation, but regression analysis showed that CR was negatively correlated with temperature across all the lakes for transplanted bottles (P=0.013, r^2=0.365). CR also correlated positively with GPP (P=0.040, r^2=0.215).

4.5 Discussion

The marine lakes of Palau serve as a natural experimental system in which variations in GPP, CR, and NCP along strong environmental gradients can be assessed. We studied a gradient of sites ranging from a cove and lakes that exchange water with the oligotrophic Western Pacific, to stratified meromicitc lakes that resemble other low-oxygen marine ecosystems. Differences among sites are reflected in their biogeochemical properties, including the presence of anoxia at 18 m depth in NLK, 12 m depth in OTM, and 6 m depth in TLN (Figure 4-2A), as well as accompanying variability in nutrient concentrations (Figure 4-3). Within and across lakes, GPP, CR, and NCP showed predictable patterns with depth and in relation to variations in DO, nutrients, temperature and light with depth and across lakes. Coupled with the natural gradients available in marine lakes, experimental manipulations allowed us to test how changes in N, C, light, and temperature may subsequently alter these patterns.

4.5.1 Patterns in GPP, CR, and NCP within and across marine lakes

The holomictic lakes in this study displayed depth patterns in GPP, CR, and NCP that are similar to those that observed throughout much of the ocean. GPP was higher near the surface and declined with depth, while CR was less variable with depth, resulting in net autotrophy near the surface, shifting to near balance or heterotrophic conditions at depth. While the shape of depth profiles were similar to the open ocean (e.g., compare with rates observed along the Atlantic Meridional Transect; Serret et al., 2001), the rate magnitudes in several marine lakes were on the high end of those observed in other marine systems. For example, ULN behaved like a holomictic lake in terms of the metabolic depth profile, but had absolute rates more similar to the meromictic lakes.

Meromictic lakes generally displayed higher overall rates for both GPP and CR that were comparable to other high-nutrient marine ecosystems (Blight et al., 1995; Serret et al., 2001; Gist et al., 2009). Interestingly, the meromictic lakes NLK and OTM displayed consistent depth patterns in GPP, CR, and NCP that differed from those in the holomictic lakes: GPP typically exceeded CR at 1 m depth, as well as near the chemocline (18 m in NLK and 10-12 m in OTM), leading to net autotrophy; CR was greater than GPP in between these depth horizons, leading to net heterotrophy. In NLK, this variation with depth was driven by variations in CR, as GPP was relatively constant with depth. In OTM, variations in both GPP and CR produced these patterns with depth. We attribute net heterotrophy at mid-depths (10 m in NLK and 7 m in OTM) to microbial consumption of sinking organic matter; however, heterotrophy was the exception rather than the rule in marine lakes, as most depths and lakes that were sampled were autotrophic (Figure 4-4). This suggests that despite the presence of productive forested watersheds surrounding marine lakes (a major difference from the open ocean), terrestrial organic material

does not play a large role in their metabolism and C cycle. Previous work in OTM supports this idea. Orem et al. (1991) found that although the sediment of OTM was approximately 50% organic matter, it was dominated by vascular plant material (66 to 91%), suggesting that allochthonus organic matter is not readily metabolized within the lake. Lake microbial communities are also dominated by common marine bacteria ill-equipped to consume terrestrial organic material (Meyerhof et al., 2016).

The peak in GPP near the chemocline in OTM is likely sustained by upward diffusion of nutrients due to the sharp gradient present in this lake. However, OTM is also unique in that it is a 'jellyfish lake' that harbors millions of medusa; the activity of these organisms could lead to biomixing that transfers nutrients into the upper water column (Katija & Dabiri, 2009; Breitburg et al., 2010). Our results from OTM are in line with Hamner et al. (1982), who found similarly high NCP values in the oxygenated surface zone of OTM (0.336 mol O_2 m^{-2} d^{-1} or 30.6 mmol O_2 m^{-3} d^{-1} assuming a chemocline of 11m). In both NLK and OTM, low CR and high NCP near the chemocline suggest a substantial flux of organic matter from the upper portion of the lake into deeper layers. However, Lyons et al. (1996) estimated that in OTM only 4% of autochthonous organic matter is deposited on the lake bottom, with vertical stratification slowing the decent of phytoplankton-derived organic matter. Most organic matter produced in the upper oxygenated zone is therefore remineralized in the lower layers of the lake (either in the suboxic zone or the anoxic zone). Low oxygen would not necessarily halt aerobic respiration, as CR has been directly measured in extremely low oxygen concentrations (Tiano et al., 2014). Particulate organic matter has also been observed to be rapidly recycled in the suboxic portions of the Black Sea (Karl & Knauer, 1991), and aerobic remineralization accounted for ~45-100% of the organic matter that was degraded in the Eastern Tropical South Pacific OMZ (Kalvelage et al., 2015). Aerobic and anaerobic metabolism of sinking organic matter regenerates nutrients, and may create a positive feedback as remineralized nutrients fluxed upward further stimulate GPP. This phenomenon has been observed in OMZs (Karstensen et al., 2008; Deutsch et al., 2011), but is particularly clear in these meromictic marine lakes given the sharp nutrient gradients and high rates of GPP and CR.

4.5.2 Effects of N and C on GPP, CR, and NCP in experimental additions

As the results above indicate, GPP, CR, and NCP rates are tightly linked to nutrient and DO concentrations within and across marine lakes. We analyzed patterns in GPP, CR, and NCP in relation to natural nutrient, oxygen, temperature, and light gradients using regression. Observational measurements within and across the lakes demonstrate the effect of nutrients on these processes because holomictic lakes are well-mixed, with lower concentrations of nutrients, while meromictic lakes are stratified, with much higher concentrations of nutrients (especially below the chemocline). GPP and CR generally increased from ocean-like lakes to deoxygenated meromictic lakes (Figures 4-4 and 4-6); regression analyses showed that GPP was positively correlated with several nutrients (independently and in multiple regression) while CR was related to nutrients during multiple regression. We further tested the effects of N, as well as organic C, using addition experiments that provided additional insight into how N and C influence GPP and CR. One of our hypotheses was that N removal in stratified, deoxygenated meromictic lakes may lead to N limitation of GPP and/or CR, while holomictic lakes may be P-limited and show no response to N additions. We would expect N-limitation to occur in low-oxygen environments

because N is removed through anaerobic activity (Francis et al., 2007; Ward et al., 2009), leading to N deficits relative to P (Beman et al., 2005).

Additions of N alone increased GPP in the holomictic lakes NLN and ULN, and the meromictic lakes NLK and OTM, confirming our hypothesis for these lakes (Figures 4-6 and 4-7). However, TLN had a slightly negative N* value and GPP did not respond to N alone—indicating that either phytoplankton require less N than the typical Redfield ratio dictates (N:P::16:1; Martiny et al., 2013), or that they utilize additional sources of N. For example, Bronk et al. (2007) outlined how the dissolved organic nitrogen pool is a possible N source for phytoplankton. As expected, C addition alone had little effect on GPP in most lakes, while co-additions of N and C showed similar GPP responses to additions of N alone. The only exception was RCA, where N and C increased GPP, while N alone had no effect.

In contrast to GPP, CR rates responded strongly to N additions, C additions, and particularly to combined N and C additions. Both NLN and NLK had heterotrophic communities that were stimulated by N addition, resulting in significantly higher CR. However, the effects of N alone were overshadowed by the synergistic effects of adding both N and C. All lakes but MLN showed sharp increases in CR following N and C co-addition. In nearly all cases where both N and C were added, CR increased to such a degree that the system became heterotrophic—i.e., CR increased much more than GPP (Figure 4-6). In general, these responses were strong in meromictic lakes (with the exception of NLK) compared with holomictic lakes, and in the less connected holomictic lakes (NLN and ULN) compared with the ocean-like lakes (HLO and MLN). In the lakes that did not undergo a metabolic shift in NCP (MLN and NLK), NLK showed an increase in CR in tandem with an increase in GPP, resulting in overall increased NCP. MLN showed a significant decrease in CR following addition of C alone, but no significant response to N or N and C; NCP did not change significantly and all values were close to 0. Finally, N and C additions increased CR far more than addition of N or addition of C alone (Figure 4-6), and the response was more than additive (Figure 4-7), indicating that the combination of N and C had synergistic effects on CR. These findings confirm and extend the hypotheses above, as CR displayed N-limitation in a few instances and N and C co-limitation in nearly all instances.

It is well-known that N limits primary production throughout broad areas of the ocean (Moore et al., 2013), and our experiments show that GPP responded positively to N additions in many marine lakes. However, the heterotrophic microbial community also utilizes inorganic nutrients and can be limited by N; this is a result of high microbial N demands (low C:N ratios), high abundances, and their high affinity for N (e.g., small surface to volume ratios)—factors that apparently lead to microbial control of N cycling across a wide range of ecosystems (Taylor & Townsend, 2010). Microbial N limitation has been tested in the ocean through experimental N additions that show changes in activity, abundance, and community composition. Like our experiments, this work shows that microbial responses to N are complex and commonly depend on more than N alone. For example, Mills et al. (2008) found that N and P co-limited bacterial production in the North Atlantic, while Carlson et al. (2002) found that N had no effect on its own, but the combination of N, P, and DOC increased bacterial production in the Sargasso Sea. However, microbial responses vary across different studies: Caron et al. (2000) observed increased bacterial and phytoplankton production in the Sargasso Sea following additions of N

and P—which were not added separately—whereas Rivkin & Anderson (1997) observed that N alone increased bacterial production or growth in the Sargasso Sea, Caribbean Sea, and Gulf Stream. These results and our own demonstrate that the quantity, timing, and stoichiometry of organic matter are key determinants of CR and/or bacterial production.

In our experiments, the effects of combined N and C additions on CR and NCP may be explained by several underlying responses. In lakes without a clear response to N or C alone, our results are indicative of co-limitation of CR by N and labile C. In lakes where CR did respond to either N or C, the joint effects of N and C were more than additive. One possibility is that this reflects complementarity among different microbial groups. Another possibility is that nitrifying archaea and bacteria respond to the N additions and draw down DO (this can be a significant sink for DO), but there is little evidence for this in our nutrient data: oxidized N concentrations were only slightly elevated following N additions to dark bottles (Table 4-2). Importantly, co-addition of N and C to light bottles yielded negative NCP values and a sharp shift to heterotrophy. This is indicative of rapid microbial response to C and N that would ultimately lead to the consumption of DO. A second implication of this finding is that the microbial community represents a significant sink for N, as we found that 55-98% of added N was taken up over the course of the incubations (Table 4-2).

4.5.3 Effects of light, temperature, and oxygen on GPP, CR, and NCP

In contrast to the strong effects of N and C on GPP, CR, and NCP in marine lakes, the effects of light and temperature were comparatively minor. Our regression results showed that although GPP was typically higher closer to the surface, GPP did not correlate significantly with light intensity. Nutrient availability was instead a more important influence on GPP in regression. Despite the lack of correlation between light and GPP when all lakes were assessed together, depth transplants reinforced the importance of light, as samples that were moved to shallower depths increased in terms of GPP, while samples that were moved to deeper depths decreased. Light limitation has been documented in tropical lakes before (Guildford et al., 2003; Lewis, 1974) and the variation in observed responses here can be explained by a combination of transplant distance and the microbial community. For example, HLO likely showed large changes in transplanted GPP because samples underwent the largest depth change (17 m) and because the lake is holomictic, meaning the photosynthetic community at the bottom of the lake was similar to the upper zone and able to take advantage of the higher light levels. OTM, on the other hand, showed very little change in GPP—likely due to the fact that deep samples that were transplanted to higher light levels possessed photosynthesizers adapted to the light levels at the chemocline, and were not able to take advantage of greater light intensities. This is similar to the phenomenon observed in stratified oceanic environments, where phytoplankton in deeper layers become light saturated at lower light levels than surface phytoplankton (Ryther & Menzel, 1959).

Depth transplants also illustrated the effects of temperature change on CR. Although observed temperature differences were small, such that the maximum temperature difference observed in depth transplants was less than 1ºC, CR generally increased in bottles moved from deeper, slightly cooler waters to the surface, and vice versa. This is in accordance with metabolic theory (López-Urrutia et al., 2006; Regaudie-de- Gioux & Duarte, 2012), although these increases were

rarely significant and were not large in magnitude. Because these are dark bottle incubations, these changes cannot be explained by responses to increases or decreases in GPP driven by variations in light levels at different depths.

Oxygen concentration was also important in predicting GPP and CR within and across lakes. GPP tended to decrease as oxygen increased, while CR displayed a hump-shaped pattern with DO, with highest rates found at intermediate DO concentrations (Figure 4-5). The correlation between low O_2 concentrations and increased GPP is most likely due to the higher concentration of nutrients coming from low oxygen waters. The observation that CR was highest at moderate oxygen concentrations (~100-160 mmol O_2 m^{-3}) was likely a function of heterotrophic microorganisms being most active at the interface between well-oxygenated surface waters and the nutrient- and labile organic matter-rich deeper waters. However, it is also possible that the intermediate oxygen concentration zone possessed the most microbial activity (for which CR is a rough proxy) as it is an interface between well oxygenated and low oxygen waters, leading to higher diversity (Beman & Carolan, 2013) and allowing for redundancy and a wider range of responses, which can stabilize ecological function from random physical and biological fluctuations (McGrady-Steed et al., 1997; Naeem & Li 1997; Bell et al., 2005; Tilman et al., 2006).

4.5.4 Implications for oxygen, carbon, and nutrient cycling

Assembled together, our results highlight the links between the production and consumption of DO by GPP and CR, and the dependence of these processes on the availability of nutrients and carbon. In meromictic lakes with steep depth gradients in DO and dissolved nutrients, we found distinct variation in GPP and CR with depth—including strong net autotrophy near the chemocline. The depth of the chemocline is consistent in our data and in earlier work (Hamner et al., 1982; Hamner & Hamner, 1998; Colin, 2009; Meyerhof et al., 2016), suggesting biogeochemical coupling between GPP in oxygenated waters and the regeneration of nutrients in deeper layers. Our experimental additions demonstrate that N can limit CR, and that this is as common as limitation of CR by the availability of labile C. As the oceans lose oxygen and low oxygen regions expand, N loss through anaerobic processes will likely be enhanced, leading to lower N availability. If N-limitation of CR is widespread in the ocean, and especially OMZs, this could lead to a negative feedback on CR and slow the overall rate of deoxygenation.

However, C and N co-limitation of CR was far more prevalent in our experiments than N or C-limitation. To our knowledge, this is the first demonstration of this phenomenon in low-oxygen marine ecosystems of any kind, and we found that the magnitude of this response was frequently greatest in deoxygenated lakes. N and C co-additions consistently resulted in net heterotrophy, indicating that the relative proportions of N and C, and their chemical forms, are critical determinants of NCP and net DO consumption. Our results suggest that pulses of N and C (but not N or C alone) sharply decrease NCP. Further work should examine how variations in the stoichiometry, chemical composition, quantity, and timing of organic matter inputs interact to affect CR and NCP along depth gradients in low-oxygen ecosystems. Our findings are also indicative of substantial uptake of N by microbial communities. The extent and duration of this N sink will be regulated by microbial growth efficiency, grazing, and viral lysis—in addition

organic matter stoichiometry and nutrient concentrations—underlining the need to understand all aspects of marine ecosystems, and their interactions, in a changing ocean.

4.6 References

Bakun, A., Field, D. B., Redondo-Rodriguez, A., & Weeks, S. J. (2010). Greenhouse gas, upwelling-favorable winds, and the future of coastal ocean upwelling ecosystems. *Global Change Biol.* 16, 1213–1228. doi: 10.1111/j.1365-2486.2009.02094.x

Behrenfeld, M. J., et al. (2006). Climate-driven trends in contemporary ocean productivity. *Nature* 444, 752–755. doi: 10.1038/nature05317

Bell, T., Newman, J. A., Silverman, B. W., Turner, S. L., & Lilley, A. K. (2005). The contribution of species richness and composition to bacterial services. *Nature* 436, 1157–1160. doi: 10.1038/nature03891

Beman, J. M., Arrigo, K. R., & Matson, P. A. (2005). Agricultural runoff fuels large phytoplankton blooms in vulnerable areas of the ocean. *Nature* 434, 211–214. doi: 10.1038/nature03370

Beman, J. M., & Carolan, M. T. (2013). Deoxygenation alters bacterial diversity and community composition in the ocean's largest oxygen minimum zone. *Nat. Commun.* 4:2705. doi: 10.1038/ncomms3705

Blight, S. P., et al. (1995). Phasing of autotrophic and heterotrophic plankton metabolism in a temperate coastal ecosystem. *Mar. Ecol. Prog. Ser. Oldendorf* 128, 61–75. doi: 10.3354/meps128061

Bograd, S. J., & Lynn, R. J. (2001). Physical-biological coupling in the California Current during the 1997–99 El Niño-La Niña Cycle. *Geophys. Res. Lett.* 28, 275–278. doi: 10.1029/2000GL012047

Breitburg, D. L., Crump, B. C., Dabiri, J. O., & Gallegos, C. L. (2010). Ecosystem engineers in the pelagic realm: alteration of habitat by species ranging from microbes to jellyfish. *Integr. Comp. Biol.* 50, 188–200. doi: 10.1093/icb/icq051

Bronk, D., See, J., Bradley, P., & Killberg, L. (2007). DON as a source of bioavailable nitrogen for phytoplankton. *Biogeosciences* 4, 283–296. doi: 10.5194/bg-4-283-2007

Burnett, B., Narita, H., & Harada, K. (1988). Uranium-series isotopes in sediment and water from an anoxic marine lake in Palau, Micronesia. *Chem. Geol.* 70, 125. doi: 10.1016/0009-2541(88)90551-7

Carlson, C. A., et al. (2002). Effect of nutrient amendments on bacterioplankton production, community structure, and DOC utilization in the northwestern Sargasso Sea. *Aquat. Microb. Ecol.* 30, 19–36. doi: 10.3354/ame030019

Caron, D. A., Lin Lim, E., Sanders, R. W., Dennett, M. R., & Berninger, U.-G. (2000). Responses of bacterioplankton and phytoplankton to organic carbon and inorganic nutrient additions in contrasting oceanic ecosystems. *Aquat. Microb. Ecol.* 22, 175–184. doi: 10.3354/ame022175

Colin, P. L. (2009). *Marine Environments of Palau*. Honolulu, HI: Mutual Publishing LLC, 416.

Dalsgaard, T., Thamdrup, B., Farías, L., & Revsbech, N. P. (2012). Anammox and denitrification in the oxygen minimum zone of the eastern South Pacific. *Limnol. Oceanogr.* 57, 1331–1346. doi: 10.4319/lo.2012.57.5.1331

Dawson, M. N. (2006). Island evolution in marine lakes. *JMBA Global Mar. Environ.* 3, 26–29.

Dawson, M. N., & Hamner, W. M. (2005). Rapid evolutionary radiation of marine zooplankton in peripheral environments. *Proc. Natl. Acad. Sci. U.S.A.* 102, 9235–9240. doi: 10.1073/pnas.0503635102

del Giorgio, P. A., & Williams, P. J. l. B. (2005). *Respiration in Aquatic Ecosystems*. Oxford: Oxford University Press, 328.

Deutsch, C., Brix, H., Ito, T., Frenzel, H., & Thompson, L. (2011). Climate-forced variability of ocean hypoxia. *Science* 333, 336–339. doi: 10.1126/science.1202422

Diamond, D. (1997). "Determination of nitrate in brackish or seawater by flow injection analysis," in *QuikChem Method 31-107-04-1-A for Lachat Instruments* (Milwaukee, WI: Lachat Instruments).

Diamond, D., & Huberty, A. (1996). "Determination of ammonia by flow injection analysis," in *QuikChem Method 31-107-06-5-A for Lachat Instruments* (Milwaukee, WI: Lachat Instruments).

Doney, S. C., et al. (2012). Climate change impacts on marine ecosystems. *Mar. Sci.* 4, 11–37. doi: 10.1146/annurev-marine-041911-111611

Elser, J., et al. (2000). Biological stoichiometry from genes to ecosystems. *Ecol. Lett.* 3, 540–550. doi: 10.1046/j.1461-0248.2000.00185.x

Francis, C. A., Beman, J. M., & Kuypers, M. M. (2007). New processes and players in the nitrogen cycle: the microbial ecology of anaerobic and archaeal ammonia oxidation. *ISME J.* 1, 19–27. doi: 10.1038/ismej.2007.8

Gilly, W. F., Beman, J. M., Litvin, S. Y., & Robison, B. H. (2013). Oceanographic and biological effects of shoaling of the oxygen minimum zone. *Ann. Rev. Mar. Sci.* 5, 393–420. doi: 10.1146/annurev-marine-120710-100849

Gist, N., Serret, P., Woodward, E. M. S., Chamberlain, K., & Robinson, C. (2009). Seasonal and spatial variability in plankton production and respiration in the Subtropical Gyres of the Atlantic Ocean. *Deep Sea Res. II* 56, 931–940. doi: 10.1016/j.dsr2.2008.10.035

Gregg, W. W., Casey, N. W., & McClain, C. R. (2005). Recent trends in global ocean chlorophyll. *Geophys. Res. Lett.* 32, 1–5. doi: 10.1029/2004GL021808

Gruber, N. (2008). *The Marine Nitrogen Cycle: Overview and Challenges. Nitrogen in the Marine Environment, 2nd Edn.* Cambridge, MA: Academic Press.

Gruber, N., & Sarmiento, J. L. (1997). Global patterns of marine nitrogen fixation and denitrification. *Global Biogeochem. Cycles* 11, 235–266. doi: 10.1029/97GB00077

Guildford, S. J., Hecky, R. E., Taylor, W. D., Mugidde, R., & Bootsma, H. A. (2003). Nutrient enrichment experiments in tropical great lakes Malawi/Nyasa and Victoria. *J. Great Lakes Res.* 29, 89–106. doi: 10.1016/S0380-1330(03)70541-3

Hamner, W., Gilmer, R., & Hamner, P. (1982). The physical, chemical, and biological characteristics of a stratified, saline, sulfide lake in Palau. *Limnol. Oceanogr.* 27, 896–909. doi: 10.4319/lo.1982.27.5.0896

Hamner, W. M., & Hamner, P. P. (1998). Stratified marine lakes of Palau (Western Caroline islands). *Phys. Geogr.* 19, 175–220.

Huberty, A., & Diamond, D. (1998). "Determination of phosphorus by Flow injection analysis colorimetry," in *QuikChem Method 31-115-01-3-A for Lachat Instruments* (Milwaukee, WI: Lachat Instruments).

Kalvelage, T., et al. (2015). Aerobic microbial respiration in oceanic oxygen minimum zones. *PLoS ONE* 10:e0133526. doi: 10.1371/journal.pone.0133526

Karl, D. M., & Knauer, G. A. (1991). Microbial production and particle flux in the upper 350 m of the Black Sea. *Deep Sea Res. A.* 38, S921–S942. doi: 10.1016/S0198-0149(10)80017-2

Karstensen, J., Stramma, L., & Visbeck, M. (2008). Oxygen minimum zones in the eastern tropical Atlantic and Pacific Oceans. *Prog. Oceanogr.* 77, 331–350. doi: 10.1016/j.pocean.2007.05.009

Katija, K., & Dabiri, J. O. (2009). A viscosity-enhanced mechanism for biogenic ocean mixing. *Nature* 460, 624–626. doi: 10.1038/nature08207

Keeling, R. F., Körtzinger, A., & Gruber, N. (2010). Ocean deoxygenation in a warming world. *Mar. Sci.* 2, 199–229. doi: 10.1146/annurev.marine.010908.163855

Lam, P., & Kuypers, M. M. (2011). Microbial nitrogen cycling processes in oxygen minimum zones. *Ann. Rev. Mar. Sci.* 3, 317–345. doi: 10.1146/annurev-marine-120709-142814

Landing, W. M., Burnett, W. C., Lyons, W. B., & Orem, W. H. (1991). Nutrient cycling and the biogeochemistry of manganese, iron. and zinc in Jellyfish Lake, Palau. *Limnol. Oceanogr.* 36, 515–525. doi: 10.4319/lo.1991.36.3.0515

Lewis, W. M. (1974). Primary production in the plankton community of a tropical lake. *Ecol. Monogr.* 44, 377–409. doi: 10.2307/1942447

López-Urrutia, A., San Martin, E., Harris, R. P., & Irigoien, X. (2006). Scaling the metabolic balance of the oceans. *Proc. Natl. Acad. Sci. U.S.A.* 103, 8739–8744. doi: 10.1073/pnas.0601137103

Lyons, W. B., et al. (1996). Jellyfish Lake, Palau: regeneration of C, N, Si, and P in anoxic marine lake sediments. *Limnol. Oceanogr.* 41, 1394–1403. doi: 10.4319/lo.1996.41.7.1394

Martiny, A. C., et al. (2013). Strong latitudinal patterns in the elemental ratios of marine plankton and organic matter. *Nat. Geosci.* 6, 279–283. doi: 10.1038/ngeo1757

McGrady-Steed, J., Harris, P. M., & Morin, P. J. (1997). Biodiversity regulates ecosystem predictability. *Nature* 390, 162–165. doi: 10.1038/36561

Meyerhof, M. S., Wilson, J. M., Dawson, M. N., & Michael Beman, J. (2016). Microbial community diversity, structure and assembly across oxygen gradients in meromictic marine lakes, Palau. *Environ. Microbiol.* 18, 4907–4919. doi: 10.1111/1462-2920.13416

Mills, M. M., et al. (2008). Nitrogen and phosphorus co-limitation of bacterial productivity and growth in the Oligotrophic Sub-Tropical North Atlantic. *Limnol. Oceanogr.* 53, 824–834. doi: 10.4319/lo.2008.53.2.0824

Moore, C., et al. (2013). Processes and patterns of oceanic nutrient limitation. *Nat. Geosci.* 6, 701–710. doi: 10.1038/ngeo1765

Morán, X. A. G., Fernández, E., & Pérez, V. (2004). Size-fractionated primary production, bacterial production and net community production in subtropical and tropical domains of the oligotrophic NE Atlantic in autumn. *Mar. Ecol. Prog. Ser.* 274, 17–29. doi: 10.3354/meps274017

Naeem, S., & Li, S. (1997). Biodiversity enhances ecosystem reliability. *Nature* 390, 507–509. doi: 10.1038/37348

Orem, W. H., Burnett, W., Landing, W., Lyons, W., & Showers, W. (1991). Jellyfish Lake, Palau: early diagenesis of organic matter in sediments of an anoxic marine lake. *Limnol. Oceanogr.* 36, 526–543. doi: 10.4319/lo.1991.36.3.0526

Paulmier, A., & Ruiz-Pino, D. (2009). Oxygen minimum zones (OMZs) in the modern ocean. *Prog. Oceanogr.* 80, 113–128. doi: 10.1016/j.pocean.2008.08.001

Paulmier, A., Ruiz-Pino, D., & Garçon, V. (2011). CO_2 maximum in the oxygen minimum zone (OMZ). *Biogeosciences* 8, 239–252. doi: 10.5194/bg-8-239-2011

Regaudie-de-Gioux, A., & Duarte, C. M. (2012). Temperature dependence of planktonic metabolism in the ocean. *Global Biogeochem. Cycles* 26, 1–10. doi: 10.1029/2010GB003907

Rivkin, R. B., & Anderson, M. R. (1997). Inorganic nutrient limitation of oceanic bacterioplankton. *Limnol. Oceanogr.* 42, 730–740. doi: 10.4319/lo.1997.42.4.0730

Robinson, C., & Williams, P. J. l. B. (2005). "Respiration and its measurement in surface marine waters," in *Respiration in Aquatic Ecosystems*, eds P. A. del Giorgio and P. J. l. B. Williams (Oxford: Oxford University Press), 147–180. doi: 10.1093/acprof:oso/9780198527084.003.0009

Ryther, J. H., & Menzel, D. W. (1959). Light adaptation by marine phytoplankton. *Limnol. Oceanogr.* 4, 492–497. doi: 10.4319/lo.1959.4.4.0492

Schroeder, S. (1997). "Determination of nitrite in brackish or seawater by flow injection analysis," in *QuikChem Method 31-107-05-1-A for Lachat Instruments* (Milwaukee, WI: Lachat Instruments).

Serret, P., Robinson, C., Fernández, E., Teira, E., & Tilstone, G. (2001). Latitudinal variation of the balance between plankton photosynthesis and respiration in the eastern Atlantic Ocean. *Limnol. Oceanogr.* 46, 1642–1652. doi: 10.4319/lo.2001.46.7.1642

Stramma, L., Johnson, G. C., Sprintall, J., & Mohrholz, V. (2008). Expanding oxygen-minimum zones in the tropical oceans. *Science* 320, 655–658. doi: 10.1126/science.1153847

Taylor, P. G., & Townsend, A. R. (2010). Stoichiometric control of organic carbon–nitrate relationships from soils to the sea. *Nature* 464, 1178–1181. doi: 10.1038/nature08985

Tiano, L., et al. (2014). Oxygen distribution and aerobic respiration in the north and south eastern tropical Pacific oxygen minimum zones. *Deep Sea Res. I* 94, 173–183. doi: 10.1016/j.dsr.2014.10.001

Tilman, D., Reich, P. B., & Knops, J. M. (2006). Biodiversity and ecosystem stability in a decade-long grassland experiment. *Nature* 441, 629–632. doi: 10.1038/nature04742

Ulloa, O., Canfield, D. E., DeLong, E. F., Letelier, R. M., & Stewart, F. J. (2012). Microbial oceanography of anoxic oxygen minimum zones. *Proc. Natl. Acad. Sci. U.S.A.* 109, 15996–16003. doi: 10.1073/pnas.1205009109

Ward, B. B., et al. (2009). Denitrification as the dominant nitrogen loss process in the Arabian Sea. *Nature* 461, 78–81. doi: 10.1038/nature08276

Williams, P. J. l. B. (2000). “Net production, gross production and respiration: what are the interconnections and what controls what,” in *The Changing Ocean Carbon Cycle: A Midterm Synthesis of the Joint Global Ocean Flux Study*, eds R. B. Hanson, H. W. Ducklow, J. G. Field, & Joint Global Ocean Flux Study (Cambridge: Cambridge University Press), 37–60.

Wright, J. J., Konwar, K. M., & Hallam, S. J. (2012). Microbial ecology of expanding oxygen minimum zones. *Nat. Rev. Microbiol.* 10, 381–394. doi: 10.1038/nrmicro2778

4.7 Tables

Table 4-1 Lake and experiment information.

	Location	Lake Type	Total Depth	Chemocline Depth	Date	Depths	Experiment
Ocean	RCA	Ocean	30	NA	11/19/2015	1	N and C Addition
Lakes	HLO	Holomictic (ocean-like)	25	NA	11/18/2014	1, 10, 20	None
					11/19/2014	1, 10, 20	Transplant
					10/22/2015	1, 10	N Addition
					11/3/2015	1, 20	None
					11/4/2015	1, 10, 20	Transplant
	MLN	Holomictic (ocean-like)	25	NA	10/30/2015	1	N and C Addition
	NLN	Holomictic	14	NA	11/21/2014	1, 7, 14	Transplant
					10/16/2015	1	N and C Addition
	ULN	Holomictic	10	NA	11/10/2014	1, 5, 8	None
					11/11/2014	1, 5, 8	Transplant
					11/6/2015	1	N and C Addition
	NLK	Meromictic (stratified)	38	18	11/13/2014	1, 10, 18	None
					11/13/2015	1	N and C Addition
	OTM	Meromictic (stratified)	30	11	11/5/2014	1, 7, 12	None
					10/13/2015	1, 7, 10	Transplant
					10/27/2015	1, 10	None
					11/17/2015	1	N and C Addition
	TLN	Transitional (stratified)	10	6	11/10/2015	1	N and C Addition

Table 4-2 Average nutrient concentrations in different treatments following experimental additions of NH_4^+ (5 μM NH_4Cl), C (100 μM), and both N + C.

Experimental Treatment		**NH_4^+ (μM)**	**$NO_2^- + NO_3^-$ (μM)**	**PO_4^{3-} (μM)**
Light bottles	Control	0.56 ±0.31	1.23 ±0.16	0.07 ±0.03
	N	1.84 ±1.85	1.21 ±0.20	0.06 ±0.02
	N + C	0.94 ±0.45	1.13 ±0.08	0.01 ±0.01
	C	1.71 ±1.25	0.82 ±0.15	0.07 ±0.01
Dark bottles	Control	1.12 ±0.56	1.18 ±0.23	0.13 ±0.02
	N	4.28 ±0.94	1.34 ±0.19	0.12 ±0.02
	N + C	0.96 ±0.29	1.12 ±0.15	0 ±0
	C	0.57 ±0.11	0.87 ±0.13	0.04 ±0.01

4.8 Figures

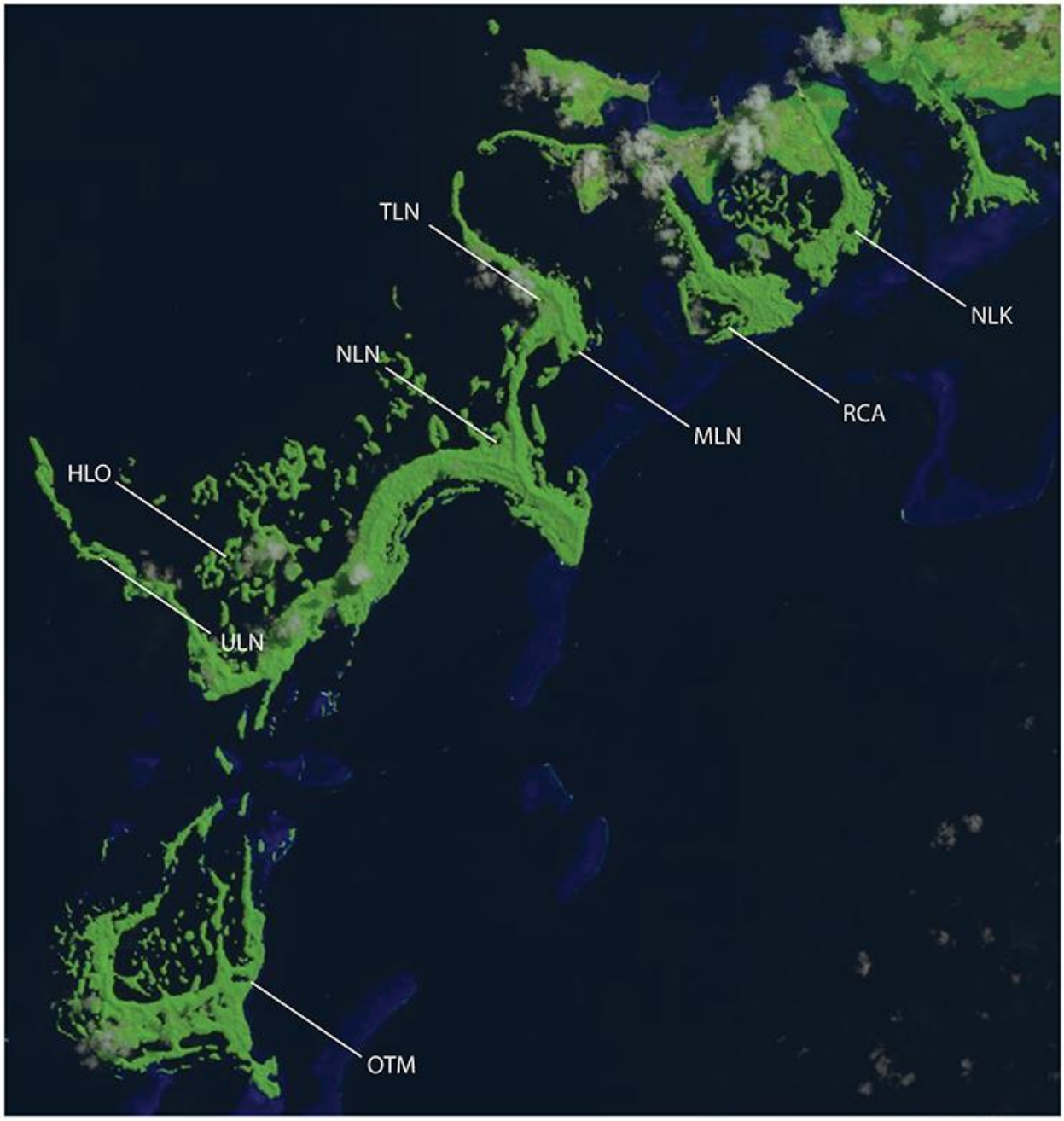


Figure 4-1 Landsat image of Palau showing the location of sampling sites. Risong Cove (RCA) is a protected cove that is completely connected to the surrounding ocean; Heliofungia (HLO), Mekeald (MLN) are ocean-like holomictic lakes; Ngeruktabel (NLN), and Uet era Ngchas (ULN) are less-connected holomictic lakes; and Ngermeuangel Lake (NLK), Ongeim'l Tketau (OTM aka Jellyfish Lake), and T Lake (TLN) are stratified meromictic lakes.

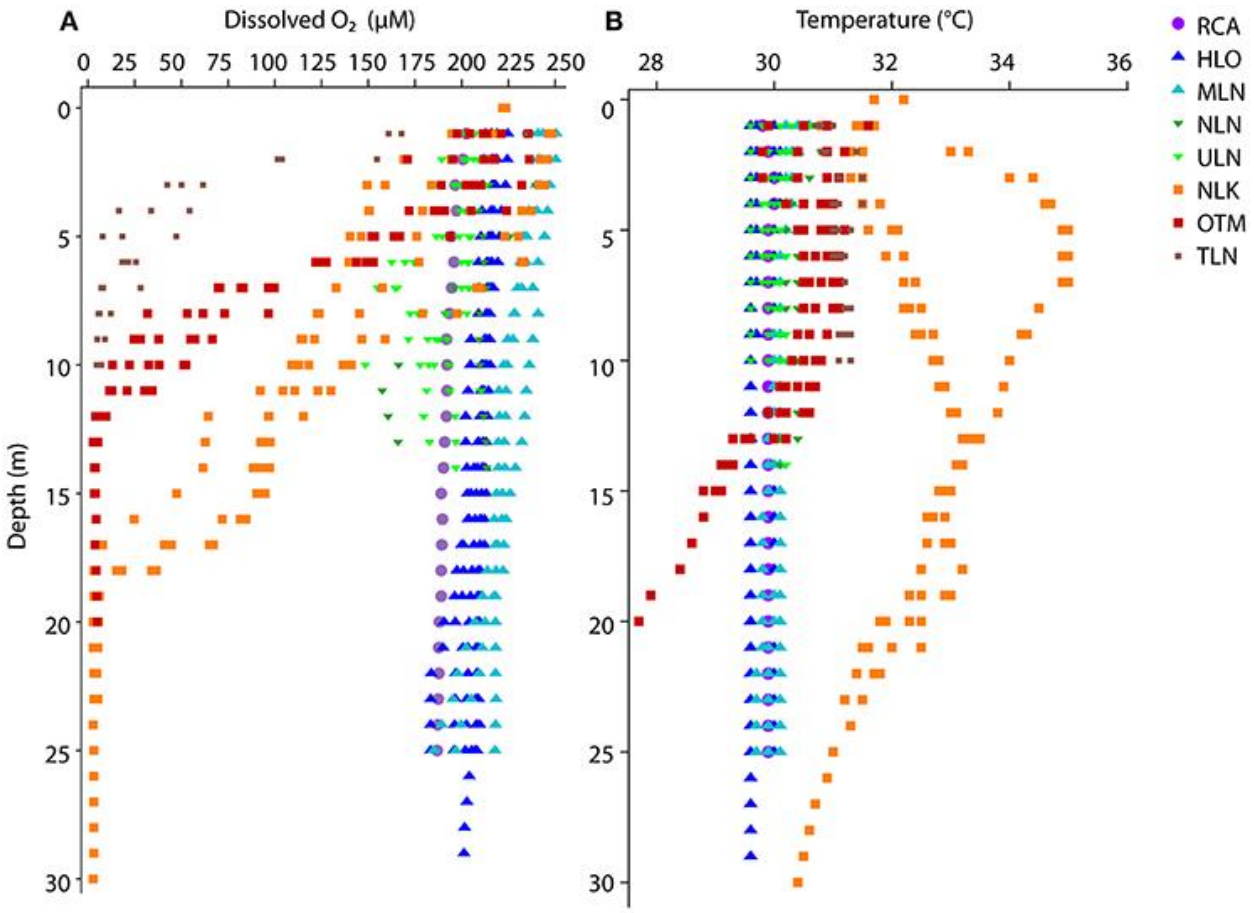


Figure 4-2 Depth profiles of (A) dissolved oxygen and (B) temperature for each lake in which rates were measured. Colors denote the various lakes and the cove, and include all profiles collected; many of the lakes had very similar profiles on the different dates visited. HLO, MLN, NLN and ULN are holomictic lakes, whereas OTM, NLK, and TLN are meromictic lakes and show sharp decreases in oxygen with depth.

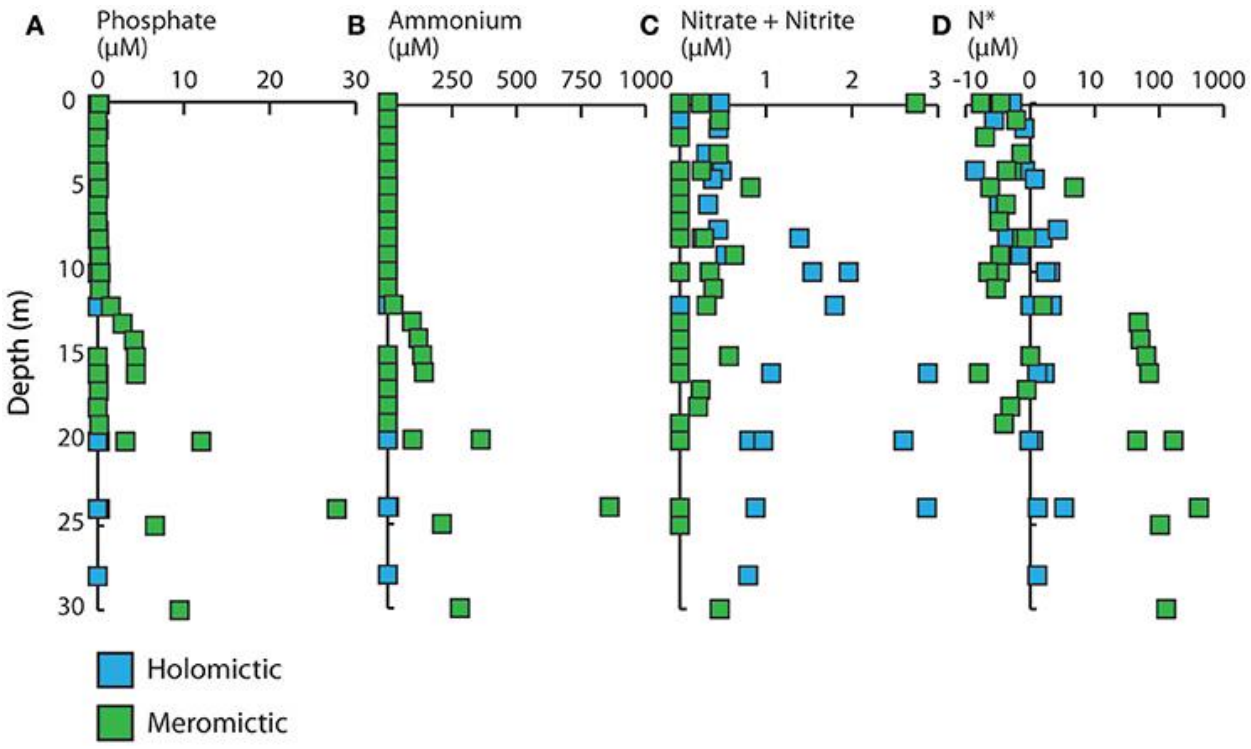


Figure 4-3 Depth profiles of (A) PO_3^{-4}, (B) NH_4^+, (C) $NO_3^- + NO_2^-$, and (D) N^* in holomictic and meromictic lakes. Colors denote the lake types. $N^* < 0$ = N-deficient, $N^* > 0$ = P-deficient.

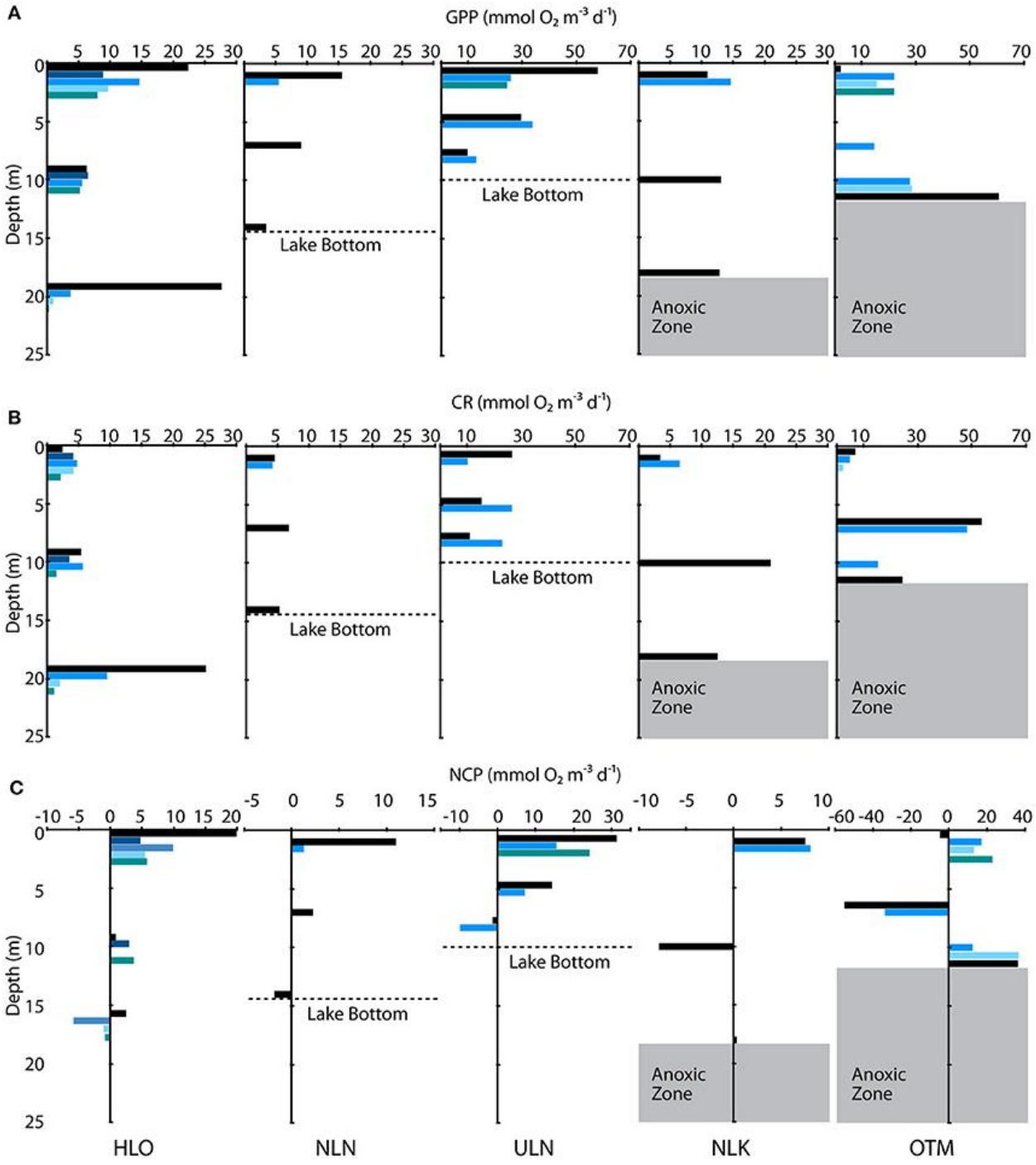


Figure 4-4 Depth profiles of (A) GPP, (B) CR, and (C) NCP collected in five lakes listed at the bottom of the figure. Colored bars indicate different measurement periods in 2014 and 2015. Dashed lines denote the lake bottom in NLN and ULN, and the gray shaded area shows the anoxic zone in NLK and OTM. GPP and CR data are plotted on the same axes for each lake, but note the differences between GPP and CR axes for ULN and OTM compared with the other lakes. NCP axes differ across all lakes.

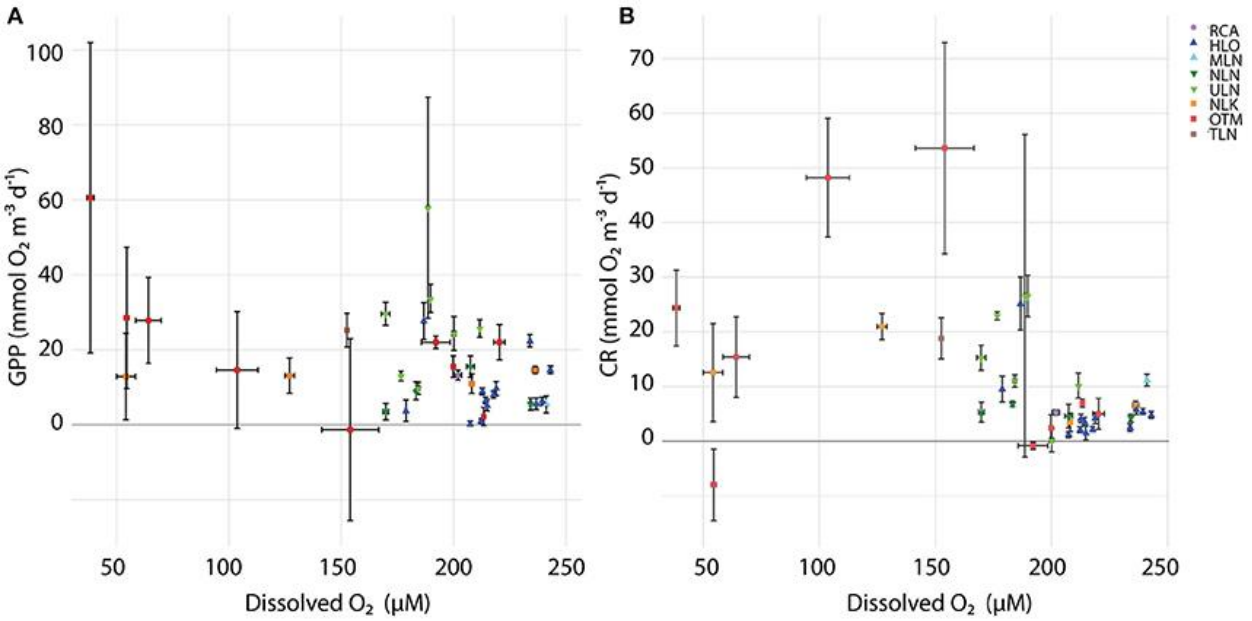


Figure 4-5 Relationships between oxygen concentration against (A) GPP and (B) CR. Error bars denote standard error and colors denote different sampling times.

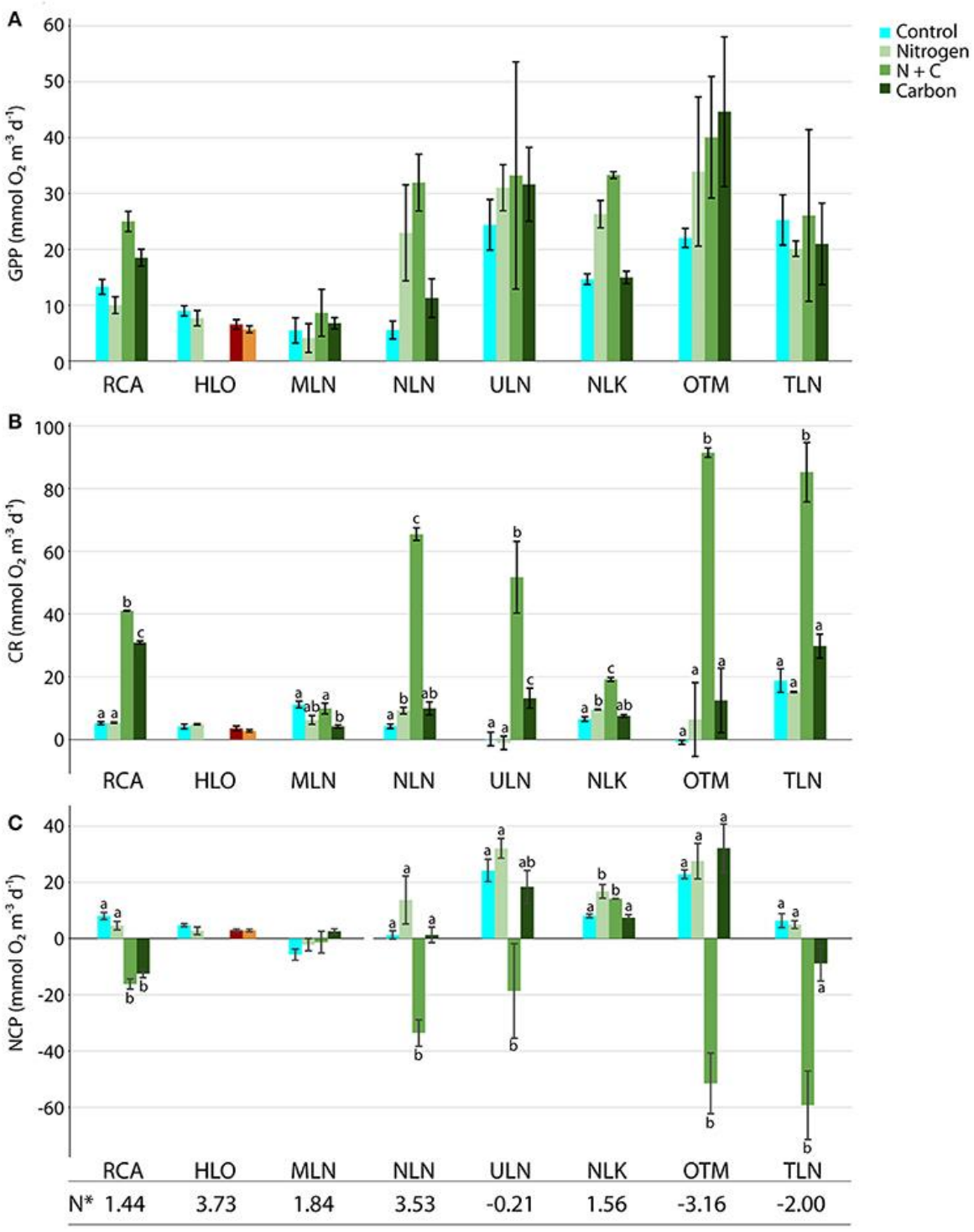


Figure 4-6 Effects of experimental additions of nitrogen, carbon, and nitrogen + carbon on (A) GPP, (B) CR, and (C) NCP. Colors denote the treatments and error bars denote standard error. (Orange and red bars denote a second N addition experiment conducted at 10 m depth in HLO.) Letters show Tukey HSD test results for each lake—i.e., whether additions are different from one another and/or the control. *N** values are labeled below each lake.

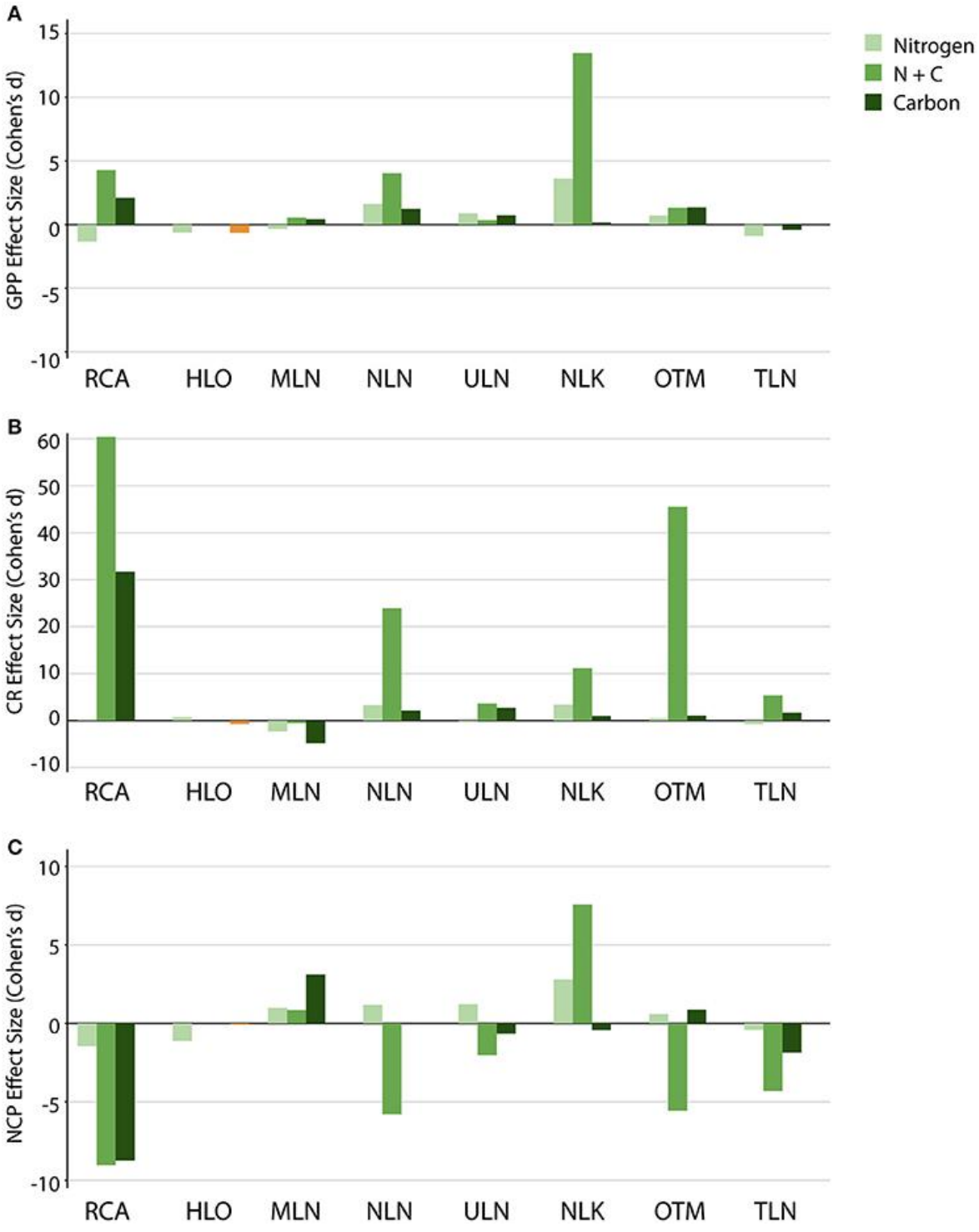


Figure 4-7 Effect sizes (Cohen's *d*) for experimental additions. Effect sizes are shown for additions of nitrogen, carbon, and nitrogen + carbon on (A) GPP, (B) CR, and (C) NCP. Colors denote treatment (orange and red bars denote a second N addition experiment conducted at 10 m depth in HLO).

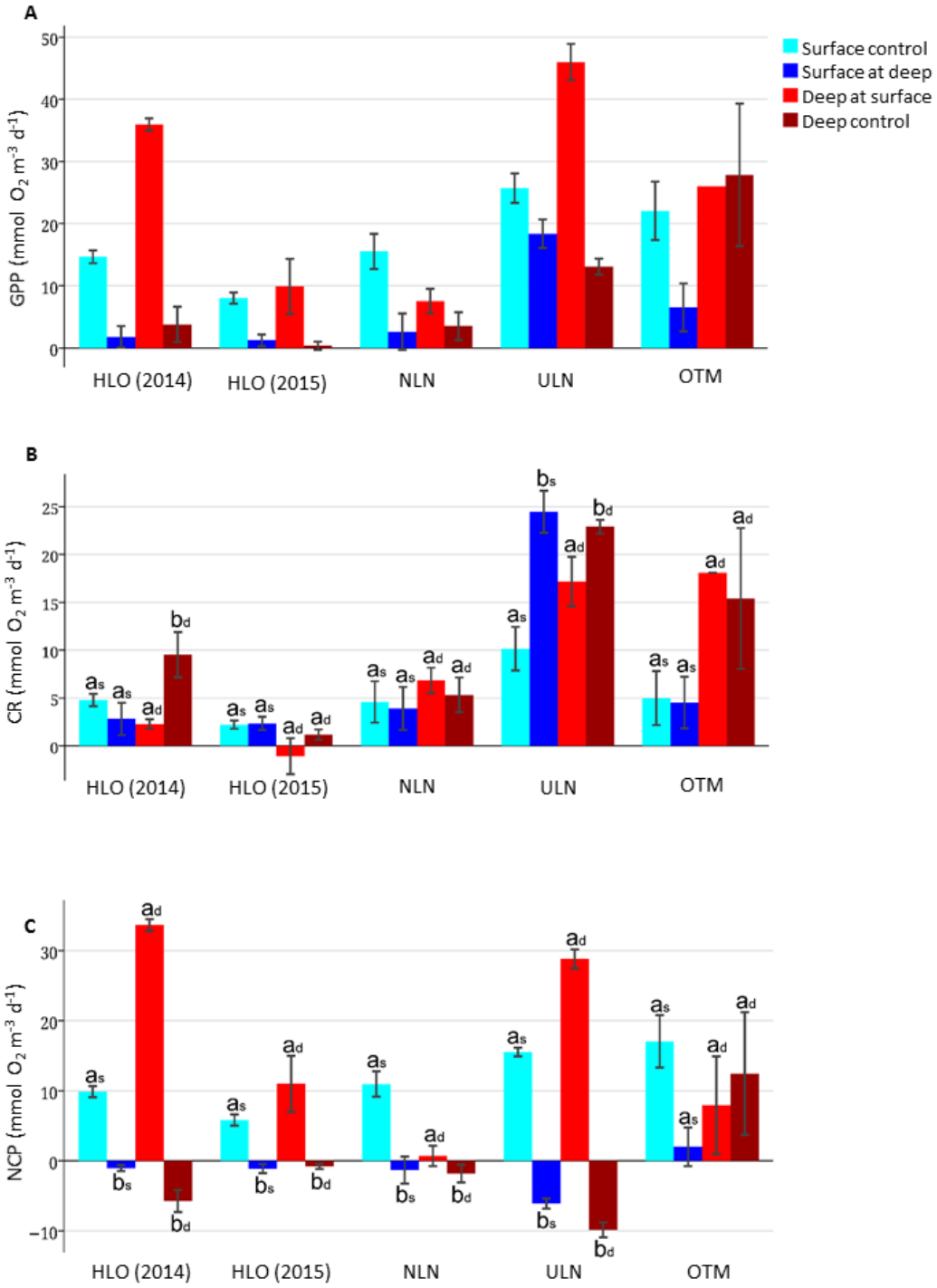


Figure 4-8 Effect of depth transplants on (A) GPP, (B) CR, and (C) NCP. Colors denote the treatments and error bars denote standard error. Error bars are not shown for OTM deep at surface CR and GPP because oxygen contamination resulted in only a single valid CR measurement. Letters show Tukey HSD test results for each lake—i.e., whether transplant is different from the control. Note: end water concentrations (not rates) were compared for Tukey HSD tests so water originating from deep water could not be compared to water originating from surface (subscripts denote water origin).

5 Conclusion

The idea that microorganisms are ecosystem engineers is becoming an accepted concept and this dissertation has helped to tease apart some of the ways microorganisms affect their surroundings (through the production and consumption of oxygen) and, in turn, how environmental conditions affect microbial community composition and activities. The overall purpose of this dissertation was to assess biological oxygen cycling in ocean systems, factoring in gaps in the literature. I ultimately chose to focus on the factors influencing community respiration (CR) because there are relatively fewer studies regarding respiration and because oxygen consumption can be used as a proxy for ecosystem function. While studying CR in any location is important for understanding ecosystem function, by studying CR in these three very different locations of the ocean (and very different scales of the ocean) I was able to understand controls on CR and how CR may change in certain areas of the ocean as currents, temperatures, and nutrient inputs change.

In chapter 2, I showed that CR was variable across the Pacific via data continuously collected by oceanic drones. 605 independent CR rates were calculated (an unmatched effort for the Pacific) and compared with coincident temperature, turbidity, and chlorophyll measurements in the Pacific Ocean and, of particular note, was the fact that different variables correlated with CR in different areas of the ocean—particularly that different oceanic provinces demonstrate differences in the coupling between primary production and CR, with strong coupling in productive provinces, and decoupling in less productive regions. This finding has implications for understanding carbon and metabolic balance in the sea, as it reinforces the importance of integrating CR over time and depth, but also lateral space. Sampling one station (or a few stations) repeatedly does not accurately capture the metabolic activities of an ocean basin, a concept that has been demonstrated before but has not gained wide acceptance. I personally expected CR to correlate more strongly with temperature across the large gradients measured, but this work ultimately supported the idea that temperature is not a strong regulating factor in non-high latitude regions. Changes in the microbial community are likely a contributing factor to the changes in CR observed throughout this study and, while a direct effect on CR from temperature changes due to climate change may not be in store for lower latitudes, changes in the supply of organic matter and nutrients from changes in water mass movement (which will certainly be affected by temperature changes) could affect CR.

In chapter 3, I showed that a subset of the microbial community correlated with CR in Monterey Bay. Nearshore Eastern Boundary Currents are some of the most productive ecosystems in the world, but also boast some of the highest rates of CR (leading to large oxygen minimum zones in certain areas), making them an ideal location to tease apart the controls on high but variable rates of CR. While several microbial subnetworks (and the entire community, based on ESOM) correlated strongly with upwelling, the two microbial subnetworks that correlated with CR did not directly correlate with upwelling; suggesting that although upwelling typically alters the environmental variables partially responsible for changes in CR (e.g. temperature and DO), the microbial groups and networks most strongly related to shifts in CR are controlled by other factors. While stronger upwelling events may have different effects on the microbial community, that would in turn affect microbial functioning, this work shows us what to expect during moderate changes in upwelling. This work also demonstrated that the critically important process

of CR is regulated by a combination of variations in the physical and chemical environment, microbial responses to these changes, and ecological and biogeochemical interactions between microbial groups. The fact that CR correlated with non-diatom eukaryotic phytoplankton is an indication that regime shifts in the dominant phytoplankton present may affect CR by changing the subset of the microbial community that correlates with CR. These types of phytoplankton regime shifts in Monterey Bay have been observed in the past with both climate change and temporary changes in stratification, such that increased stratification correlated with higher CR by increasing non-diatom eukaryotic phytoplankton. Finally, the fact that many of the heterotrophic microbial groups that were associated with the various subnetworks are widespread and display similar dynamics elsewhere suggests that these finding can be applied elsewhere.

In chapter 4, I demonstrated that CR and GPP are tightly linked to both DO and nutrient concentrations in the marine lakes of Palau, but can uncouple via the stimulation of CR—inducing net heterotrophy—though the addition of both N and C. This effect was seen across a majority of the marine lakes (both holomictic and meromictic). Through a combination of observational measurements and experimental manipulations I was able to show both the natural effect of nutrients on GPP and CR (they tended to increase as nutrients increase from holomictic to meromictic lakes) and how the same microbial community would respond to influxes of C and N (CR increased much more than GPP). The biogeochemical controls on metabolism in these tropical marine lakes may be applicable to other marine ecosystems—particularly nearshore, low-latitude environments. The resulting net heterotrophy following N and C stimulated CR may indicate a potential positive feedback to climate change and reinforcement of low oxygen waters as we witness oceanic currents change or increased runoff.

Each one of these experiments ultimately informs us about possible feedbacks to global change in certain ecosystems. While it is tempting apply these findings to the entire ocean and estimate CR and net metabolism worldwide, the highly intricate and interconnected nature of the biological, chemical, and physical processes that take place on Earth's entire surface make forecasting global responses more involved than one dissertation made up of three observational and experimental studies can tackle—something that was made all too clear in Chapter 2. The contributions this work has made to understanding how biology, physics, and chemistry interact to govern important microbial functions should be limited to ecosystems similar to the ones studied; but could, perhaps, one day be combined with other research to create breathable atmosphere on a new planet.